Quartz arenites of the uppermost Cambrian - lowermost Ordovician Kamouraska Formation, Québec, Canada: gravity flow deposits of eolian sand in the deep sea

Pierre Malhame

Department of Earth and Planetary Sciences
McGill University
Montréal, Québec

A thesis submitted to McGill University in partial fulfillment of the requirements of the degree of Masters of Science

June 2007

Your file Votre référence
ISBN: 978-0-494-38419-0
Our file Notre référence
ISBN: 978-0-494-38419-0

TABLE OF CONTENTS

LIST OF FIGURES AND TABLES

ABSTRACT

The uppermost Cambrian-Lower Ordovician Kamouraska Formation in the external Humber Zone of the Quebec Appalachians consists of dominant thick massive to graded quartz arenite beds, subordinate pebble conglomerate and intercalated thin shale and siltstone beds. It was deposited by hyperconcentrated to concentrated density flows in a meandering submarine canyon on the continental slope bordering the Iapetus Ocean. Turbidity currents deposited beds with turbidite structure divisions. The sandstones consist of well sorted, well rounded quartz sand with frosted grains. Scanning electron microscopy reveals the presence of textures supporting eolian transport before redeposition in the deep sea. The Kamouraska quartz arenites are considered an ancient equivalent of Pleistocene eolian-sand turbidites on an abyssal plain off West Africa consisting of Sahara sand. Sand provenance is attributed to eolian equivalents of the Cairnside Formation of the Potsdam Group. The quartz arenites of the Kamouraska Formation provide a variant to tectonic sandstone provenance proposed in the scheme of Dickinson and Suczek (1979).

RÉSUMÉ

La Formation de Kamouraska (Ordovicien inférieur), affleurant dans la zone externe de Humber des Appalaches du Québec, consiste principalement de lits épais d'arénites quartziques à texture massive à granoclassée, de conglomérat à galets, et de lits de shale et siltstone intercalés. Les travaux de terrain suggèrent une mise en place par des courants gravitaires hyperconcentrés à concentrés sur la pente continentale de l'océan Iapétus, dans un canyon sous-marin à méandres. Des courants de turbidité ont déposé des lits aux divisions de coulées turbiditiques. Les grès consistent de grains de quartz bien triés et arrondis aux surfaces dépolies. La microscopie à balayage électronique révéle la présence de textures indiquant un transport éolien avant la redéposition en eaux profondes. Les arénites quartziques de la Formation de Kamouraska sont interprétées comme un ancien équivalent des turbidites sableuses (Pléistocène) d'origine éolienne mise en place sur la plaine abyssale au large de Afrique de l'ouest et dont la source est le Sahara. La provenance du sable de la Formation de Kamouraska est attribuée aux équivalents éoliens de la formation de Cairnside (Groupe de Potsdam). Les arénites quartziques de la Formation de Kamouraska sont une variante à la provenance tectonique de grés proposée dans la classification de Dickinson and Suczek (1979).

1. INTRODUCTION

The Kamouraska Formation crops out on the south shore of the St. Lawrence Estuary. Known outcrops occur in the Saint-Raphael area (Lebel and Hubert, 1995a), L'Islet-Kamouraska area (Hubert, 1965; Hubert, 1973), Rivière-du-Loup area up to Rimouski (Vallières, 1984), and intermittently in parts of eastern Gaspé (between Rimouski and Cap-des-Rosiers): south of Matane, south of Les Méchins and south of Grande-Vallée (Slivitzky et al., 1991). Dresser (1912) was the first to use the term Kamouraska Formation. According to Dresser (1912), the Kamouraska Formation comprises all quartzite occurrences along with their associated limestone conglomerates on the south shore of the Gulf of St. Lawrence between Montmagny and Rivière-du-Loup. Hubert (1965) revived the term Kamouraska Formation and refined its definition. He differentiated the quartz arenites from the feldspathic arenites in the L'Islet-Kamouraska area. Hubert (1965) applied the term Kamouraska Formation to the quartz arenites and their associated conglomerates and the term Saint Damase Formation to the underlying feldspathic arenites and conglomerates. Hubert (1965, 1973) interpreted the depositional environment of the Kamouraska Formation as shallow marine (beach and near-shore sands) due to the massive bedding, lack of sedimentary structures and the dominance of mature well-sorted quartz sand. The associated conglomerates were interpreted as alluvial fan deposits based on section correlations which revealed a fan-like geometry for the conglomerate deposits (Hubert, 1973). Subsequent research has shown that the formation must have been deposited in deep water on the continental slope or rise by means of turbidity currents as it is underlain and overlain by deep-water sediments (St.Julien & Hubert, 1975; Vallières, 1984; Lebel and Hubert, 1995a). "Elevator stratigraphy/tectonics" involving a change in the depositional environment from deep sea to shallow water and then back to deep sea in a short period of time is not compatible with modern concepts of continental margin evolution. Therefore the original environmental interpretation of Hubert (1973) was abandoned.

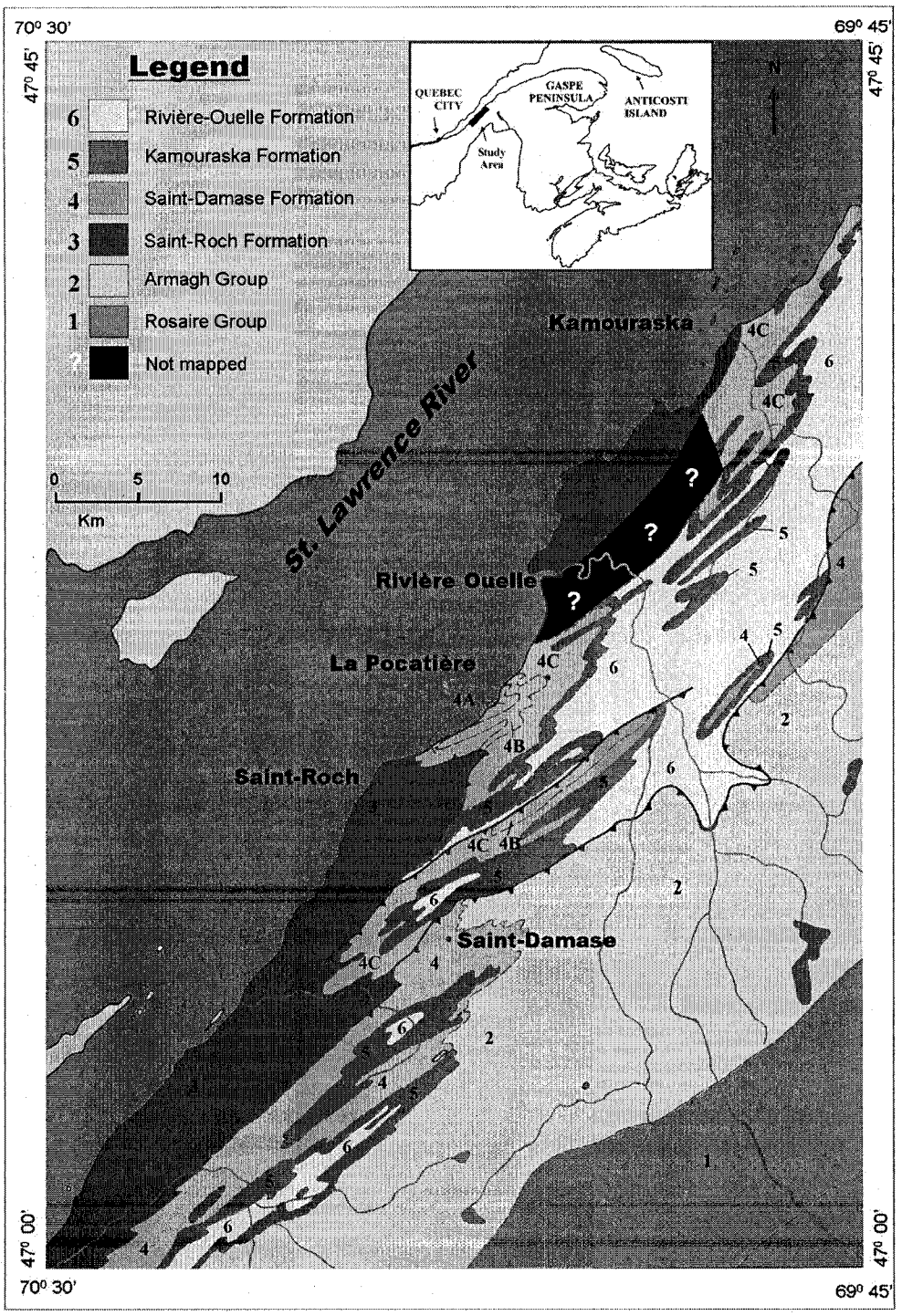

Figure 1: Geologic map of the study area in the L'Islet-Kamouraska region. Note that the Kamouraska Formation is exposed on the flanks of a succession of anticlines (after Hubert, 1973).

The main objective of this study pertains to the unique occurrence of quartz arenites in the deep sea. The focus is primarily on the mode of deposition of the quartz arenites of the Kamouraska Formation and their provenance including the depositional environment of the source area before the sands were redeposited in the deep sea. For this study the L'Islet - Kamouraska area of Hubert (1973) has been revisited. Field work was conducted in a 90 km stretch on the south shore of the St. Lawrence between the town of Cap-Saint-Ignace in the south (approximately at the boundary between Montmagny and L'Islet counties) and the village of Saint-André in the north (northernmost Kamouraska County), covering all occurrences of the Kamouraska Formation in the area (Fig. 1).

2. REGIONAL GEOLOGIC SETTING

The geological history of the area dates back to the opening of the Iapetus Ocean (590 Ma; according to evidence from Quebec) at the end of the Precambrian (Kamo et al., 1995). Evidence from rift-drift volcanic rocks in Western Newfoundland suggests multiple stages of magmatism ranging from 615 Ma (Kamo et al., 1989) to 555-550 Ma (Cawood et al. 1996, 2001). At that time, the newly formed basin attracted sediments from the surrounding areas and an Atlantic-type continental margin developed. The first sediments to fill the basin were earliest Cambrian rift volcanics interlayered with early rift-drift sediments (St. Julien and Hubert, 1975). As the basin evolved, passive margin sediments predominated from earliest Middle Cambrian until accretion and uplift in Middle Ordovician time (St. Julien and Hubert, 1975; Doolan et al., 1982; Sandford, 1993). Tectonism and sea-level changes played an important role in influencing the types of sediments present (James et al., 1989; Lavoie et al., 2003).

Two major structural events highlight the rise of the Appalachian Mountains: the Taconian Orogeny (late Middle to early Late Ordovician) and the Acadian Orogeny (middle to early Late Devonian). These events resulted in folding, nappe emplacement and dynamothermal metamorphism in the Quebec

Appalachians (St. Julien and Hubert, 1975). Towards the end of the Early Ordovician, the Atlantic-type continental margin of the Iapetus Ocean was converted into a west America-type convergent margin with the development of an east-dipping subduction zone. This resulted from the collision of a volcanic island arc with the continent in which both oceanic and continental rocks became imbricated in an accretionary wedge (Dewey and Bird, 1970; Osberg, 1978; Stanley and Ratcliffe, 1985; Cawood et al., 1995; Castonguay et al., 1997).

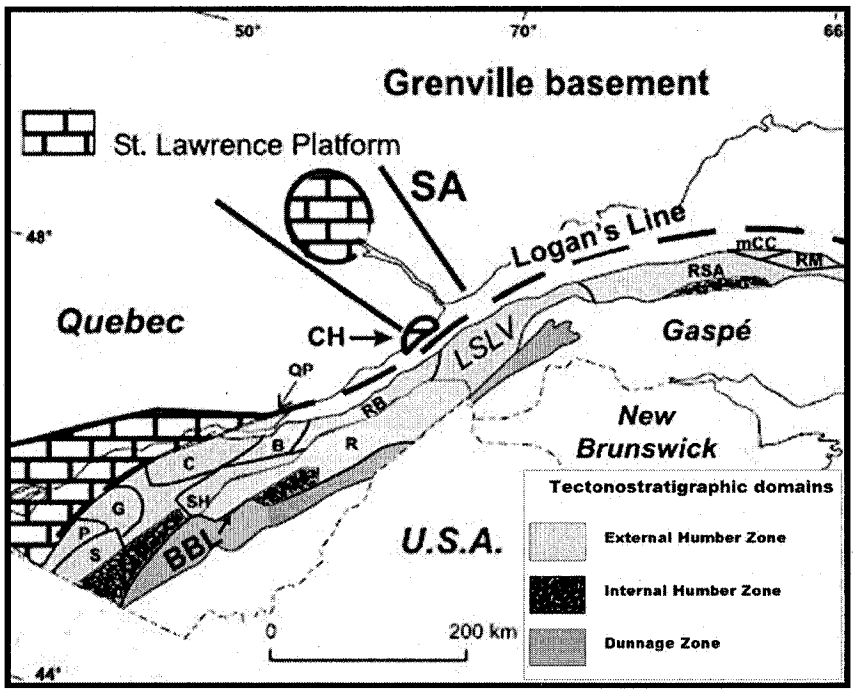

Figure 2: Tectonostratigraphic map of the Quebec Appalachians. CH = Charlevoix area; BBL = Baie Verte – Brompton Line; SA = Saguenay Graben. Nappes of the Humber Zone are S = Stanbridge; P = Philipsburg; G = Granby; SH = Sainte-Hénédine; LSLV = Lower St. Lawrence Valley Nappe; C = Chaudière; QP = Quebec Promontory; B = Bacchus; RB = Rivière Boyer; R = Richardson; RSA = Rivière Sainte-Anne; RM = Rivière Marsoui; mCC = Cap Chat mélange (modified after Lavoie et al., 2003).

Williams (1978, 1979) subdivided the Canadian Appalachians into five broad tectonostratigraphic zones. From west to east these are the Humber, Dunnage, Gander, Avalon and Meguma zones. In Quebec, only two of these exist; the Humber and Dunnage zones (Fig. 2). A third domain that occurs in Quebec is known as the Autochthonous-Parautochthonous Domain (St. Julien and Hubert, 1975), which comprises the Lower Paleozoic rocks of the St. Lawrence Platform.

The Humber Zone and the Autochthonous-Parautochthonous Domain record the development/destruction of an Atlantic-type continental margin, along with the evolution of the convergent-foreland basin (Williams and Stevens, 1974; St. Julien and Hubert, 1975; St. Julien et al., 1983; Lavoie et al., 2003). The Dunnage Zone represents remnants of the Iapetus Ocean with island-arc sequences and mélanges derived from oceanic lithosphere (Kean and Strong, 1975; St. Julien and Hubert, 1975; Pinet and Tremblay, 1995).

The Kamouraska Formation crops out in the Humber Zone. This zone is bordered to the west by the St. Lawrence Platform (Fig. 2). In Quebec, the western limit of the Humber Zone coincides with the westernmost transport of allochthonous thrust sheets (St. Julien and Hubert, 1975; Lavoie et al., 2003) referred to as Logan's Line (Fig. 2). West of Logan's Line the autochthonous sediments form the platform rocks. These rocks lie on the Precambrian Grenville basement and were weakly deformed and metamorphosed as they were marginally involved in tectonic stacking. A restricted frontal zone exists and was deformed during the Taconian orogeny. This marginal zone, known as the "parautochthonous" or "zone of imbricated thrust sheets", is characterized by a series of southeast-dipping thrust faults that result in imbricated slices of the southeastern part of the platform (St. Julien and Hubert, 1975; St. Julien, 1979; St. Julien et al. 1983; Castonguay et al., 2001). This frontal zone is rooted in the autochthonous St. Lawrence Platform and therefore not considered a part of the Humber Zone.

To the east, the Humber Zone is bordered by the Dunnage Zone (Fig. 2). The boundary is defined by a southeast-dipping thrust fault known as the Baie Verte - Brompton Line (Fig. 2), (St. Julien and Hubert, 1975, Williams and St. Julien, 1978; Williams, 1995). It is followed to the southeast by a steeply dipping structural belt (Williams and St. Julien, 1982) characterized by ophiolite occurrences that separate the Humber polydeformed schists to the northwest from the less deformed volcanic sequences of the Dunnage Zone to the southeast

(Williams, 1995).

The Humber Zone has a uniform width of about 100 km (Williams, 1995). It is divided into an internal and an external domain based on structural and metamorphic styles (St. Julien and Hubert, 1975; Pinet and Tremblay, 1995; Williams, 1995; Lavoie et al., 2003). In the external Humber Zone, the rocks are weakly deformed and metamorphosed. Deformation and metamorphism increase towards southeast in the internal Humber Zone. Stratigraphic and structural relationships become less clear. In Quebec, the deformed and metamorphosed rocks of the internal Humber Zone are thrust above the less deformed and less metamorphosed external Humber Zone.

The Humber Zone succession in Quebec is preserved in a number of distinct, stacked structural nappes (Fig. 2; Lebel and Kirkwood, 1998). The Kamouraska Formation is known to crop out in the Rivière Boyer, the Lower St. Lawrence Valley, and the Rivière Saint-Anne nappes (Fig. 2). Field work was restricted to the Rivière Boyer Nappe (Fig. 2), specifically in the L'Islet-Kamouraska area that was covered by Hubert (1973).

3. STRATIGRAPHY OF THE RIVIÈRE BOYER NAPPE

The oldest rocks that characterize the basal parts of the Rivière Boyer nappe do not crop out on the surface (Fig. 3). They have been primarily inferred from adjacent areas. The Montagne de Saint-Anselme Formation has been proposed to exist at the bottom of the Rivière Boyer Nappe (Vallières, 1984; Lebel and Hubert, 1995a; Lebel and Hubert, 1995b). This was based on exposures in the basal rocks of the adjacent Saint-Malachie area, south west of the Rivière Boyer Nappe, and the basal rocks of the Richardson Nappe, east of the Rivière Boyer Nappe (Vallières et al., 1978; Vallières, 1984). The Montagne de Saint-Anselme Formation is composed of volcanics intercalated with feldspathic arenites and conglomerates. A belt of aeromagnetic anomalies has been documented in the

Rivière Boyer Nappe and the Richardson Nappe (Relevés Géophysiques inc., 1978). This anomaly belt has been associated with the presence of a volcanic unit at a depth of 2000 m in the northwest and 2500 m in the southeast, representing a subsurface extension of the Montagne de Saint-Anselme Formation. The Montagne de Saint-Anselme Formation dates back to the latest Precambrian and has been associated with the opening of the Iapetus Ocean.

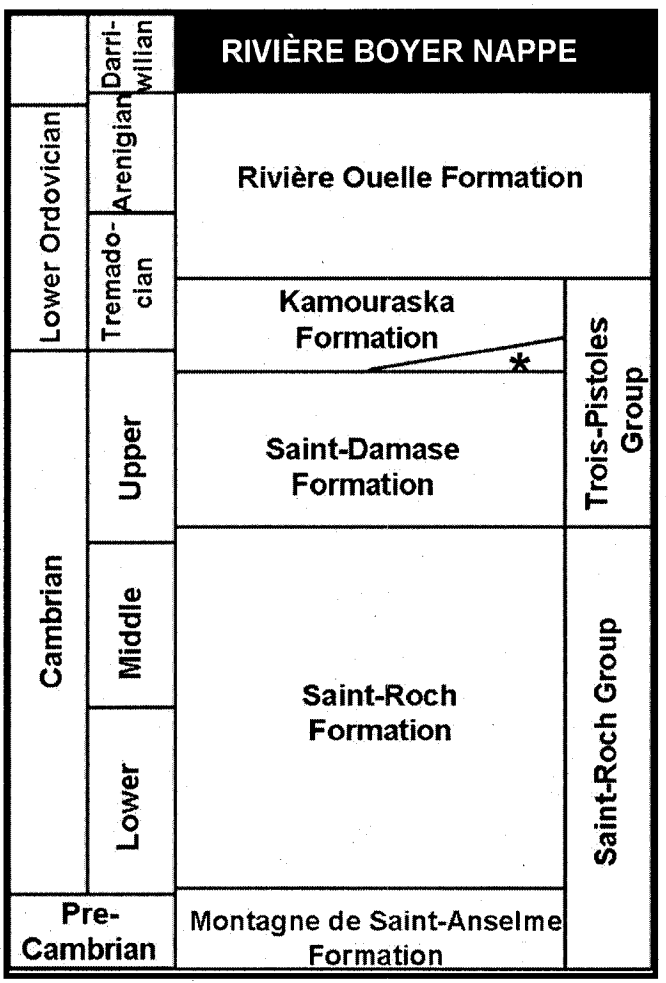

Figure 3: Stratigraphy of the Rivière Boyer Nappe. (*) = Rivière-du-Loup Formation (age correlation modified after Lavoie et al. 2003).

The basal rocks exposed on the surface are those of the Saint-Roch Formation (Hubert, 1973). These rocks overly the subsurface Montagne de Saint-Anselme Formation with their contact unexposed. The Saint-Roch Formation is a very heterogeneous unit composed of mudstone intercalated with bands of

conglomerate, feldspathic wacke, subarkose, siltstone, shale and limestone. Essentially, the formation is characterized by an alternation of fine intervals of pelitic red-green mudstone and coarse intervals of grey-green sandstone and conglomerate, at about equal proportions (Lebel and Hubert, 1995a). From the northeast towards the southwest, the coarse intervals of the sandstone and conglomerate increase gradually in thickness at the expense of the finer red mudstone intervals (Lebel and Hubert, 1995a). Lebel and Hubert (1995a) document three major thinning and fining upward cycles of massive feldspathic wacke which display a gradual upward increase in compositional maturity to subarkose.

Vallières (1984) elevated the status of the Saint-Roch Formation to that of a group. He noticed that the Saint-Roch Formation can be divided into two units in the Rivière-du-Loup area: the informal "green sandstone" unit (characterized by distinctive green sandstone and conglomerate), and the Orignal Formation (characterized by red and green shale). The informal "green sandstone" unit is a distinctive massive unit of feldspathic sandstones that owe their green color to the presence of 15-20% recrystallized chloritic matrix (Vallières, 1984). This unit can be traced for long distances from Québec City to Gaspé Peninsula (Lavoie et al., 2003) and is probably equivalent to the Charny Group (Rasetti, 1946; formerly known as the Sillery Formation - Logan, 1863) in the region of Quebec City (Vallières, 1984; Lavoie et al., 2003) and to other formations in different nappes of the Humber zone. The Orignal Formation overlies the informal "green sandstone unit" and is characterized by the widespread occurrence of laminated red, green and grey mudstone. Vallières (1984) grouped the subsurface Montagne de Saint-Anselme Formation, the informal "green sandstone" unit, and the Orignal Formation into one group, creating what is now known as the Saint-Roch Group in the Rivière-du-Loup area.

This promotion of the Saint-Roch Formation to group status has not been adopted by Lebel and Hubert (1995a) in the Saint-Raphael nor the L'Islet-

Kamouraska areas of the Rivière Boyer nappe. The reason for rejecting this proposal was because a top unit resembling the Orignal Formation has not been recognized in the Saint-Raphael or the L'Islet-Kamouraska areas. Instead, the top of the Saint-Roch Formation resembled more the beds of the overlying Saint-Damase and Rivière-du-Loup formations of the Trois-Pistoles Group (Lebel and Hubert, 1995a). However the "group" designation has been adopted by many workers (e.g., Lavoie et al., 2003) and this usage is followed here (Fig. 3).

The St. Roch Group has been interpreted as a deep marine deposit (Hubert, 1973; Lajoie, 1979) that was laid down on the Cambrian continental rise-basin plain complex, in part by turbidity currents (Strong and Walker, 1981; Lebel and Hubert, 1995a). Trilobite fragments recovered from the lower parts of the Saint-Roch Group indicate a Lower Cambrian age (Hubert, 1965). The palynological analysis of the green mudstone within the "green sandstone" unit revealed the presence of late Early to early Middle Cambrian achritarch assemblages (Appendix A in Burden, 2001). The upper contact of the Saint-Roch Group is transitional with the Saint Damase Formation (Lebel and Hubert, 1995a). The Saint Damase Formation has been dated as Upper Cambrian (Hubert, 1965), hence placing the age of the top of Saint-Roch Group at the boundary between Middle and Upper Cambrian (Fig. 3).

The Trois-Pistoles Group overlies the Saint-Roch Group. Vallières (1984) applied the term Trois-Pistoles Group to the threefold Upper Cambrian/lowermost Ordovician rock assemblage of the coarse-grained basal Saint Damase Formation, the fine-grained middle interval of the Rivière-du-Loup Formation, and the coarse-grained upper Kamouraska Formation (Fig. 3). This threefold assemblage is well established in the Rivière-du-Loup area (Vallières, 1984). In the L'Islet-Kamouraska area (study area) this threefold assemblage is less clear because the fine-grained middle interval of the Rivière-du-Loup Formation is limited to a maximum of 15m (Hubert, 1973). In the Saint-Raphael area (south of study area) the Rivière-du-Loup Formation is entirely absent (Lebel and Hubert, 1995a).

The Saint Damase Formation is characterized by thick graded feldspathic arenites and polymictic limestone conglomerates. In the L'Islet-Kamouraska area, the Saint Damase Formation is divided into three members (Hubert, 1973): A lower feldspathic arenite member (Des Aulnaies Member), a middle lenticular quartz arenite member (La Pocatière Member) and an upper feldspathic arenite member (Saint-Anne Member). These divisions were only identified in the L'Islet-Kamouraska area and are absent in other areas. The rocks of the Saint Damase Formation are of early Late Cambrian age (Rasetti, 1946) and have been interpreted as turbidites (Hubert, 1973).

The thin pelitic unit in the L'Islet-Kamouraska area which is an extension of the Rivière-du-Loup Formation (Fig. 3) thins from 200 m in the Rivière-du-Loup area to 15 m in the south (Vallières, 1984). Palynological analysis of the Rivière-du-Loup Formation gives a latest Cambrian-earliest Ordovician age based on achritarchs (Appendix A in Burden, 2000).

The Kamouraska Formation which overlies the Rivière-du-Loup Formation (Fig. 3) consists of thick and massive quartz arenite beds and a basal horizon of polymictic limestone conglomerate. Shale and siltstone interbeds rarely separate the quartz arenite beds. The formation will be described in detail in subsequent sections of the thesis.

The Kamouraska Formation is topped by varicolored shales and siltstones of the Rivière-Ouelle Formation (Fig. 3). Sandstones, ribbon limestones, calcarenites and limestone conglomerates are locally abundant. The Rivière-Ouelle Formation is of Early Ordovician age based on Late Tremadocian to Arenigian graptolite and chitinozoan assemblages (Riva, 1972; Landing and Benus 1985; Lebel and Hubert, 1995a). The uppermost parts of the Rivière-Ouelle Formation have been dated by graptolites (Maletz, 1992, 2001; Lebel and Hubert, 1995a) and by an assemblage of Middle Ordovician chitinozoans found at Les Méchins on the northern shore of Gaspé Peninsula (Asselin et al., 2004). The

Rivière-Ouelle Formation consists of deep-sea shale (Hubert, 1973) possibly deposited on the slope or the continental rise.

4. FIELD OBSERVATIONS

In the study area, the Kamouraska Formation crops out in a series of hills and linear ridges which trend in the northeast-southwest direction. These ridges are the most prominent morphological features in the area and appear to be stripped off their overlying cover of the less resistant shale of the Rivière Ouelle Formation.

4.1 Measured Sections

Three detailed stratigraphic sections have been measured in the Kamouraska Formation (Fig. 4). Sections 1 and 2 were measured in the town of Saint Pacôme and show the best exposure of the quartz arenites. The third section was measured in the vicinity of Saint-Philippe-de-Néri along Highway 20. The detailed measured sections do not include the conglomerates because of the lack of continuous outcrops. Sections 1 and 2 are road cuts on opposite sides of Boulevard Bégin at Saint Pacôme and are easy to correlate because they are only 15 m apart. They were not combined in one section in order to document short-distance lateral thickness and petrographic variations. Section 3 is 11 km away from sections 1 and 2 and cannot be correlated with them. Sections 1 and 2 combined reveal the presence of the following 6 stratigraphic intervals.

Section 1 starts with a basal fine grained, relatively thin-bedded interval (Interval 1), 8m thick that contains massive beds of sandy mudstone with laminated shale lenses. This facies is interpreted as slump units that contain lenses of laminated shale. The facies is extremely rare in the Kamouraska Formation and was only encountered in this outcrop. The slumps are interrupted by thin massive beds of clay-rich fine-grained sandstone markedly different in color and clay content from the quartz arenites of the Kamouraska Formation.

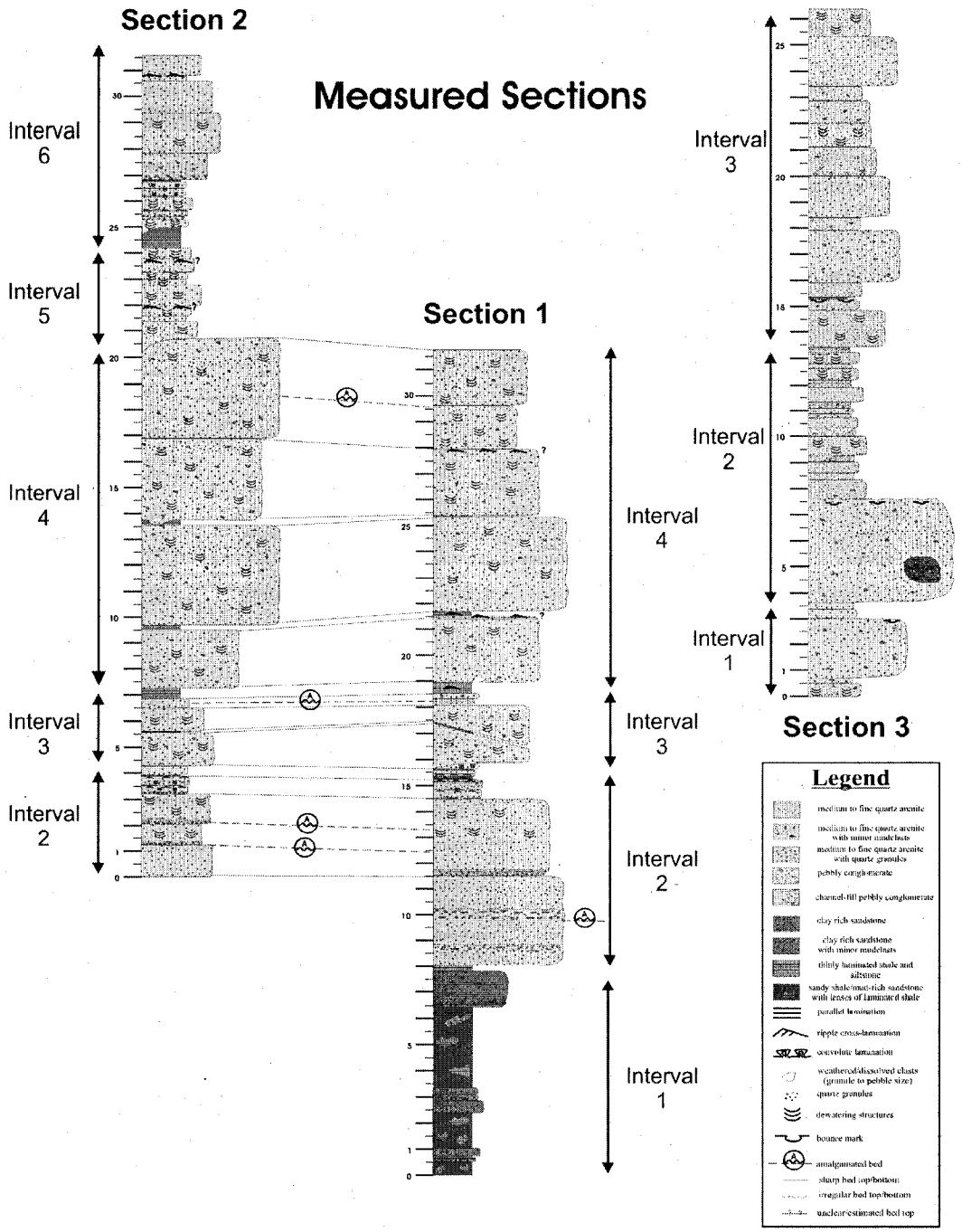

Figure 4: Sections 1 and 2 were measured in the town of Saint Pacôme, on the south and north sides of Boulevard Bégin, respectively, between Rue King and Rue du Moulin. Section 3 was measured in the vicinity of Saint-Philippe-de-Neri, along Highway 20 West, 1km east of exit 456 to Saint-Philippe-de-Neri.

These sandstone beds show an abundance of mudclasts.

Overlying Interval 2 displays the typical grayish and massive quartz arenite beds (Fig. 4). The basal bed of amalgamated sandstone and pebbly sandstone is 3.50 m thick. Primary structures such as ripple lamination at top of beds appear in the thinnest beds. Dewatering structures abound.

Interval 3 cuts erosively into the top of Interval 2. Two 1-2 m thick beds are lenticular compensating each other in thickness laterally and are separated by a thin shale bed. Abundant dewatering structures are present in the thicker beds and ripple cross-laminations at the top of thin beds at the uppermost part of the interval.

Interval 4, at the top of section 1 is almost 12 m thick consisting of thick quartz arenite beds which may be separated by thin shale interbeds. The massive beds display abundant dewatering structures.

Section 2 begins with the top portion of interval 2. Correlation between sections 1 and 2 reveals that some thick beds are amalgamated and split into two or more beds on the opposite side of the road cut.

Interval 5 shows basal scouring by a small channel chute or gully into the top parts of Interval 4, and is characterized by thinner beds. The depth of the gully (comprising all beds of interval 5) does not exceed 3.5 m with a width of 8m. Interval 5 is topped by brown shale.

The lowest quartz arenite of Interval 6 cuts into the underlying shale bed at the base of this interval. The interval is characterized by thin quartz arenite beds in its lower part and increasing bed thickness upwards. Dewatering structures are abundant.

Section 3 reveals a sequence of massive quartz arenites with rare shale interbeds. Three main intervals have been recognized in this section. Interval 1 shows massive quartz arenite beds with randomly scattered mudclasts. Some show minor scattered carbonate granules.

Interval 2 begins with a giant 4-meter bed and is followed by a set of thinning and fining upwards quartz arenite beds. A boulder (1 meter in diameter) composed of mudstone containing bladed siltstone fragments occurs in the lower half of the bed. The boulder could have been dislodged from a channel wall during the deposition of the thick bed. The thin beds that follow commonly reveal dewatering structures. Mudclasts and frequently carbonate clasts were found randomly scattered within the beds. Pebbly conglomerates were observed in two beds in this interval. In one of the beds, the pebbly conglomerate is laterally replaced by clean quartz arenite. This bed is overlain by clean quartz arenite which is overlain by a similar pebbly conglomerate bed.

Interval 3 is characterized by quartz arenite beds of medium thickness (1-2 m). Dewatering structures abound. Scattered mudclasts and carbonate granules/ pebbles have also been observed.

4.2 Lithology and sedimentary structures

The Kamouraska Formation consists of three main lithologies: 1) quartz arenite (orthoquartzite), 2) conglomerate, and 3) subordinate shale and siltstone. Quartz arenite is the dominant lithology. The shales and siltstones appear as thin horizons separating some of the quartz arenite beds. The conglomerates are found in the basal parts of the Kamouraska Formation and are interbedded and frequently amalgamated with the quartz arenites.

4.2.1 Quartz arenite (orthoquartzite).--- The quartz arenites range in color from light grey and white to beige and dark grey. They are characterized by thick and

massive beds with a sheet-like geometry and average thicknesses of 1 m (Fig. 5A). Individual beds can reach a thickness of more than 4m and are frequently amalgamated with underlying and/or overlying beds. Some beds are lenticular (Fig. 5B). Grain size ranges from medium to fine sand. Disk shaped mudclasts are frequently encountered in the beds; however they don't amount to more than 1% of the bed volume (Fig. 6A). The mudclasts are usually granule- to pebble-sized; very few cobble-sized mudclasts have been found. Minor randomly scattered carbonate pebbles and granules were also observed (dominantly calcisiltite and calcilutite fragments).

Subtle grading exists in the quartz arenite beds, however it is often hard to decipher in the field due to the good sorting and the pervasive silica cementation. In the field, grading is best demonstrated by the concentration of pebble-sized mudclasts, carbonate clasts or granule-sized quartz grains at or near the base of some beds (Figs. 6B, C). Scouring at the base of the quartz arenite beds is usually in the order of 5-20 cm and is often associated with a basal lag (2-3 cm thick) of quartz granules (Fig. 6B) which is massive or reversely graded. Flute and grove casts at the base of some beds gave paleocurrent directions indicating flow to the southwest and southeast in line with observations of Hubert (1973).

The most abundant sedimentary structures in the quartz arenite beds are dewatering structures (Fig. 7). These include dish structures, type A pillars, type B pillars, type D stress pillars and consolidation lamination (Fig. 7; following the terminology of Lowe 1975).

Dish structures may be hard to detect in outcrop; however, cut and varnished samples show these structures clearly (Fig. 7A). They are usually widely spaced and less numerous towards the base but decrease in size and increase in number towards the top of beds. Type A pillars represent vertical or inclined pipes of water escape and are associated with dishes (Figs. 7A, B) and do not exceed more than a few centimeters in length.

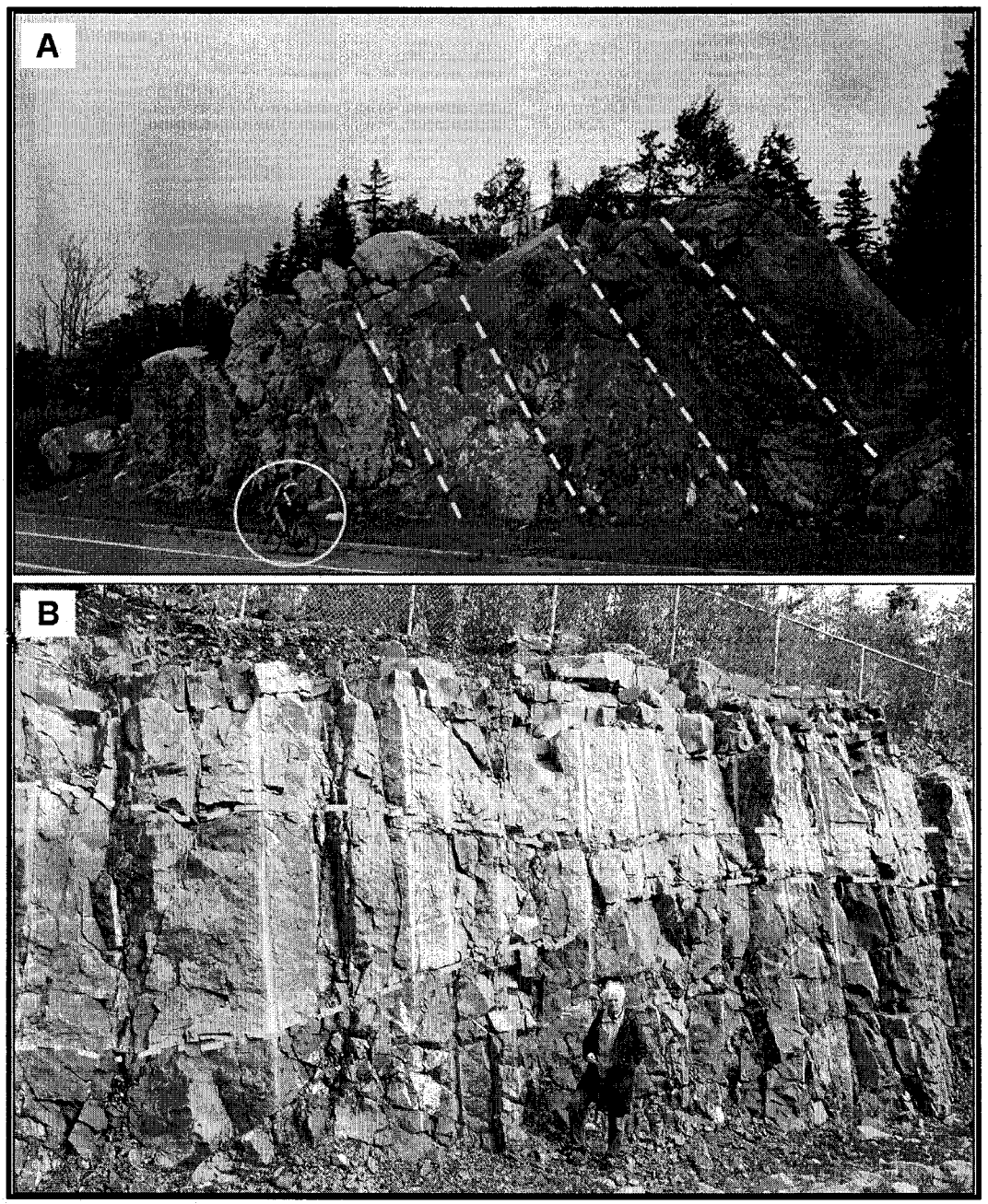

Figure 5: A) Thick and massive quartz arenite beds with a sheet-like geometry (Rue Centrale, Saint Pascal). B) Massive lenticular quartz arenite beds (Boulevard Bégin, Saint Pacôme).

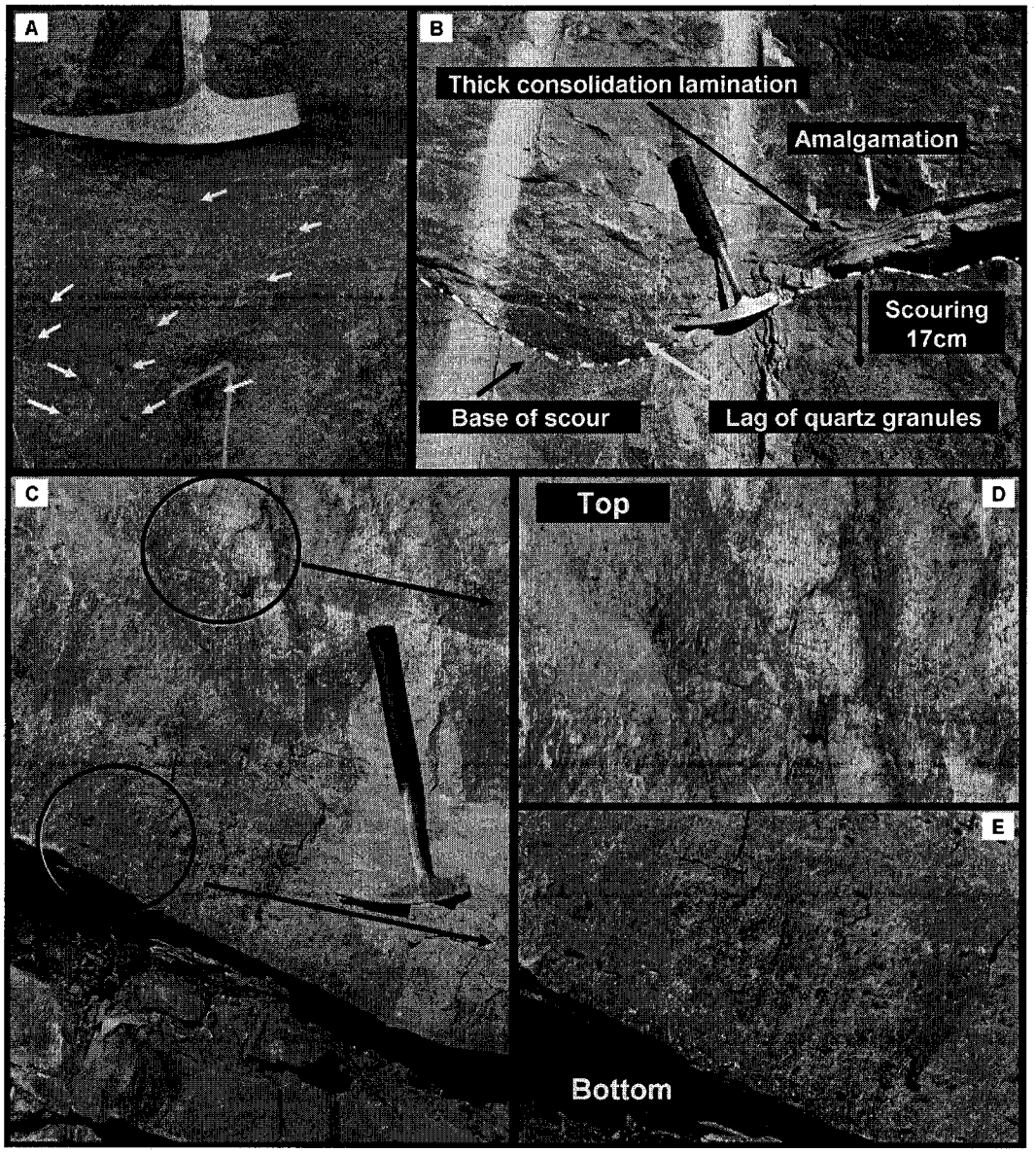

Figure 6: A) Randomly scattered granule- and pebble-sized mudclasts. B) Basal scour and concentration of quartz granule lag. The scour is 17cm deep. The thick bed is amalgamated with an underlying thinner bed, which shows thick dark, wavy and discontinuous consolidation laminations (see text). C) Graded bed showing concentration of quartz granules and granule- to pebble-sized mudclasts at the bottom of bed (Boulevard Bégin, Saint Pacôme). D) and E) Close-ups of C).

Type B Pillars are individual pillars unrelated to dish structures. They are often larger than the type A pillars and can occur vertically (discordant) or horizontally (concordant). They appear as zones of homogeneous or faintly structured sand (Lowe, 1975); sometimes showing irregular patches of clean sand (Fig. 7B). Others show simple funnel shapes of water escape (Fig. 7C). They usually form above zones of water escape in underlying layers (Lowe, 1975). Type B pillars were frequently observed to form parallel to stratification as these may be zones of highest permeability. Vertical type B pillars have also been observed (Fig. 7C). Type B pillars usually form vertically or steeply inclined zones in cross-bedded sediment (along zones of highest permeability) or in axes of anticlinal convolute lamination; however, they could also form vertically when fluid escape velocities are exceptionally high and the escaping fluid faces little resistance from the overlying permeable sediment (Lowe, 1975) as is the case in the quartz arenites of the Kamouraska Formation.

Type D stress pillars have been observed in some quartz arenite beds. They appear as series of lighter-colored vertical irregular streaks (near-perpendicular to bedding) and are regularly spaced (4-7 cm; Fig. 8A, B). Mineralogy within the type D stress pillars is similar to that of the surrounding rock (dominated by quartz with quartz overgrowth); however it differs from the surroundings by the near-absence of the darker clay cement/matrix. Grains with their long axis oriented perpendicular to bedding have also been observed in the stress pillars. Type-D stress pillars develop in sedimentary layers which have undergone soft sediment hydroplastic flowage (Lowe, 1975; hydroplastic flow is associated with grain-supported sediments having significant yield stress and pore-fluid velocities below those required for fluidization). In other words, these stress pillars appear to represent partial sediment fluidization along flow paths which develop within sediment undergoing hydroplastic shear (Lowe, 1975). This structure may form due to an earthquake at a time after deposition but before consolidation.

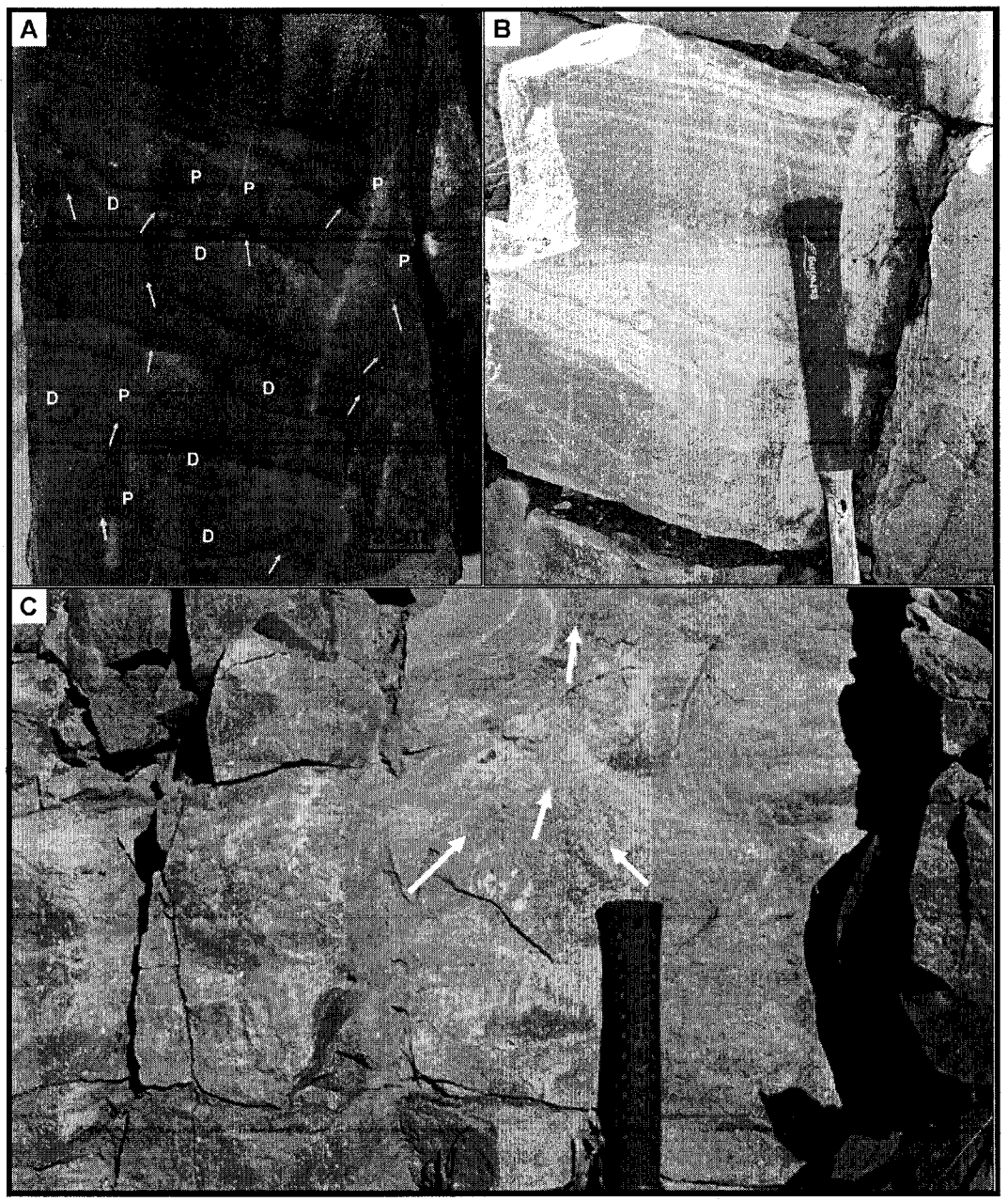

Figure 7: Cut and varnished rock showing dish structures (D) and associated type A pillars (P). Arrows indicate water escape routes. Note the presence of two vertical fractures rehealed by silica cement (light colored). B) Horizontal to inclined type B pillar associated with a fluidization channel. It appears as zone of homogeneous or faintly structured sand showing irregular patches of clean sand. Length of blue hammer handle 18.5 cm (Section 2, Boulevard Bégin, Saint Pacôme). C) Vertical, funnel-shaped type B pillar indicating water escape. The feature is not associated with dish structures. Arrows indicate water escape routes. Length of hammer handle 18.5 cm (Boulevard Bégin, Saint Pacôme).

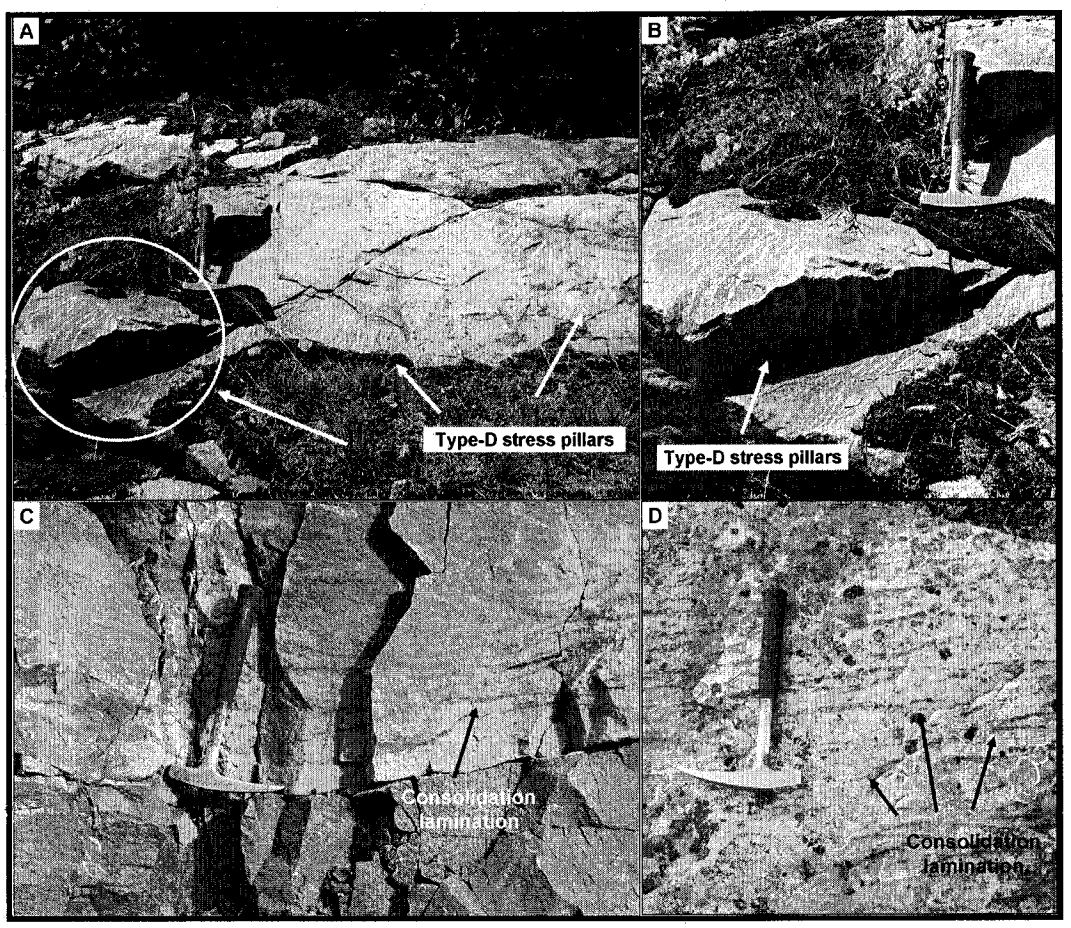

Figure 8: A) Outcrop showing type D stress pillars on top and side of bed (indicated by arrows). B) Close-up of circled area in A. Type D stress pillars appear in series of lighter-colored, narrow, vertical and irregular streaks that are regularly spaced (4-7 cm apart). Locality: Chemin du Tour-du-Lac-Trois-Saumons, Saint Aubert. C) Consolidation laminations: These are dark, diffuse and discontinuous water escape routes following zones of maximum permeability parallel to bedding (Section 2, Boulevard Bégin, Saint Pacôme). D) Thick consolidation laminations in a quartz arenite bed (Highway 132, 700 m south of intersection with Route Saint-Germain, Kamouraska).

The most abundant dewatering structures observed are consolidation laminations. These are the simplest water escape structures. They appear as fine and generally dark laminations (Fig. 8C, D). They may be faint, discontinuous and slightly wavy. They have been dominantly observed towards the bottom of beds. These horizontal flow paths form beneath impermeable or semi-permeable laminations (Lowe, 1975) or beneath a less permeable sediment plug. Subsidence associated with the central parts of consolidation laminations may give rise to dish

structures (Lowe, 1975). The dark color of consolidation laminations is due to hydrodynamically mobile material (clay and migrabitumen) which used the laminae as corridors to migrate into the rock and line the walls of the fluidization channels. The accumulation of heavy minerals at the base of fluidization channels often contributes to the production of pronounced dark laminations.

The tops of some massive quartz arenite beds show a thin ripple-laminated division. This division usually does not exceed 2-3 cm in thickness (Fig. 9) and consists of fine or very fine sand. Rarely, rippled bed tops have been observed (Fig. 9B). Some beds show a massive base followed by parallel lamination and topped by a 2-3 cm ripple-laminated division characteristic of Bouma divisions Ta, Tb, and Tc (Fig. 9C). Convolute lamination exists but is not common in the quartz arenites of the Kamouraska Formation. Few paleocurrent directions measured from rippled tops indicate flow to the south east.

4.2.2 Conglomerate.--- A monomicitic/polymicitic conglomerate horizon exists at the base of the Kamouraska Formation and displays a distinctive black to dark brown, sometimes beige weathering color. The conglomerate beds are thick and lenticular, commonly exceeding 1 m, and reaching a thickness in excess of 7 m in the northernmost parts of the study area. The conglomeratic horizon forms several lense-shaped bodies (based on section correlations by Hubert, 1973) and thins from northeast to the south, southwest and southeast. Clasts are dominantly rounded. Some bladed or elongate clasts have been observed and these are usually imbricated. Clast size varies from pebble to cobble size. Boulder size clasts exist but are rare and restricted to the northernmost parts of the study area. Rare beds of pebbly sandstone exist and are composed of small pebbles. The pebbly sandstone may show normal grading (Fig. 10A) and have been dominantly encountered in the southern parts of the study area.

The conglomerates have different clast compositions. Some conglomerate beds are exclusively made up of limestone clasts (monomicitic conglomerate).

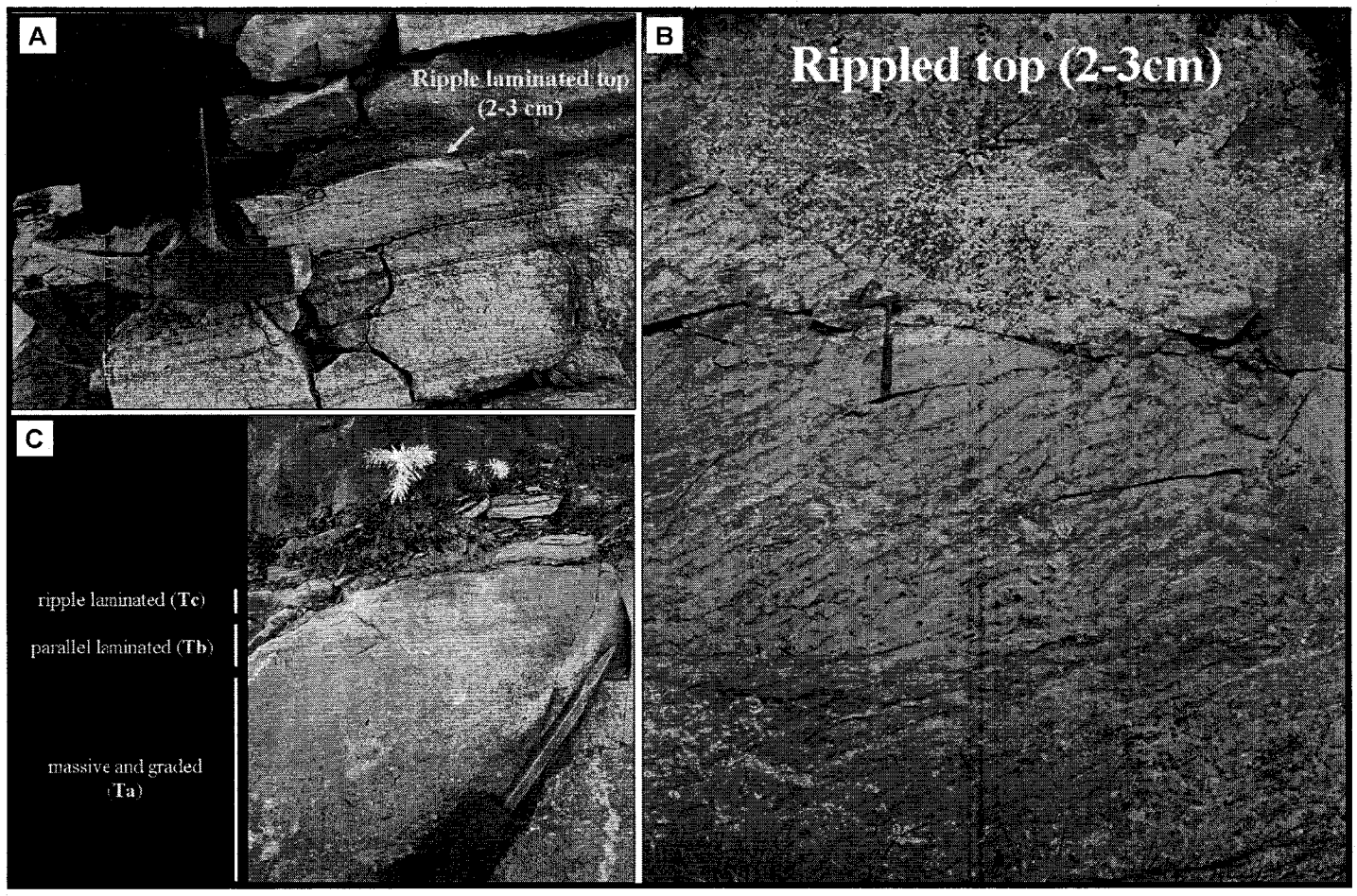

Figure 9: A) A bed with a thin ripple-laminated top (2-3cm); (Boulevard Bégin, Saint Pacôme; height of hammer head is 2.5 cm). B) Plane view of bed with low-amplitude ripples (2-3 cm); (Highway 230, 1.2 km northeast Chemin du Haut-de-la-Rivière, Rivière Ouelle; hammer for scale). C) Graded quartz arenite bed with Bouma Divisions T_{abc}; (Section 1, Boulevard Bégin, Saint Pacôme; metal part of chisel is 17 cm).

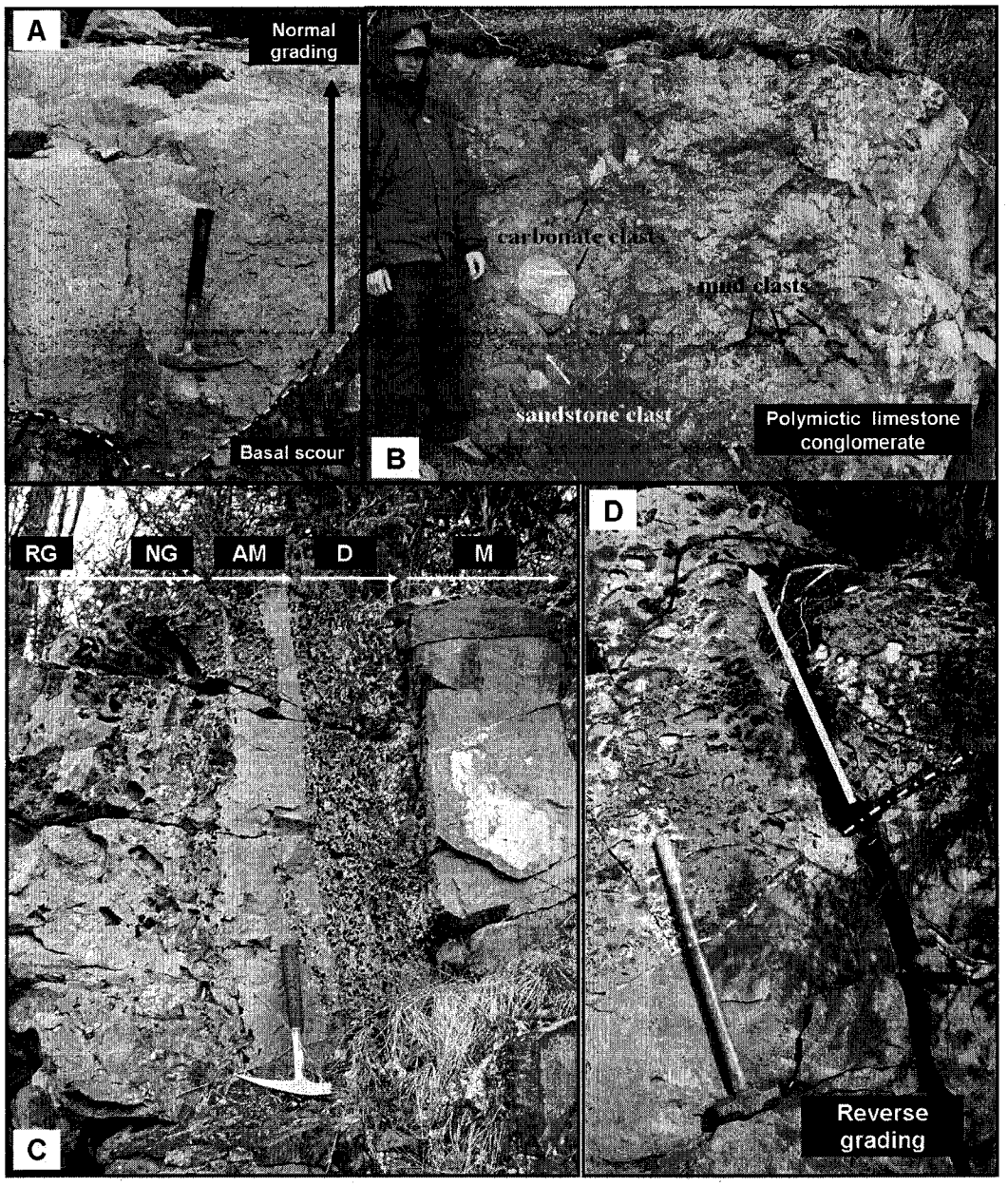

Figure 10: A) Pebbly sandstone bed grading into sandstone. The bottom of the bed shows scouring. The bed is composed of a high percentage of small pebbles that have been entirely dissolved. The bed grades into medium to fine quartz arenite (Range de-la-Canelle, Saint Pacôme). B) Thick bed of polymicitic limestone conglomerate composed of pebbles and large cobbles (Chemin des Sables east of intersection with Rue Dionne, Saint Philippe-de-Neri). C) Steeply dipping beds; from left to right shows reverse- to normally-graded (RG to NG) limestone conglomerate, followed by amalgamated quartz arenite and pebbly conglomerate (AM), overlain by disorganized pebbly conglomerate (D), and topped by massive quartz arenite (M). Also note dissolution of limestone clasts (Highway 230, 0.5 km south of Rivière Ouelle Junction, Saint Pacôme). D) Thick amalgamated quartz arenite and conglomerate. The conglomerate is reversely graded and characterized by large cobble sized clasts. Also note carbonate clast dissolution (Chemin Mississipi, Saint-Germain).

Mud clasts and sandstone clasts may co-exist with the limestone clasts (Fig. 10B, polymicitic conglomerate); however, in all cases, the limestone clasts dominate. Limestone clasts are dominantly calcisiltite and calcilutite; however calcarenite and calcirudite are also present. The conglomerate beds are usually disorganized (Fig. 10C), but may be reversely graded (Figs. 10C, D). Some beds show reverse grading at the base followed by normal grading towards the top (Fig. 10C); however, disorganized and reversely graded conglomerates dominate. The conglomerate beds are usually interbedded with quartz arenites and commonly amalgamated with these (Figs. 10 C, D). In the distal direction towards south, the conglomerates become better sorted and decrease in average and maximum grain size (Hubert, 1973). In pockets within the conglomerate horizon the carbonate clasts commonly underwent dissolution (Figs. 10C, D). The quartz arenites in proximity to the conglomerate beds may be partly carbonate cemented suggesting that the dissolved carbonate clasts may have provided the cement to the adjacent quartz arenites (see below; Figs. 10C, D).

4.2.3 Shale and siltstone.--- Rare shale and siltstone beds occur as thin intervals separating some of the quartz arenite beds. They usually range between 5 and 15 cm in thickness rarely exceeding 50 cm. Their color ranges from grey and black to brown and green. The siltstones are dominantly parallel laminated and less commonly ripple laminated. Lenticular shale pockets or discontinuous shale beds exist in the Kamouraska Formation (Fig. 11) and appear as erosional remnants sandwiched between the quartz arenite beds. In very rare instances, some of the thicker shale and siltstone beds show evidence of slumping (Fig. 12). These are characterized by a sandy texture (sandy shale/mud-rich sandstone), absence of lamination and presence of remnant parallel laminated shale pockets (Fig. 12).

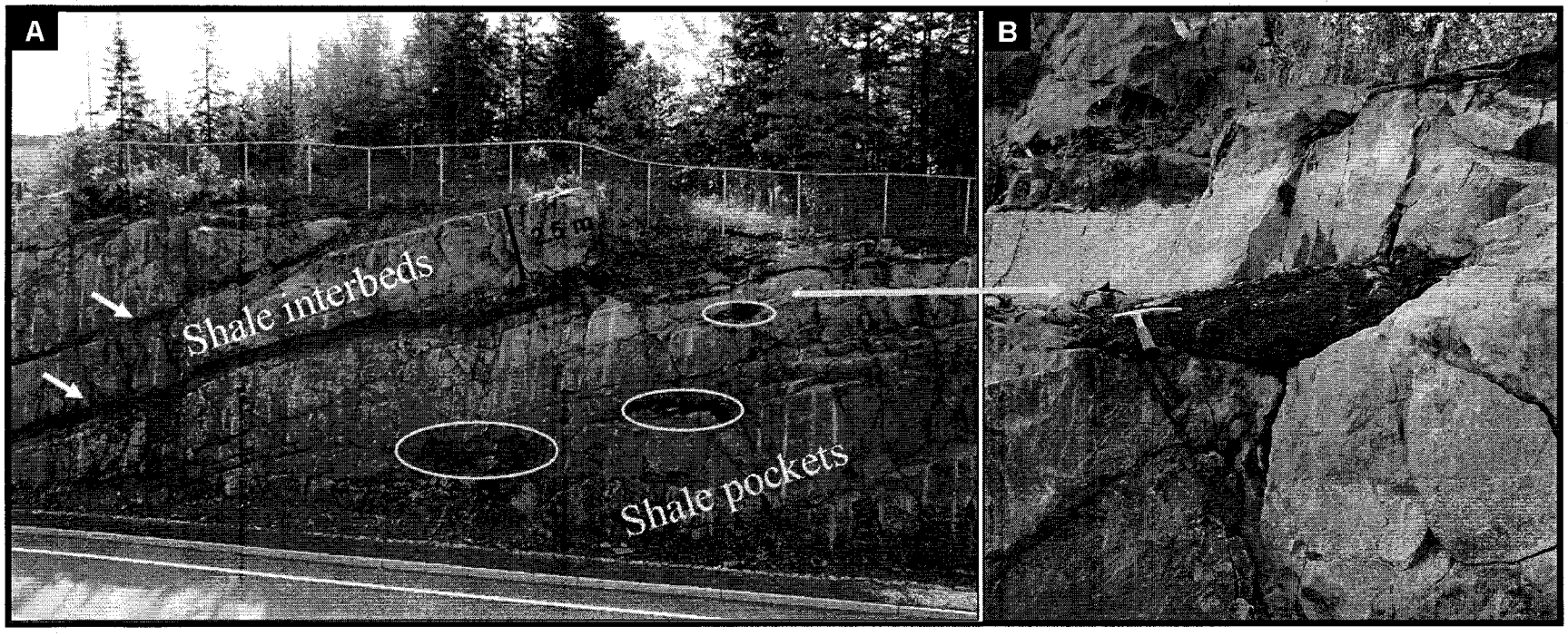

Figure 11: A) Massive quartz arenite beds and intercalated thin shale and siltstone beds (white arrows). Shale pockets are indicated by ellipses and represent remnants of shale beds that have been eroded in the process of the quartz arenite deposition. B) Close-up of one of the shale pockets (Section 1, Boulevard Begin, Saint-Pacôme).

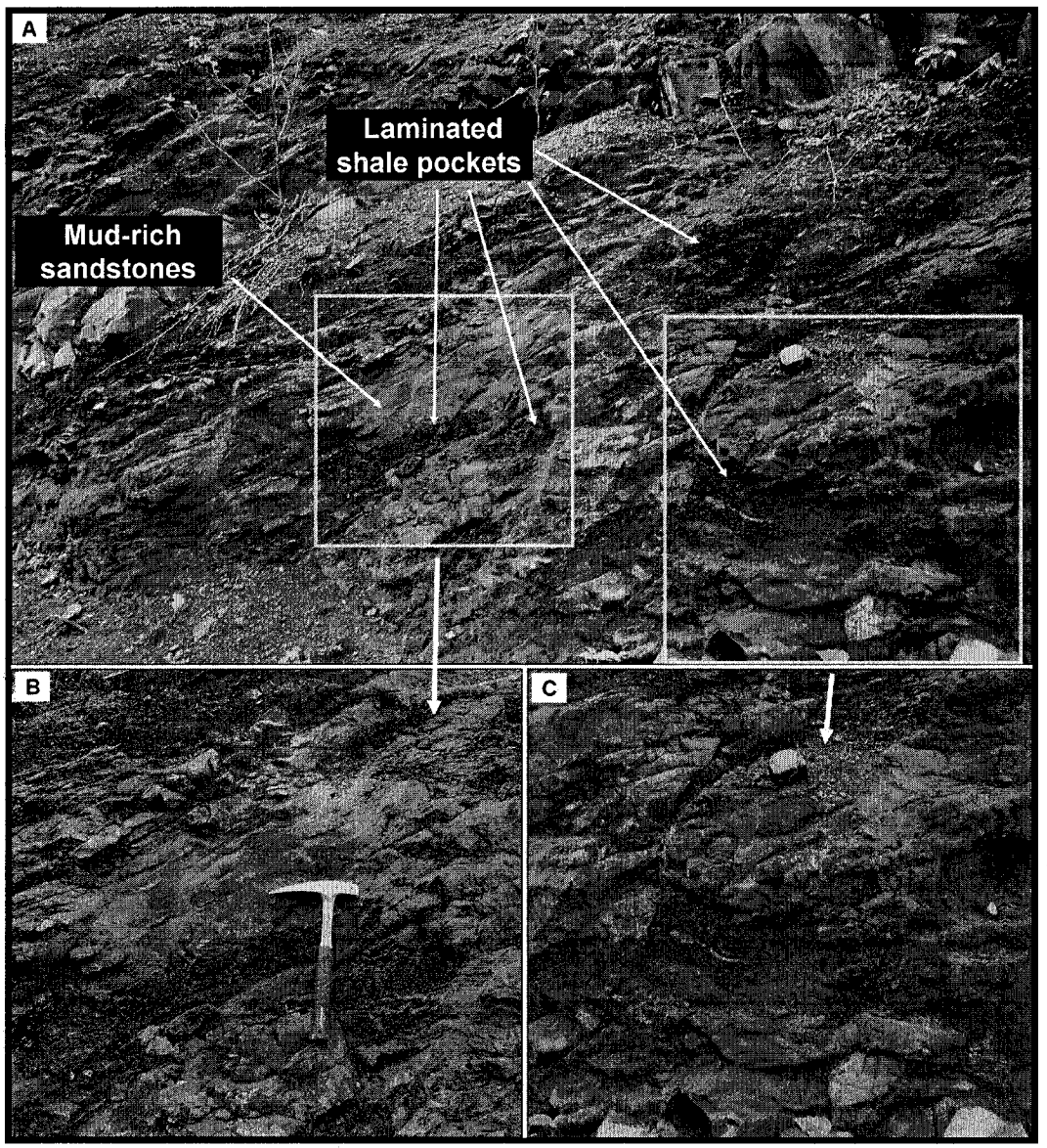

Figure 12: A) Thick mudstone unit characterized by massive sandy shale/mud-rich sandstone containing lenses of parallel laminated shale. These massive mud-rich beds are interpreted as slumped deposits that retain some undeformed sediment as parallel laminated shale lenses (measuring tape for scale). B) and C) show close-up of parallel laminated shale lenses in massive sandy shale/mud-rich sandstone(measured Section 1, Boulevard Begin, Saint-Pacôme, measuring tape for scale).

5. AGE OF THE KAMOURASKA FORMATION

The only fossils recovered from the Kamouraska Formation come from limestone clasts of the basal conglomerates that contain Upper Cambrian trilobites (Hubert, 1973). However these fossils give only a maximum age for the Kamouraska Formation as they provide the age of the clasts and not the age of the conglomerate, and the true age would be younger. Hubert (1973) assigned an Early Ordovician age to the Kamouraska Formation.

An attempt was made to date the Kamouraska Formation by palynological analysis of interbedded shale horizons. A total of 36 shale samples were acquired from shales underlying and overlying the formation and from within. The organic matter extracted from all 36 samples did not yield any faunal elements. However, palynological analysis of the underlying Rivière-du-Loup Formation indicated a latest Cambrian-earliest Ordovician age (Appendix A in Burden, 2000); and palynological analysis of the overlying Rivière-Ouelle Formation yielded Late Tremadocian to Arenigian graptolite and chitinozoan assemblages (Riva, 1972; Landing and Benus 1985; Lebel and Hubert, 1995). Since the Kamouraska Formation conformably overlies and underlies the Rivière-du-Loup and the Rivière-Ouelle formations, respectively, the Kamouraska Formation is likely earliest Ordovician age; with a possible range from latest Cambrian to earliest Ordovician (middle Tremadocian).

6. PETROGRAPHY

6.1 Quartz-arenite

The petrographic study focused on the quartz arenites that dominate the formation using 56 thin sections. Samples were collected from either tops or bottoms of beds, and when possible, from both top and bottom. The thin sections were

stained with blue epoxy for porosity. Carbonate cemented samples were stained with alizarin-red S and potassium ferricyanide for differentiating calcite and dolomite and detecting Fe-rich calcite and dolomite, respectively. Grain counting following the Gazzi-Dickinson counting method was performed on 40 thin sections (Table 1). Around 400 grains were counted per thin section on an equal-spaced grid.

Quartz dominates all samples with an average of 96. 8%. The feldspars combined average around 1% (Table 1). Potash feldspars and plagioclase are approximately of equal proportions in the formation as a whole. Microcline is the dominant potash feldspar with subordinate perthite and orthoclase. Plagioclase ranges dominantly from albite to oligoclase. Lithic fragments, namely mud clasts, limestone clasts, polycrystalline quartz, chert, plus mica and heavy minerals (zircon, tourmaline and garnet) amount to 2.2 % on average. Polycrystalline quartz and chert average 0.7%. Heavy minerals and mica are present in trace amounts. These petrographic results are comparable to those of Hubert (1973) and Lebel and Hubert (1995a). However, results form the Saint-Raphael area (Lebel and Hubert, 1995a) show slightly higher feldspar concentrations. Furthermore, Lebel and Hubert (1995a) additionally documented the presence of massive subarkose beds within the Kamouraska Formation in the Saint-Raphael area. Subarkose is very rare to absent in the L'Islet-Kamouraska area.

The quartz arenites are pervasively silica-cemented (Fig. 13A). This phenomenon is almost ubiquitous to the quartz arenites within the Kamouraska Formation. The presence of quartz overgrowths obscures the true original grain-size and shape unless dust rims or fluid inclusions permit viewing the boundary between the detrital grains and the syntactic quartz overgrowth (Fig. 13A). The original grain shapes are dominantly well rounded. This is especially true for the coarser grains. As grain size decreases the grains become more sub-rounded.

Carbonate cement is present in some samples (Fig. 13C); however silica

Table 1: Point counting data from thin sections. The symbols used are as follows: Q - all quartz grains, both monocrystalline and polycrystalline, including chert; Q_m - monocrystalline quartz; Q_p – polycrystalline quartz; F - all feldspar grains; L - all lithic fragments without Q_p; L_t - all lithic fragments; M - matrix; SL refers to sandstone sublithologies described in text.

Petrographic data of the sandstones of the Kamouraska Formation									
Sample Number	%Q	%Qm	%QP	%F	%L	%Lt	%M	Sorting	SL
PM230505-I-1	99.3	99	0.3	0.2	0.6	0.9	1	Well	1
PM230505-I-2	99.4	99	0.4	0.1	0.5	0.9	2	Moderate	2
PM230505-I-4	98	97.8	0.2	0	2	2.2	3	Well	1
PM230505-I-5	98.6	98.4	0.2	0	1.4	1.6	1	Moderate	2
PM240505-I-6	96.6	96.3	0.3	1.8	1.6	1.9	4	Moderate	4
PM240505-I-9	96.7	96.3	0.4	2.2	1.1	1.5	2	Moderate	2
PM250505-I-10a	95.6	95.4	0.2	2.4	2	2.2	4	Moderate	4
PM250505-I-11	96.2	96	0.2	2.8	1	1.2	3	Moderate	2
PM250505-I-12	95.7	95.3	0.4	2.7	1.6	2	1	poor	3
PM260505-I-16	98.9	98	0.9	0.2	0.9	1.8	2	Well	1
PM270505-I-17	98.3	97.8	0.5	0	1.7	2.2	1	Well	1
PM270505-I-18	98.2	97.7	0.5	0	1.8	2.3	2	Well	1
PM270505-I-19	98.1	97.5	0.6	0.8	1.1	1.7	1	Mod. Well	1
PM280505-I-21	99.3	98.8	0.5	0	0.7	1.2	1	Well	1
PM280505-I-22	99.6	98.7	0.9	0	0.5	1.4	1	Mod. Well	1
PM280505-I-23a	96.1	95.8	0.3	2.5	1.4	1.7	3	Moderate	2
PM290505-I-25	98.4	97.8	0.6	0.8	0.8	1.4	3	Moderate	2
PM290505-I-26a	97.1	96	1.1	1.6	1.3	2.4	2	Moderate	2
PM300505-I-28	99.2	98.4	0.8	0.2	0.6	1.4	2	Mod. Well	1
PM300505-I-29	97.6	97.1	0.5	1	1.4	1.9	1	Mod. Well	1
PM300505-I-32	99.2	98	1.2	0	0.8	2	1	Well	1
PM310505-I-33	99.3	98.1	1.2	0.2	0.5	1.7	2	Moderate	2
PM310505-I-36a	99.2	98.5	0.7	0	0.8	1.5	2	Moderate	2
PM010605-I-41	98.9	98.1	0.8	0	1.1	1.9	1	Moderate	2
PM010605-I-43	99.3	98.9	0.4	0.2	0.5	0.9	1	Mod. Well	5
PM010605-I-44	98.1	97.1	1	0	1.9	2.9	2	Moderate	2
PM010605-I-45	97.8	97.3	0.5	0.2	2	2.5	1	Well	1
PM010605-I-46a	96.3	95.6	0.7	0.4	3.3	4	2	Well	5
PM010605-I-47	99	98	1	0.2	0.8	1.8	1	Well	1
PM030605-I-48a	98.2	97.3	0.9	0.3	1.5	2.4	1	Moderate	2
PM260705-II-1 (50)	99	97.7	1.3	0	1	2.3	2	Mod. Well	1
PM300705-II-3 (52a)	93.3	92.3	1	3.4	3.4	4.4	4	Mod. Well	6
PM300705-II-3 (52b)	93.6	92.2	1.4	3.4	3	4.4	4	poor	4
PM300705-II-4 (53b)	94.2	93.6	0.6	3.4	2.4	3	8	Mod. poor	4
PM300705-II-5 (54)	93.5	91.9	1.6	4.2	2.3	3.9	3	Well	6
PM300705-II-6 (55a)	95	94.6	0.4	2.2	2.8	3.2	4	Mod. Well	6
PM300705-II-6 (55b)	94.6	94.2	0.4	2.6	2.8	3.2	7	Mod. poor	4
PM300705-II-7 (56b)	96.8	95.7	1.1	2.6	0.6	1.7	3	Moderate	2
PM04-01	99	97.7	1.3	0	1	2.3	1	Well	5
PM04-03	98.9	97.5	1.4	0	1.1	2.5	1	Well	1
Average	**97.5**	**96.8**	**0.7**	**1**	**1.5**	**2.2**	**2.3**		
Standard Deviation	**1.8**	**1.9**	**0.4**	**1.3**	**0.8**	**0.9**	**1.58**		
		Well and moderately-well sorted				**52.50%**			
		Moderately sorted				**37.5%**			
		Moderately poor and poorly sorted				**10.00%**			

cementation preceded the carbonate and plugged most of the pores. The carbonate cement is frequently localized in fractures and limited to pore-space that was left uncemented by silica. Some pockets that partially escaped the pervasive silica cementation are cemented dominantly by ferroan calcite and less commonly by non-ferroan calcite. Dolomite cement also exists but is very rare (Hubert, 1973). It should be noted that the relative abundance of ferroan calcite versus non-ferroan calcite is based on a small number of samples studied and thus might not be representative of the formation as a whole.

Localized carbonate cementation in a number of instances can be attributed to the dissolution of limestone clasts present in these or adjacent rocks. Dominant calcite cement only occurs in pockets in close proximity to the conglomerates at the base of the formation (Fig. 13C). These pockets appear to have a carbonate cement similar to that in the overlying horizons; however, the dominance of cement in these pockets could also be attributed to an earlier stage of cementation before the onset of pervasive silica cementation that plugged most of the pores.

Many feldspar grains appear fresh; some are slightly altered to clay minerals, probably kaolinite. Authigenic clay cement is present in minor amounts, however, the detrital clay matrix may in some cases exceed 3% and in very rare cases 5%. On average the detrital matrix is around 2%. In samples with clay matrix, silica cementation was hindered. Matrix as opposed to clay cement was identified based on the mode of occurrence as drapes or interstitial fill. The values reported for detrital matrix may have been overestimated because the criteria for their identification would also include diagenetic, compaction-related pseudomatrix and organic material mixed with clay and pyrite that would all be counted under the umbrella of detrital matrix. The possible overestimation is considered negligible and therefore does not affect any subsequent reasoning.

Porosity in the quartz arenites is usually less than 1%. This is due to the pervasive silica cementation involving extensive quartz overgrowth. Porosity is locally enhanced by fracturing and the presence of minor dissolved limestone clasts. Two sets of micro-fractures were identified in the thin sections studied. The first set is near perpendicular to bedding; the second near parallel. The first set is older. Fractures are usually rehealed by silica cement. Some fractures are cemented by calcite. Rare stylolites were also observed in the quartz arenites (Fig. 13B). Heavy mineral grains (dominantly zircon) were observed in contact with the stylolites (Fig. 13B).

During thin section study of the quartz arenites, six sub-lithologies were identified. Their classification was based on grain size, matrix content and sorting. Sorting was visually estimated using sorting diagrams. Figures 14 and Table 2 illustrate the details of this classification. Sub-lithologies 1, 2, 3 and 4 fall under the umbrella of medium to fine sand (Fig. 14). The medium to fine sand quartz arenites were subdivided into two categories (Fig. 14): low-matrix content and high-matrix content arenites (less or greater than 3%). Sub-lithologies 1, 2 and 3 belong to the low-matrix category; sub-lithology 4 belongs to the high-matrix category (Fig. 14).

Sub-lithologies 1, 2 and 3 were subdivided on the basis of the degree of sorting (Fig. 14). Sorting deteriorates from well to moderately well sorted quartz arenite in sub-lithology 1, to moderately sorted quartz arenite in sub-lithology 2, to poorly sorted quartz arenite in sub-lithology 3. Sub-lithology 4 of the high-matrix category of medium to fine sand varies between moderate and poor sorting (Fig. 14).

Sub-lithology 5 is made up of fine, well sorted sand with low matrix content (< 3%) (Fig. 14). Sub-lithology 6 consists of very fine sand to coarse silt with variable matrix content (usually high) and good sorting. Other specific details of these sub-lithologies are listed below and summarized in Table 2:

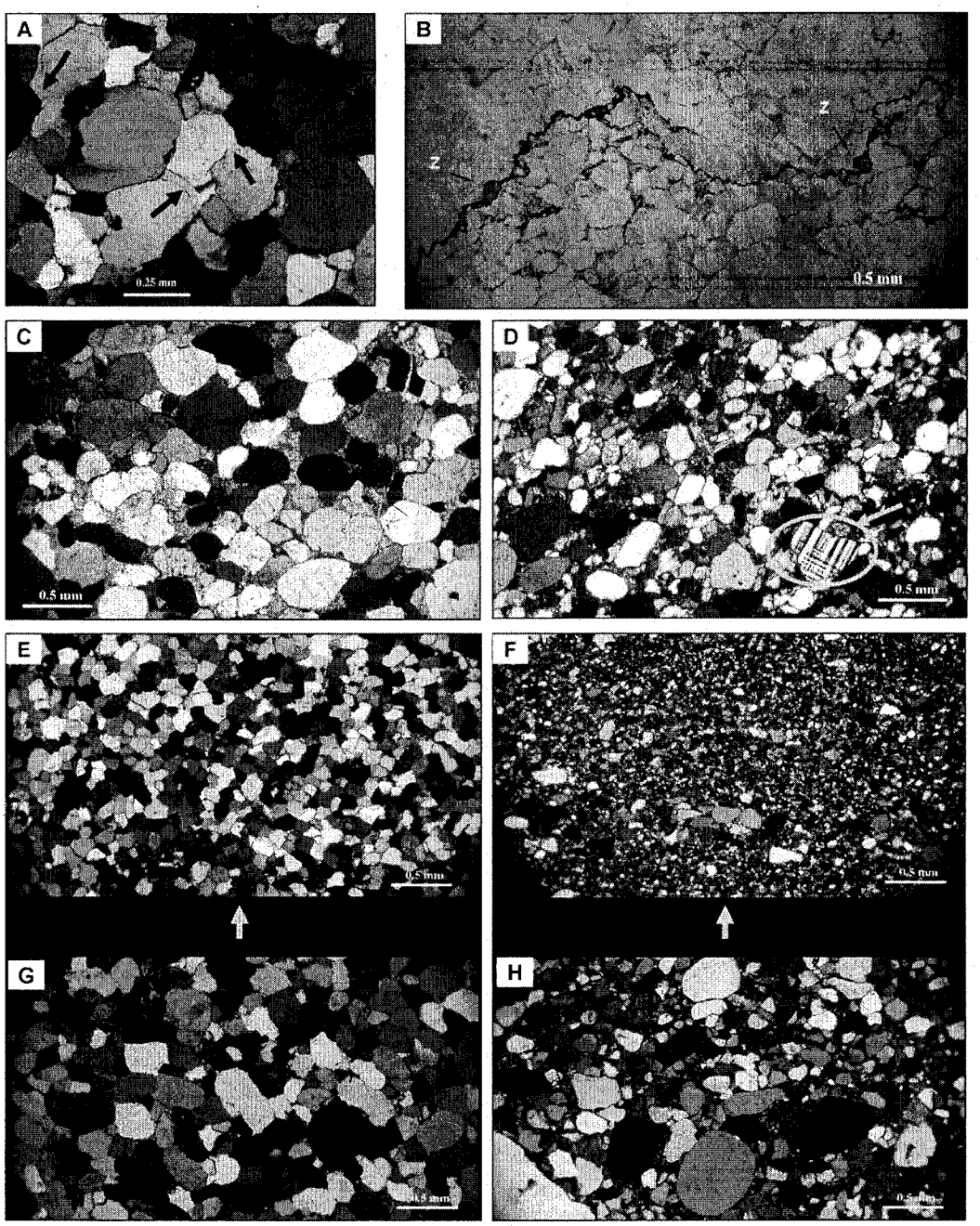

Figure 13: A) Quartz arenite with pervasive silica cementation and syntactic quartz overgrowth. Quartz grains with dust and fluid inclusion rims permit viewing the extent of the quartz overgrowth and reveal the original detrital grain shape (arrows). B) Black stylolite in the quartz arenite. Notice the accumulation of the heavy mineral zircon (Z) at this horizon. Below the stylolite, grain contacts are often sutured and this zone appears darker due to the concentration of fines. C) Well sorted and dominantly carbonate cemented quartz arenite associated with sub-lithology 1. D) Poorly sorted, medium to fine, quartz arenite (sub-lithology 3). Notice the presence of the oversized microcline clast (approximately 0.5 mm) that is coarser than average grain size. E) Sub-lithology 5. F) Sub-lithology 6. G) Sub-lithology 1. Thin sections E and G were acquired from top and bottom of the same bed respectively. Notice grading from sub-lithology 1 to sub-lithology 5. H) Sub-lithology 4. Thin sections F and H were acquired from top and bottom of the same bed respectively. Notice grading from sub-lithology 4 to sub-lithology 6.

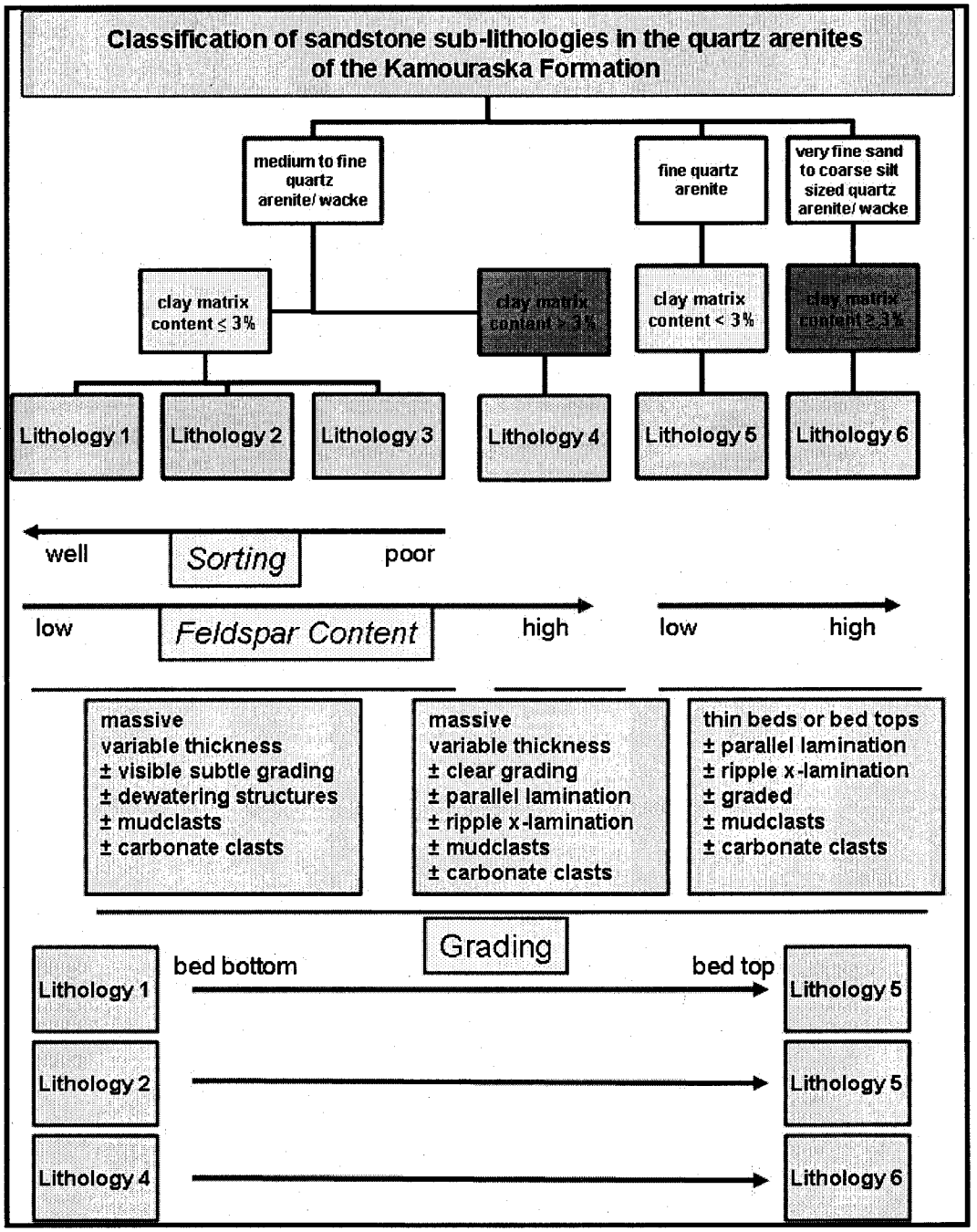

Figure 14: Classification of the different sandstone sub-lithologies of the quartz arenites from the Kamouraska Formation. Six different sub-lithologies were observed (refer to text for details). Analysis based on both field and petrographic studies.

Sub-lithology 1 is characterized by negligible feldspar content (Fig. 14 and Table 2). The highest values amount to less than 1%. The feldspar content averages 0.2% based on point counting (Table 2). Grains are dominantly rounded including the feldspars. Beds associated with sub-lithology 1 have variable thickness and are massive frequently exhibiting dewatering structures (Fig. 14). Grading is subtle.

Table 2: Characteristics of the different sandstone sub-lithologies of the quartz arenites of the Kamouraska Formation. Refer to text for details.

Characteristics of sandstone sub-lithologies in the Kamouraska Formation						
Sub-lithology	Grain size	Clay content	Sorting	Feldspar content	Bed characteristics	Lithology
1	Medium to fine sand	≤ 3%	well to moderately well sorted	(0 -1%) average (0.2 %)	Massive or graded	Quartz arenite
2	Medium to fine sand	≤ 3%	Moderately sorted	(0 -2.9%) average (1%)	Massive or graded	Quartz arenite
3	Medium to fine sand	≤ 3%	Poorly sorted	(2.7%)	Massive or graded	Quartz arenite
4	Medium to fine sand	> 3% (up to 8%)	Moderate to poor sorting	Up to (3.5%) average (2.5%)	Massive or graded; sedimentary structures	Quartz arenite or quartz wacke
5	Fine sand	< 3%	Well sorted	(0-1%) average (0.22%)	Thin massive or graded; sedimentary structures	Quartz arenite
6	Very fine sand to coarse silt	≥ 3%	Variable usually well	Up to (4.3%) average (3.3%)	Thin massive or graded; sedimentary structures	Quartz arenite or quartz wacke

In sub-lithology 2, feldspar content is variable and ranges between 0 and 2.9%. The average feldspar content is around 1% (Table 2). Some samples, typically the ones with high feldspar content (> 2%), show oversized feldspar grains that are larger than the average quartz grain (Fig. 13D). These feldspar grains show no evidence of diagenetic growth (feldspar rims do not show an extinction angle different from that in the core). Quartz grains are dominantly well rounded; feldspar grains dominantly subrounded to subangular. Beds

associated with sub-lithology 2 have variable thickness and are massive frequently exhibiting dewatering structures. Grading is subtle yet more pronounced than in sub-lithology 1.

Sub-lithology 3 is represented by only one sample having a matrix content of 1%. Feldspar content is relatively high at 2.7% (Table 2). Quartz grains are dominantly rounded; feldspar grains are subrounded to subangular. The most striking characteristic of this sample is the presence of large feldspar grains many of which have a diameter larger than 0.5 mm (Fig. 13D); the average grain size of the quartz arenite is 0.28 mm.

In sub-lithology 4, the clay matrix exceeds 3% but may reach up to 8% so that the rock would be termed a quartz-wacke. Feldspar content is high and may reach up to 3.5% (average about 2.5%) (Table 2). Grains are rounded to subrounded. Beds associated with sub-lithology 4 are massive but may show well developed grading. Sedimentary structures such as parallel and ripple cross-lamination may also be present in sub-lithology 4.

In sub-lithology 5, feldspar content is low (< 1%) and sometimes nearly absent (Table 2). Grains are subrounded to subangular. Samples belonging to this sub-lithology are often graded and laminated even at the thin-section scale. This lithology is found in thin graded beds that may show sedimentary structures such as parallel and ripple-cross lamination (Table 2). This sub-lithology is frequently found to constitute bed tops.

In sub-lithology 6, feldspar is abundant (Table 2), averaging 3.3% and may reach 4.3%. Grains are angular to subangular. Lamination is easily noticed even at the thin-section scale. This lithology is characterized by thin beds that show sedimentary structures, namely parallel and ripple-cross lamination (Table 2). This sub-lithology has also been found to comprise the tops of some beds.

Sub-lithologies 1, 2, and 3 were initially differentiated on the basis of sorting only (Fig. 14); however, after point counting it became apparent that they also vary in feldspar content. Feldspar is negligible to absent in sub-lithology 1, but becomes more abundant in sub-lithologies 2 and 3 (Fig. 14). Furthermore, some feldspar grains encountered in sub-lithologies 2 and 3 are coarser than the average grain size (Fig. 13D). Bearing in mind that quartz is more resistant than feldspar in many weathering environments; this suggests that the coarse feldspar probably had a different provenance. It is also noteworthy to add that samples that are richer in feldspar are often associated with the sub-lithologies that showed a deterioration in sorting as has been observed in sub-lithologies 2 and 3. This suggests that mixing probably occurred and that a sediment of "sub-lithology 1" has been mixed to varying degrees with a feldspar-rich source of coarser sand (possibly the same source of feldspar-rich sand that supplied the underlying feldspathic arenites of the Saint Damase Formation). As the rate of mixing increased, sub-lithology 1 was replaced by sub-lithology 2 or rarely sub-lithology 3; showing an increase in feldspar content and often accompanied with a decrease in the degree of sorting.

In support of the arguments in the previous paragraph, alternatives to the mixing theory were considered. Diagenetic bias in generation of over-sized feldspar was examined and ruled-out as none of the feldspar crystals showed rims with an extinction angle different from that in core. Furthermore, Hubert (1973) documented the presence of the same type of feldspars (microcline, perthite, orthoclase, oligoclase, albite and andesine) with about equal potash to plagioglase content in the underlying Saint-Damase Formation, hence adding further support to the mixing hypothesis and suggesting that the source of the oversized feldspars in the Kamouraska Formation could have been similar to the source that supplied the Saint-Damase feldspars.

It is also worthwhile to note that sub-lithologies 5 and 6 are special sub-lithologies that occur on their own only in very thin beds ranging from 5 to 10 cm.

However, they are usually associated with the tops of thicker beds. In some beds, sub-lithologies 1 and 2 were found to grade into sub-lithology 5 (i.e., well or moderately sorted, matrix-poor, medium to fine sandstone grading into well sorted, matrix-poor fine sandstone; Figs. 13E, G and Fig. 14). Sub-lithology 4 was found to grade into sub-lithology 6 (i.e. moderately to poorly sorted, matrix-rich, medium to fine sandstone grading into well sorted, matrix-rich very fine sandstone to siltstone; Figs. 13F, H and Fig. 14).

6.2 Conglomerate

Petrography of the conglomerates was given second priority in this study (5 thin sections of pebbly conglomerates). The thin section study of the conglomerates reveals the presence of clasts surrounded by a sandy matrix. This sandy matrix is characterized by medium to fine sand similar in character to that of the quartz arenites. This similarity was also reported by Hubert (1973) who noted that the quartz grains are frosted. The sorting of the sandy matrix varies from one place to another. Some pockets were characterized by very well sorted medium to fine sand. Grains are dominantly rounded and subrounded. The sandy matrix is generally composed of quartz and feldspar. Feldspar content is markedly higher than observed in quartz arenites, and feldspar grains are dominantly euhedral. Feldspars, namely microcline and orthoclase, as large as 0.7 mm were observed. Mica flakes are present in trace amounts but are somewhat more abundant than in the quartz arenites. The sandy matrix is often cemented with calcite or dolomite. In some samples, the sandy matrix was cemented by silica in the form of quartz overgrowths. In all samples, clay matrix and clay cement does not exceed 2-3%.

Clasts observed in thin section vary between granule and pebble size. Clast composition varies from carbonate, quartz, feldspar to other rock fragments. Quartz granules/pebbles observed are frequently polycrystalline and show aggregates of fused quartz crystals with irregular serrated contacts probably of igneous origin. Monocrystalline quartz pebbles were observed up to 5 mm in

diameter. They may contain large feldspar intergrowths (as large as 0.7 mm in diameter). Large euhedral feldspar grains have been observed that may be as large as 6 mm. Carbonate clasts usually predominate and vary from calcilutite (micrite), calcisiltite, and calcarenite to calcirudite. In the thin sections studied, all these carbonate fragments are dolomitized by fine (sucrose) dolomite. Some samples show partial dolomitization by coarse dolomite of a later stage. Shell fragments and other debris in the calcirudites were largely obliterated by the dolomite. Carbonate clasts have been preferentially removed by dissolution providing secondary porosity to the rocks. Other fragments observed are sandstone fragments of medium to fine, well sorted and well rounded sand that is cemented by dolomite. Similar fragments of very fine sandstone and siltstone were also observed. Well rounded mudclasts are also present in these rocks.

Porosity is generally low in the range of 1-2% but is enhanced in rocks where carbonate clasts have suffered partial or complete dissolution. Some pockets show the presence of diagenetic pyrite which might have formed in the sulfate reduction zone.

The pebble fraction was reported to make up 90% of the rock in coarser conglomerates (Hubert, 1973) but towards the distal areas (in southern parts of the study area) sandy matrix may reach up to 65% (Hubert, 1973). The thin sections studied show sandy matrix making up 30% and pebble fragments 70% of the rock.

7. GRAIN SIZE ANALYSIS OF THE QUARTZ ARENITES

The fact that the quartz arenites of the Kamouraska Formation are pervasively silica cemented makes grain-size analysis by either sieving or thin section study impractical because the disintegration of rock samples is impossible in the presence of heavy silica cement. In thin sections with pervasive quartz overgrowth detrital grain boundaries are commonly not visible.

The solution to this problem was a search for carbonate-cemented samples that could be disintegrated by using acid. Carbonate-cemented quartz arenites are rare in the Kamouraska Formation; however, some basal horizons in close proximity to the limestone conglomerates effervesce vigorously with 10% hydrochloric acid (HCl) indicating the presence of carbonate cement. Carbonate cement was also detected in randomly occurring pockets away from the conglomerates at stratigraphically higher zones. A total of 35 samples were collected, crushed and then attacked by 38% hydrochloric acid (HCl). Only five samples successfully disintegrated and were all associated with horizons in close proximity to the conglomerates. The remaining samples showed partial or no disintegration. Grain size analysis was only performed on the five disintegrated samples.

Wet sieving was first conducted in order to extract the fine fraction (< 32 μm). The coarser fraction trapped in the sieves was dried and sieved again by dry sieving. The fine fraction was then analyzed using the pipette method. Figure 15 shows the grain size curves of the 5 samples with their corresponding histograms.

The dominant grain sizes vary between medium and fine sand. The average grain size graphically derived from the median (M) is 0.26 mm; the average grain size graphically calculated from the geometric mean (Gm) is 0.25 mm (Fig. 15) which is the boundary between medium and fine sand. The near vertical grain size distribution curves provide a visual indicator for good sorting. The standard deviation σ calculated for the samples GSA 3, GSA 7 are 0.6 and 0.66, respectively (and sorting coefficient S_o of 1.38 and 1.42, respectively); indicating moderately well-sorted sand (moderately well-sorted sand has a standard deviation σ = 0.5-0.71). Samples GSA 22, GSA 10 and GSA 11 have a standard deviation σ of 0.73, 0.86 and 0.89 respectively (sorting coefficient S_o of 1.38, 1.49 and 1.5 respectively); and indicate moderately sorted sand (moderately sorted sand has standard deviation σ = 0.71-1.00). Sample GSA 22 strands the boundary between moderately well sorted and moderately sorted sand. Sorting

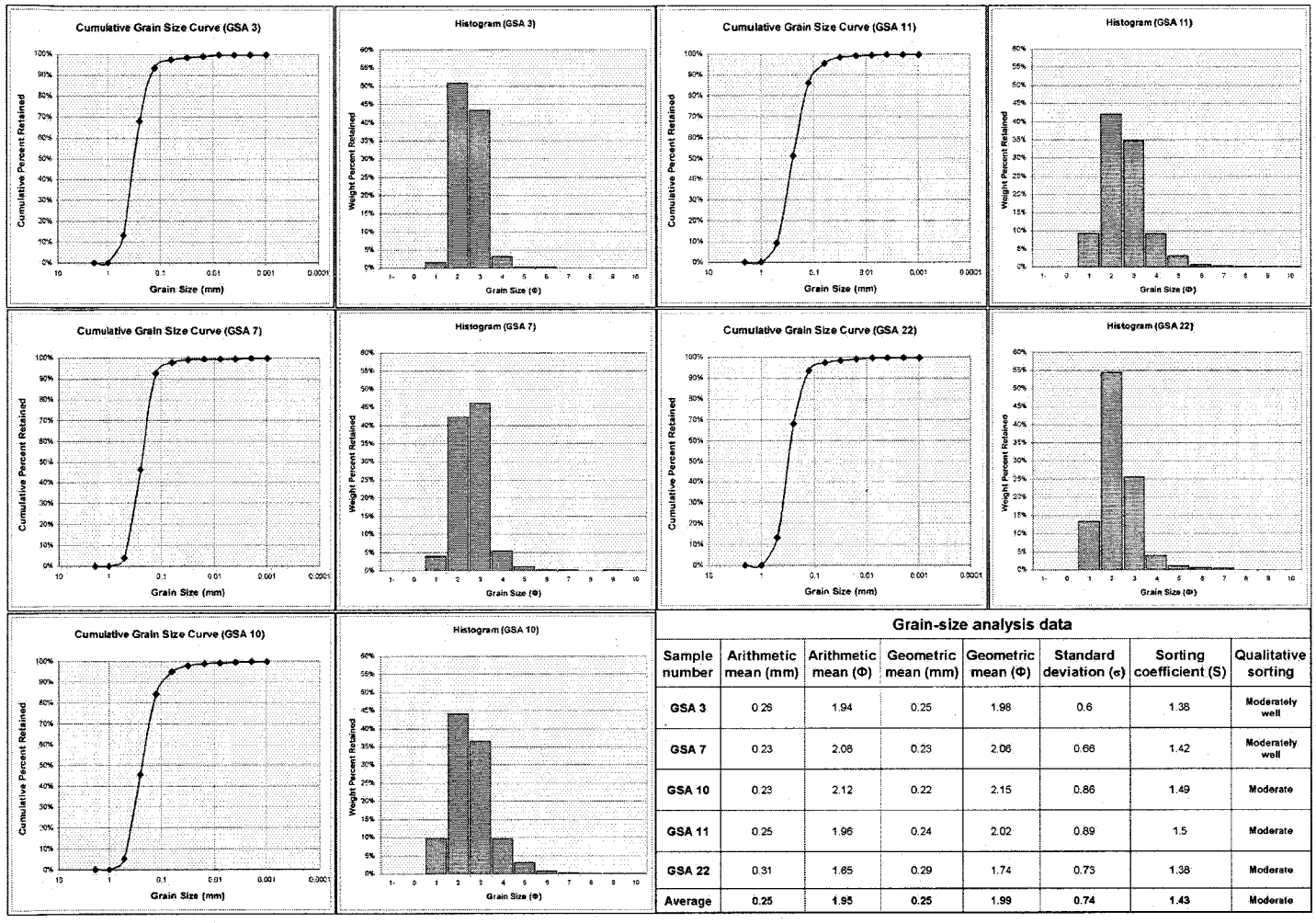

Grain-size analysis data

Sample number	Arithmetic mean (mm)	Arithmetic mean (Φ)	Geometric mean (mm)	Geometric mean (Φ)	Standard deviation (σ)	Sorting coefficient (S)	Qualitative sorting
GSA 3	0.26	1.94	0.25	1.98	0.6	1.38	Moderately well
GSA 7	0.23	2.08	0.23	2.06	0.66	1.42	Moderately well
GSA 10	0.23	2.12	0.22	2.15	0.86	1.49	Moderate
GSA 11	0.25	1.96	0.24	2.02	0.89	1.5	Moderate
GSA 22	0.31	1.65	0.29	1.74	0.73	1.38	Moderate
Average	0.25	1.95	0.25	1.99	0.74	1.43	Moderate

Figure 15: Grain size analysis of the quartz arenites of the Kamouraska Formation. Refer to text for explanation.

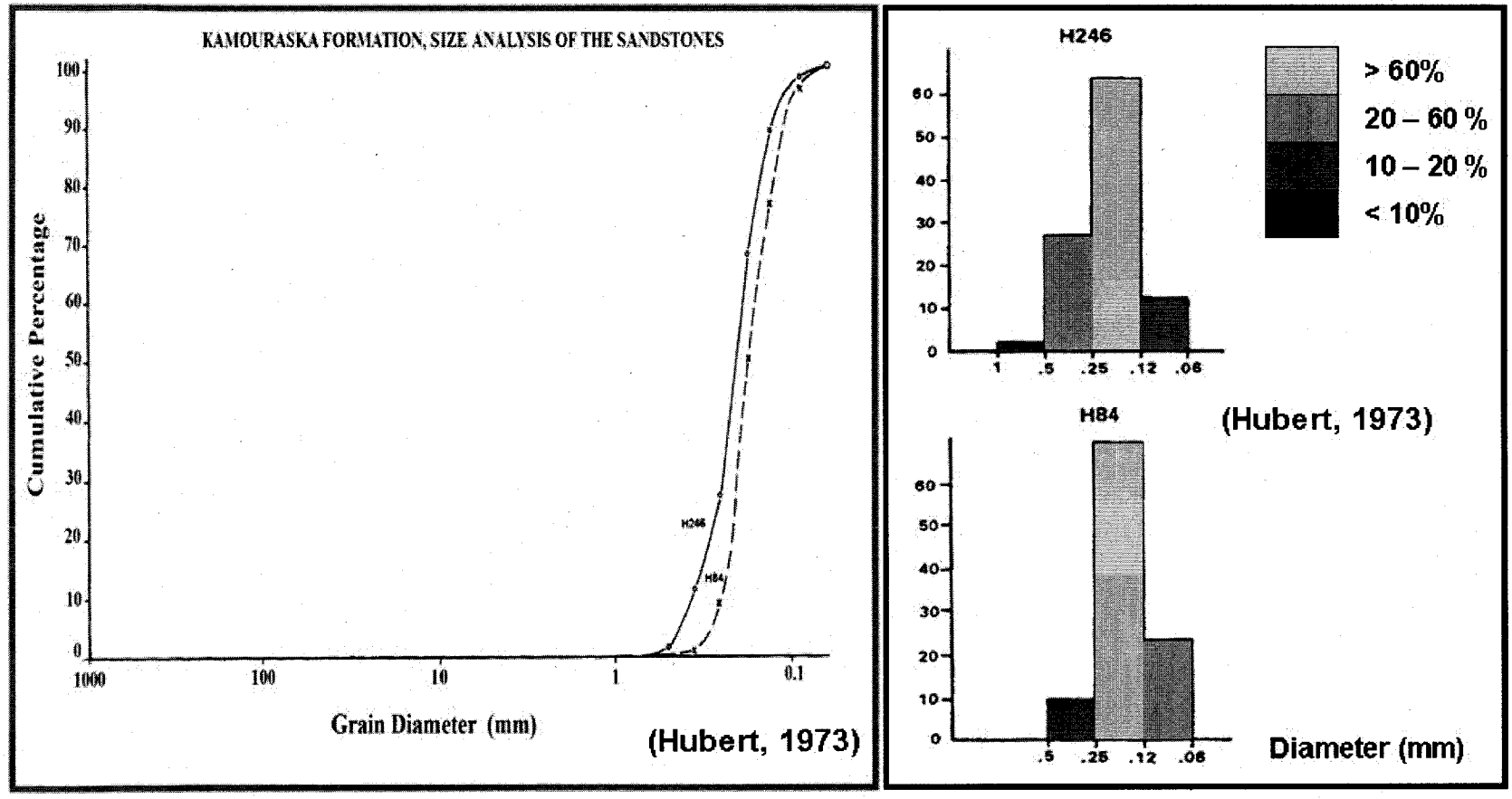

Figure 16: Grain size analysis of the quartz arenites using thin sections (after Hubert, 1973). See text for details.

coefficient S_o for GSA 22 is the same as GSA 3 which is moderately-well sorted. The sorting coefficient used is $S_o = (Q_{25}/Q_{75})^{1/2}$, where Q_{25} and Q_{75} represent the 25 and 75 percentiles of the distribution, respectively.

The number of samples used is not sufficient for making conclusions about average sorting. Furthermore the samples used for grain size analysis were sampled from the basal parts of the Kamouraska Formation in close proximity to conglomerate beds and this favors the selection of samples with poorer sorting. These figures may be considered a minimum estimate for the quality of average sorting for the quartz arenites. Hubert (1973) conducted grain size analysis on two quartz arenite samples using thin sections. His results give a sorting coefficient S_o of 1.27 for both samples indicating that the quartz arenites are well sorted (Fig. 16).

The grain size analysis conducted, coupled with the petrographic study of the quartz arenites, suggests that indeed sorting varies. It does confirm Hubert's (1973) results that well sorted and moderately well sorted quartz arenites abound, however not throughout the formation. The estimates from this study show that more than 50% of the beds studied in thin sections fall into the well sorted or moderately well sorted category (Table 1). Moderately sorted quartz arenites also constitute an important part of the Kamouraska quartz arenites. Poorly sorted quartz arenites exist but are rare. The decrease in sorting is attributed to mixing as has been discussed in the petrography section.

8. GRAIN-SURFACE MORPHOLOGY FROM SCANNING ELECTRON MICROSCOPY (SEM)

The quartz grains obtained from the disintegrated rocks (i.e. the ones used for grain size analysis) were visualized using a binocular microscope. The grains are well rounded and frosted. Many grains approach a perfect sphere and show clear

pitting, especially those larger than 0.25 mm. The grain surface textures were imaged using the scanning electron microscope (SEM).

Quartz grains were glued to a carbon tape mounted on a thin section. The quartz grains were then carbon coated. Around 100 quartz grains were mounted per section. Grain sizes larger than 0.25 mm were selected for observation as diagenesis might be involved and have affected smaller grains more than larger ones. Only the prominent surface features of the grains were documented in this study.

The surface relief observed on the grains varies between low and medium amplitude. The following grain surface textures were observed (Figs. 17 and 18): 1) bulbous edges, 2) smoothed-over upturned plates, 3) irregular/dish-shaped depressions, and 4) V-shaped scars. A description of these textures follows:

1) Bulbous edges are the most common surface textures. Mahaney (2002) describes bulbous edges as prominent, protruding and rounded grain edges with the shape of a parabolic curve. This texture is more than simple grain rounding. It is a result of a combination between mechanical breakage (surface abrasion) and chemical precipitation of silica (Mahaney, 2002), (Figs. 17 and 18).
2) Upturned plates are impacted surfaces with small to large plates partially torn loose from the mineral surface (Mahaney, 2002). Upturned plates result from breakage of quartz along cleavage planes in the quartz lattice (Pye and Tsoar, 1990). The sharp plate edges become smoothed out and tend to give rise to a rolling microtopography (Fig. 17).
3) Irregular depressions are usually equidimensional (dish shaped) or elongate (Fig. 18). These depressions tend to be large, and have been reported in the literature up to 250μm. These irregular depressions are attributed to grain impact (Krinsley et al., 1976).

4) V-shaped scars are fractures embedded on the grain surface that can be of variable size (Mahaney, 2002), generally ranging between 0.05-5 μm (in rare cases up to 25 μm; Krinsley and Doornkamp, 1973).

The bulk of the textural imprints listed above suggest that the quartz grains have gone through an eolian stage in their history for the following reasons:

The bulbous edge texture (Fig. 17 and 18) is almost ubiquitous to eolian environments (Mahaney and Andres, 1996; Mahaney, 2002). This texture is related to grain saltation which causes edge breakage and is coupled with solution/reprecipitation of silica thus creating a rolling microtopography. When grains saltate, they lose their edges. Experiments mimicking eolian transport conducted by Kuenen (1960) resulted in simple edge breakage that lacked the smoothing observed on desert sand. The solution and reprecipitation of silica occurs in deserts during the night and day, respectively. The desert dew during the night has a high pH from dissolved evaporites and causes silica dissolution. During the day the dew evaporates and the silica reprecipitates in depressions thus smoothing over the grain surface and creating a rolling microtopography (Margolis and Krinsley, 1971; Krinsley and Doornkamp, 1973; Mahaney, 2002).

The smoothed over upturned plates (Fig. 17) are very characteristic of eolian environments (Krinsley and Doornkamp, 1973; Mahaney, 2002). Upturned plates result from cleavage scarps and are frequently modified in the desert environment by solution and reprecipitation of silica (Krinsley et al. 1976; Mahaney, 2002). Frosting observed on eolian grains has been attributed to the presence of upturned plates. Experimental evidence suggests that the spacing and size of upturned plates may be broadly related to wind energy (Krinsley and Wellendorf, 1980).

Irregular depressions (Fig. 18B, C and D) usually form by a single (mechanical) event during periods of violent abrasion related to strong winds.

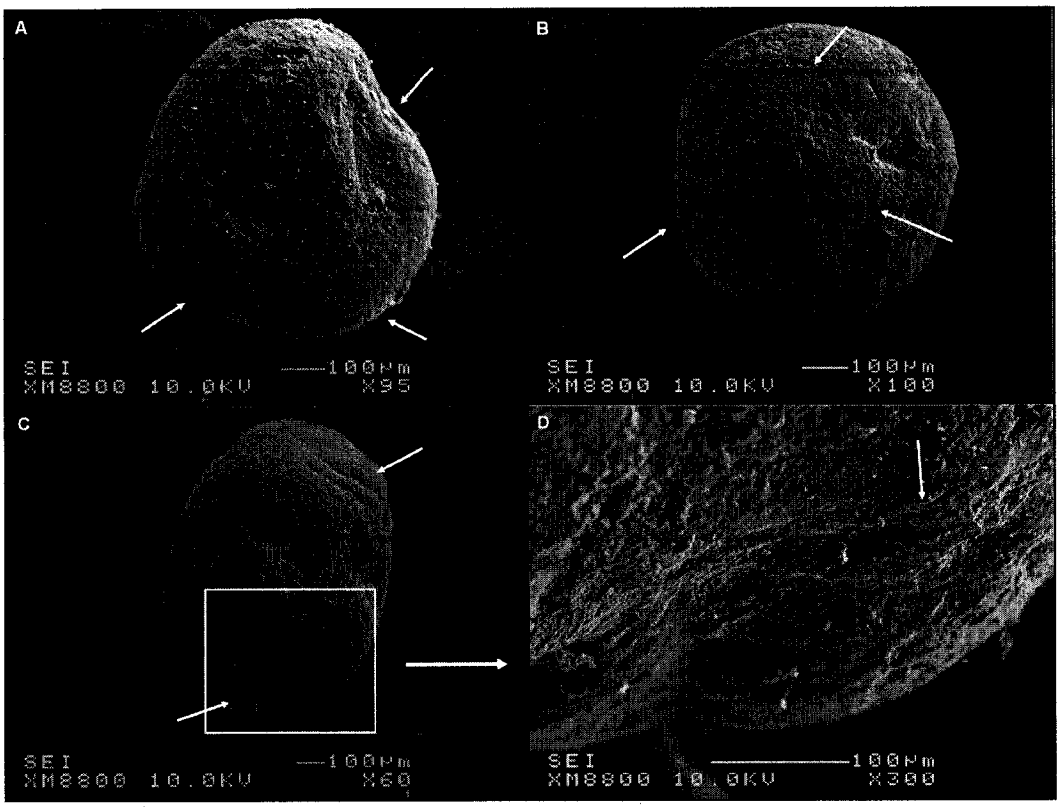

Figure 17: A) Rounded quartz grain with bulbous edges showing numerous upturned plates (arrows). B) Near spherical quartz grain with abundant upturned plates (arrows). Grain also shows small depressions attributed to grain collision during saltation. C) Rounded elongate grain with bulbous edges and upturned plates (arrows). D) Close-up of C), showing zone of smoothed-out upturned plates (arrow).

They are the result of direct as opposed to glancing impact between saltating or creeping grains (Mahaney, 2002). The depressions correspond to chips that have been broken off (Krinsley and Doornkamp, 1973). Such depressions are found on grains in eolian environments. The length or diameter of irregular depressions observed on quartz grains is on the order of 100 µm.

V-shaped scars (also known as percussion scars) have been observed but were not further documented. No attempt was made at imaging these fine features as they are very small in size (0.05-5 µm) and prone to healing by diagenesis. In general, very small features were disregarded in order to avoid confusion with possible diagenetic phenomena. V-shaped percussion scars are the most diagnostic features found on water transported quartz. They are produced by

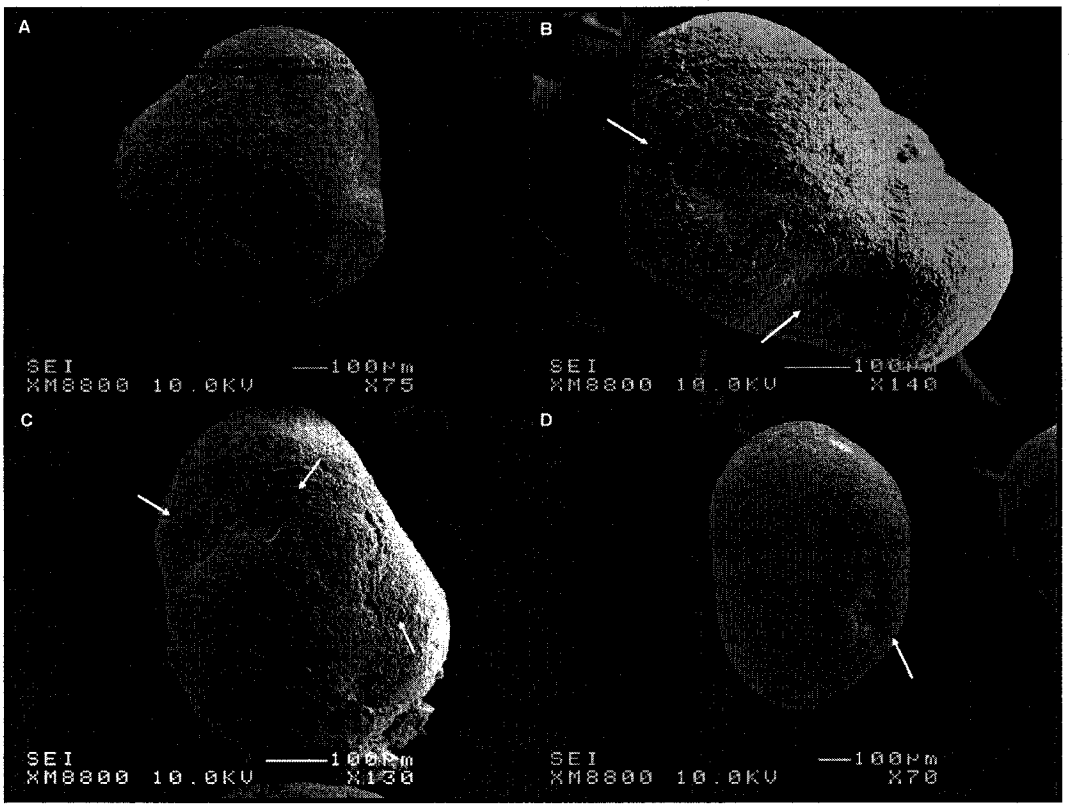

Figure 18: A) Rounded grain (originally triangular) with bulbous edges. Grain has its edges and a rolling topography was created. B) Elongate grain with bulbous edges and large depressions related to impact of saltating grains. Grain-covering silica plates are related to precipitation of silica. C) Quartz grain with irregular depressions (arrows at top) and abundant upturned plates (bottom right). D) Quartz grain with triangular depression. This depression could be related to grain collision in an eolian environment or during violent collision in subaqueous transport which creates V-shaped impact scars. However, the large size of the V-shaped scar (>100 µm) is not typical of those produced during subaqueous transport.

vibrational energy which is released from the grains during high speed collisions in subaqueous transport (Mahaney, 2002).

9. MODE OF DEPOSITION

The fact that the Kamouraska Formation is underlain and overlain by deep water shale suggests that deposition occurred in a deep-sea environment. First the mode of transport and deposition of the quartz arenites will be considered, second that of the basal conglomerates will be discussed.

9.1 Quartz arenites

Field observations suggest that the quartz arenites have been transported into the deep sea by means of rapid sediment gravity flows. This proposal is supported by the following observational facts:

1) The common massive bedding indicates rapid deposition either of pseudoplastic quick beds (Middleton, 1967; Middleton and Hampton, 1973), from high-density turbidity currents (Lowe, 1982); sustained high-density flows (Kneller and Branney, 1995); hyperconcentrated/concentrated density flows (Mulder and Alexander, 2001), or from non-cohesive debris flows (Gani, 2004).

2) The observed graded beds indicate deposition out of suspension (Bouma, 1962; Middleton, 1967; Middleton and Hampton, 1973; Lowe, 1982; Mulder and Alexander, 2001) and eliminate the possibility of the controversial sandy debris flows (which would be reversely graded; Shanmugam, 1996) and hyperconcentrated density flows (which lack vertical particle sorting; Mulder and Alexander, 2001).

3) The prominent dewatering structures in the quartz arenite beds of the Kamouraska Formation indicate rapid deposition from subaqueous turbulent flows involving entrapment of excess pore-water (connate water) and subsequent dewatering (Lowe and LoPiccolo, 1974; Lowe, 1975; Lowe, 1982).

4) The presence of randomly scattered carbonate granules and pebble-sized mudclasts (up to cobble size) reflect flow competence (Hiscott and Middleton, 1979; Mutti and Nilsen, 1981; Lowe, 1982; Mutti and Normark, 1987; Piper et al., 1988). Larger clasts are harder to entrain and have a higher settling velocity. This is why they are associated with more competent flows (Hiscott and Middleton, 1979; Lowe, 1982). As flows decelerate deposition occurs due to loss of capacity not competence (Hiscott, 1994a).

5) The ripple cross-lamination at the top of some beds reflects the waning energy of a turbidity current (Bouma, 1962; Lowe 1982; Kneller and Branney, 1995).

6) Bouma divisions $T_{a,b,c}$ in some thin beds are characteristic turbidite divisions (Bouma, 1962) clearly attesting to deposition from turbidity currents.

7) The presence of scours and flute casts at the base of some of the quartz arenite beds and the occurrence of sandwiched shale lenses (i.e., remnants of eroded shale beds) reflect rapid erosive flows (Walker, 1978, Hiscott and Middleton, 1979) also called ignitive flows (Parker et al., 1986).

The quartz arenites of the Kamouraska Formation are characterized by population 1 grains of Lowe (1982) (clay, silt, fine sand up to medium sand) and low matrix content (< 2%). The low matrix content reflects cohesionless (frictional) flows of medium to fine sand (Hampton, 1975). Population 2 grains of Lowe (1982) (coarse sand to small pebble-sized gravel) represent a small percentage of these deposits. These cannot be suspended in low concentration flows (Pantin, 1979; Lowe, 1982). Consequently, the flows must have been concentrated. These characteristics coupled with thick bedding (dominantly massive and graded beds) suggest deposition from high-density turbidity currents (Lowe, 1982; Mutti, 1992).

Following Lowe's (1982) structural and textural divisions of the deposits from high-density turbidity currents, the quartz arenite beds are classified as belonging dominantly to the S_3-type turbidite structure. These are massive beds with abundant dewatering structures. The S_3-type beds tend to grade into a parallel- and ripple-laminated top or Bouma divisions T_{bc} laid down from low-density turbidity currents. This vertical succession reflects flow evolution from a high-density to a low-density turbidity current (or from a concentrated density flow to a turbidity current in the terminology of Mulder and Alexander, 2001).

This evolution results from flow dilution and the waning energy of the flow (Kneller and Branney, 1995).

A traction S_1-type layer (following the Lowe, 1982, nomenclature) sometimes exists at the base of the bed and is associated with scouring of underlying sediment 5-20 cm deep (Fig. 6B). It may be characterized by the presence of a quartz granule lag (or rarely pebble/granule-sized lag of carbonate clasts or mudclasts) that does not exceed 2-3 cm, at the base of the bed. This division is normally graded; however, the basal 2-3 cm may be massive or reversely graded. It should be noted that scouring in these beds is not necessarily restricted to granule-sized material, but occurs also with coarse or medium to fine sand. The overlying massive S_3-type layer comprises the bulk of the bed (Fig. 6B).

The S_1-division was introduced here to represent a thin zone of scour and lag material at the basal parts of beds. Traction carpet S_2 layers, also known as "near-horizontal stratification bands" or "inversely graded stratification bands" have been documented by Lowe (1982) to overlie the basal scouring and lag (associated with traction) and to underlie the massive structureless S_3-division. The term "traction carpets" is a misnomer (Pickering et al., 1989) that was first introduced by Dzulynski and Sanders (1962) and later elaborated on by Hiscott and Middleton (1979, 1980) and Lowe (1982). Traction carpets are attributed to flow unsteadiness and the concentration of a coarse-grained basal flow (Lowe, 1982) known as the basal inertia-flow layer (Bagnold, 1954) which is developed beneath, and driven by, an overlying turbulent flow (Dzulynski and Sanders, 1962). It is believed that the coarse-grained basal flow is maintained by dispersive pressure (Bagnold, 1954) resulting from grain collisions (Middleton, 1967; Hiscott and Middleton, 1979, 1980; Lowe, 1982). The inversely graded stratification bands (traction carpets) result from progressive collapse or freezing of inertia layers which develop beneath an overriding high-density turbidity current (Hiscott and Middleton, 1980). Hiscott (1994b), based on experimental

results of Savage and Sayed (1984) suggested a different model for traction carpets. He documented the inability of dispersive pressure to generate stratification bands thicker than 2 cm, and adopted the "sweep-fallout model" which, however, has raised other concerns (Sohn, 1995; Sohn 1997). Most recent discussions by Hand (1997), Legros (2002), Le Roux (2003) and others have provided valuable insight into the formation of basal reverse grading in concentrated density flows. However the problems pertaining to the formation of traction carpets with spaced stratification remain unresolved. Beds with complete Lowe (1982) divisions have rarely been documented in the literature (Shanmugam, 2006). Traction carpets have not been encountered in the quartz arenite beds of the Kamouraska Formation. Reverse grading in the quartz arenites was only limited to the basal 2-3cm in the S_1-division (Fig. 19).

It is believed that the coarse clasts associated with the S_1-division could have been transported as a lag (Lowe, 1982) but were frequently lifted into the lower inertia flow layer (Bagnold, 1954) due to higher shear and dispersive pressure associated with this basal zone (Middleton, 1967; Lowe, 1976; Hiscott and Middleton, 1979, 1980; Lowe, 1982, Hiscott, 1994b). The presence of randomly scattered coarse carbonate or quartz clasts within the quartz arenite beds suggests that the lower inertia flow layer could have also been fed by grains falling out of the overlying turbidity flow. The entrainment of larger clasts into the lower inertia flow layer causes it to expand (Legros, 2002). Flow expansion leads to a decrease in grain interaction (Legros, 2002). This decrease results in lowering of dispersive pressure between grains (Legros, 2002). For this reason, Legros (2002) suggested discarding dispersive pressure as a likely mechanism to generate reverse grading. However, Le Roux (2003) re-emphasized its importance and explained that flow expansion is halted as dispersive pressure becomes equal to static pressure (when dispersive pressure equals static pressure the flow compacts). As the flow compacts, grain interaction and subsequently dispersive pressure are re-established. The reverse grading observed in the basal 2-3 cm can be explained by the following:

At the time of flow expansion at the base of the flow, smaller particles fall in holes between the larger clasts and result in reverse grading (kinetic sieve mechanism; Middleton, 1970). With the onset of flow compaction, a friction dominated zone of limited accommodation is established at the base of the flow (Le Roux, 2003). This phenomenon prompts pushing of larger clasts upwards; a mechanism known as kinematic squeezing (Le Roux, 2003) and couples the effects of the kinetic sieve mechanism in the production of reverse grading. The presence of scours suggests that sweeps caused by turbulent eddies (Hesse and Chough, 1980; Cheel and Middleton, 1986; Hiscott, 1994b) could have also played a role in the entrainment of these coarse clasts during intermittent durations of transport. However, the thickness of 2-3 cm attributed to this reversely graded zone does not necessarily require a mechanism involving large sweeps associated with turbulent eddies (Hiscott, 1994b). Furthermore, the transport-lag mechanism proposed by Hand (1997) could provide another plausible mechanism for the reverse grading observed in the 2-3cm thick basal lag zone.

The presence of randomly scattered carbonate granules and pebble-sized mudclasts (up to cobble size) throughout some of the bed has other implications for the deposition of the massive S_3-division. Population 1 grains are dominantly maintained in suspension by turbulence independent of concentration. However, at high concentrations, hindered settling becomes an important sediment support mechanism rendering the flow capable of suspending larger clasts (population 2 grains) (Middleton, 1967; Lowe, 1982). The presence of randomly scattered mudclasts and carbonate granules suggests that a particle support mechanism besides turbulence must have been active. In the absence of dispersive pressure and matrix buoyancy (matrix < 2%) hindered settling becomes the likely source of sediment support for the slightly larger clasts in these flows.

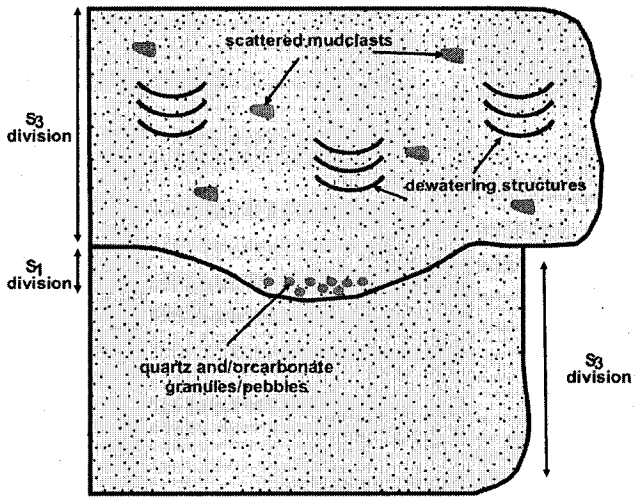

Figure 19: Bed structure in the quartz arenites of the Kamouraska Formation. Beds are usually of the S_3 type. Some beds show a basal scour of 5-20cm, delineating the S_1 division. Scouring is often associated with a lag deposit. See text for details.

Mudclasts are a special clast category because they have a lower density than quartz and behave differently in turbulent flows. Mudclasts are highly susceptible to degradation in turbulent flows (Postma et al., 1988; Nelson et al., 1992; Shanmugam and Moiola, 1995; Shanmugam, 2006). Most likely many mudclasts incorporated into the flows did not survive the ride. However, mudclasts are continuously added to the flows by scouring and erosion as the currents move down submarine canyons. Probably most of these clasts incorporated into the flows are degraded into silt and clay after an unknown distance of transport and the resulting fine particles are subsequently lifted to the top of the flows. However, clasts incorporated during the final stages (or clasts that are quickly deposited just after having been incorporated in the flow) could have survived. Some studies have advocated laminar flows for the preservation of mudclasts (Shanmugam and Moiola, 1995; Shanmugam, 2006). However, no evidence was found in this study for laminar flow in the currents that deposited the quartz arenite beds. The mudclasts are scattered with random orientations. Furthermore the dominant discoidal shape of the mudclasts would favor rounding in a turbulent flow as opposed to angular imbricated mudclasts observed in laminar debris flows.

9.2 Conglomerates

The basal conglomerate beds are characterized by grain populations 1, 2 and 3. Population 3 grains are pebble and cobble sized clasts (Lowe, 1982). The fact that population 3 grains have been entrained suggests a high particle concentration and more intense grain interaction. Turbulence is an inefficient particle support mechanism for coarse clasts. Dispersive pressure, hindered settling and matrix buoyancy lift are important mechanisms in supporting population 3 grains (Middleton, 1967; Lowe, 1982; Shanmugam and Moiola, 1995; Mulder and Alexander, 2001; Shanmugam, 2006). The reverse grading observed in these deposits suggests intense grain interaction and reflects the role of dispersive pressure in sediment support especially in the presence of a wide spectrum of grain sizes. Disorganized conglomerate beds further suggest rapid deposition and lack of grain segregation. Matrix strength tends to be low in these deposits because of their low clay content (<2%). These flows are dominantly frictional. The role of the sandy matrix in providing a buoyancy lift cannot be neglected and the intense grain interaction further supports a frictional flow. Conglomerate beds, unlike the quartz arenites, are not continuous. They quickly thin out and disappear in a southerly direction (Hubert, 1973) suggesting deposition by frictional freezing.

9.3 Revised terminology and flow evolution

Despite the use, to this point, of the term "high-density turbidity current", the more specific terms "concentrated density flows" for the flows that deposited the quartz arenites and "hyperconcentrated density flows" for the conglomerates are preferred following the terminology of Mulder and Alexander (2001). This avoids the problem of ascribing the two types of deposits to the same mechanism, namely high-density turbidity currents.

Following the reasoning of Mulder and Alexander (2001), sediment gravity flows in the Kamouraska Formation should have evolved from

hyperconcentrated flows (depositing the conglomerates) to concentrated flows (depositing the massive quartz arenite beds) to turbidity currents (depositing the T_{bc} divisions on the top of some massive beds). As the flow becomes diluted and loses the coarsest fractions, transition from one flow type to the next occurs and the role of turbulence as sediment support mechanism is increased (Fisher, 1983). Dispersive pressure on the other hand decreases due to lower flow concentrations and less grain interaction. Particle segregation becomes more pronounced and suspension sedimentation results in graded bedding as opposed to poorly segregated ungraded or reversely graded deposits of hyperconcentrated flows.

In this discussion a simplified model of flow evolution in the Kamouraska Formation has been presented which in reality is probably more complex than described. As has been pointed out, the conglomerate beds show a decrease in grain size and thickness from north to south along with a change from coarse grained (boulder-, cobble- and pebble-sized) conglomerates to pebbly conglomerates to pebble-rich sandstone (Fig. 10). This suggests that probably more detailed stages of flow evolution exist and that flow evolution proceeded in a transitional fashion. The type of flow evolution described as a proximal to distal (N to S) trend could also be one between laterally coexisting flow stages if the overall paleocurrent (or channel) direction was from northeast to southwest.

10. ENVIRONMENT OF DEPOSITION

The evidence presented here suggests that the Kamouraska Formation was laid down by sediment gravity flows in a deep-water depositional system, commonly referred to by previous workers as "submarine fan" (Barnes and Normark, 1985). Facies models for submarine fans have received much attention in the past, however, in the last 2 decades submarine canyon systems on the slope and deep-sea channel systems on the rise have received increasing attention as alternatives to fans (e.g. Damuth et al., 1983; Carlson and Karl, 1988; O'Connel et al., 1987;

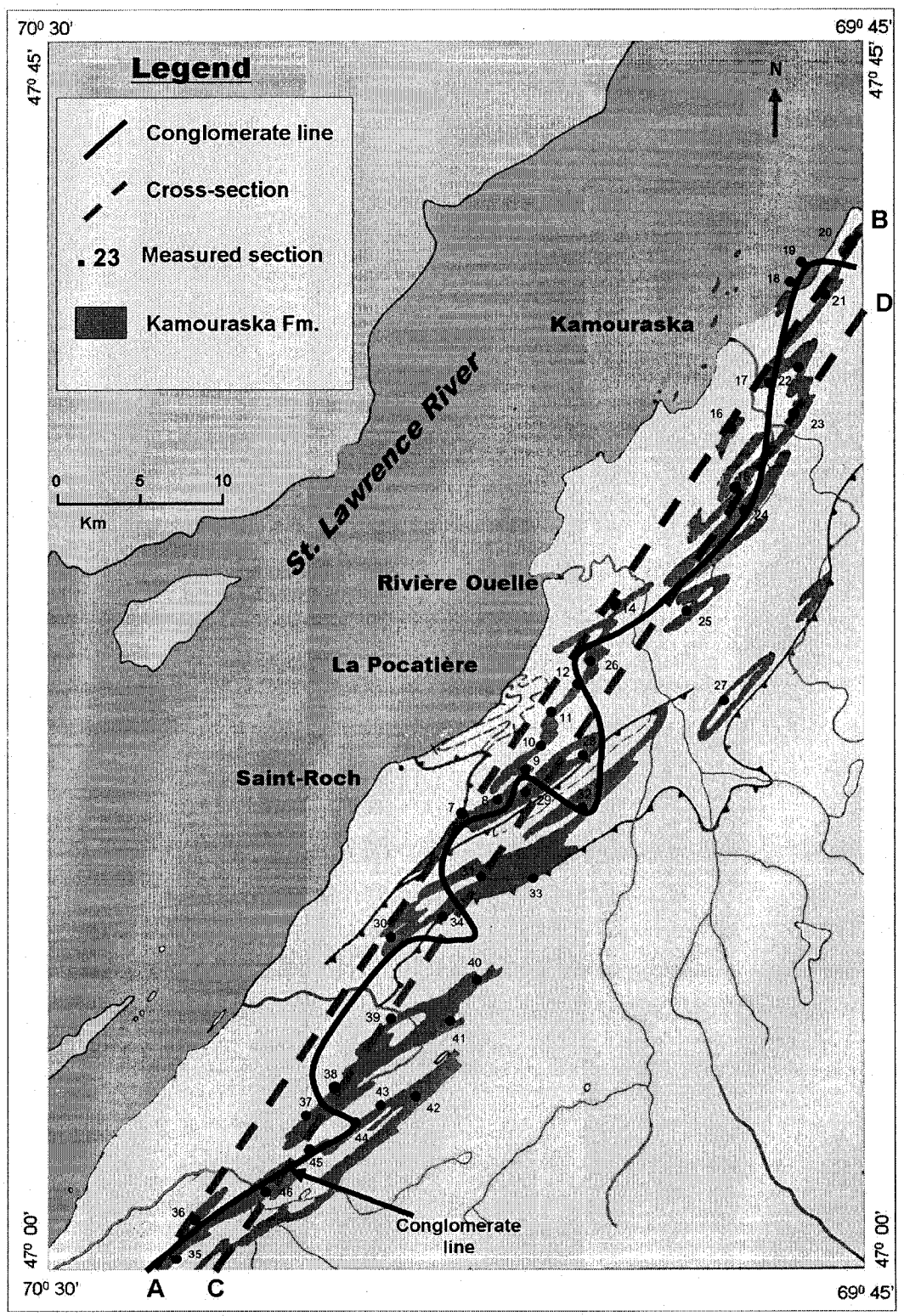

Figure 20: Sections from Hubert (1973) using his numbers. The solid black line (the "conglomerate line") depicts the eastern limit of the occurrence of polymictic conglomerate. East of the conglomerate line pebbly sandstone may still exist. Notice the nose-shaped eastward protrusions of the conglomerate line (especially at sections 44, 34and 38). Lines A-B and C-D are the lines onto which the profiles in Figures 21 and 22 have been projected.

Clark et al., 1992; Hagen et al., 1994; Kolla et al., 2001; Babonneau et al., 2002; Normark and Carlson, 2003; Krastel et al., 2004; Paull et al., 2005) and need to be considered as depositional models for ancient coarse-grained deep-water clastics.

The 3 measured sections provide clues on the mode of the deposition of the Kamouraska Formation and give hints at possible depositional environments. Many characteristics support the mode of emplacement by channelized flows: massive (up to 4 meters) thick quartz arenite beds; discontinuous conglomerate beds (that may be very coarse grained); the scarcity of shale interbeds; the presence of randomly scattered rip-up mudclasts; the abundance of scouring and erosional bases; abundant dewatering structures, amalgamation and bed lenticularity as pointed out by Mattern (2002) for a Cretaceous sand-rich deep-water system in the Alps.

A regional view of the geometry of the Kamouraska Formation is obtained from sections measured by Hubert (1973). Hubert (1973) inspected 40 sections in the Kamouraska Formation ranging in thickness from 175 to more than 300 m. Although these are not detailed measured sections they broadly separate the various different lithologies of polymicitic conglomerate, pebbly sandstone, quartz arenites and shale/siltstone horizons in the Kamouraska Formation, and will be used to approximate their geometry. Based on Hubert's sections, the eastern boundary of the basal conglomerate could be mapped (Fig. 20). The basal conglomerate horizons rapidly decrease in thickness form northwest to southeast. East of the conglomerate line drawn in Figure 20, conglomerates are not present, but pebbly sandstone may exist. The conglomerate belt was also delineated in the Saint-Raphael Area (south of the study area) (Lebel and Hubert, 1995a). The basal conglomerate belt thins out in the Saint Raphael area and disappears south of Montmagny, approximately 11 km south of our study area.

Measured sections west of the conglomerate line were projected onto a profile placed along the hatched line A-B in Figure 20. The basal conglomerate

horizon shows considerable variation in thickness along the projected profile and reaches a thickness of 120m in section 14, whereas quartz arenite horizons show considerably less variation along strike. This may reflect incomplete exposure at the base of the sections which may not show the true stratigraphic base of the formation. Since this is the more likely explanation for the considerable thickness variation, the sections in Figure 21 were correlated using the top of the conglomerates. A parallel line (C-D), 2.6 km southeast of line A-B connects sections in which the basal conglomerate is absent (Fig. 22). Shale and siltstone horizons are more abundant along C-D.

The abrupt thinning and disappearance of the conglomerate to the southeast coupled with an increase in shale/siltstone horizons might reflect a proximal-distal relationship from northwest to southeast, perpendicular to the paleoslope. The conglomerate-line shows three nose-shaped eastward protrusions (Fig. 20, around sections 44, 34, and 32). The areas in between might reflect thinning and disappearance of the conglomerates in areas between southeast directed canyons on the slope (or channels on the rise). This model would require the presence of several, more or less parallel southeast directed channels, but it does not explain the presence of the thick quartz arenites in the intervening areas.

Considering the fact that the conglomerates occupy the basal parts of the formation, a model different from northwest-southeast running canyons (or channels) may be more realistic assuming a southwestward running, relatively large meandering canyon (or channel) depicted in Figure 23. Meandering would encompass the observed paleocurrent directions that vary from southwest to southeast. The basal conglomerate horizon would exist along the deepest parts of the canyon (channel). The disappearance of the polymictic conglomerate horizons to the southeast is thus explained by their restriction to the basal parts of the conduit and the early part of its history. The thinning of the conglomerate belt to the southwest is a result of a proximal-distal trend with increasing transport distance. The nose-shaped protrusions previously attributed to flow directions

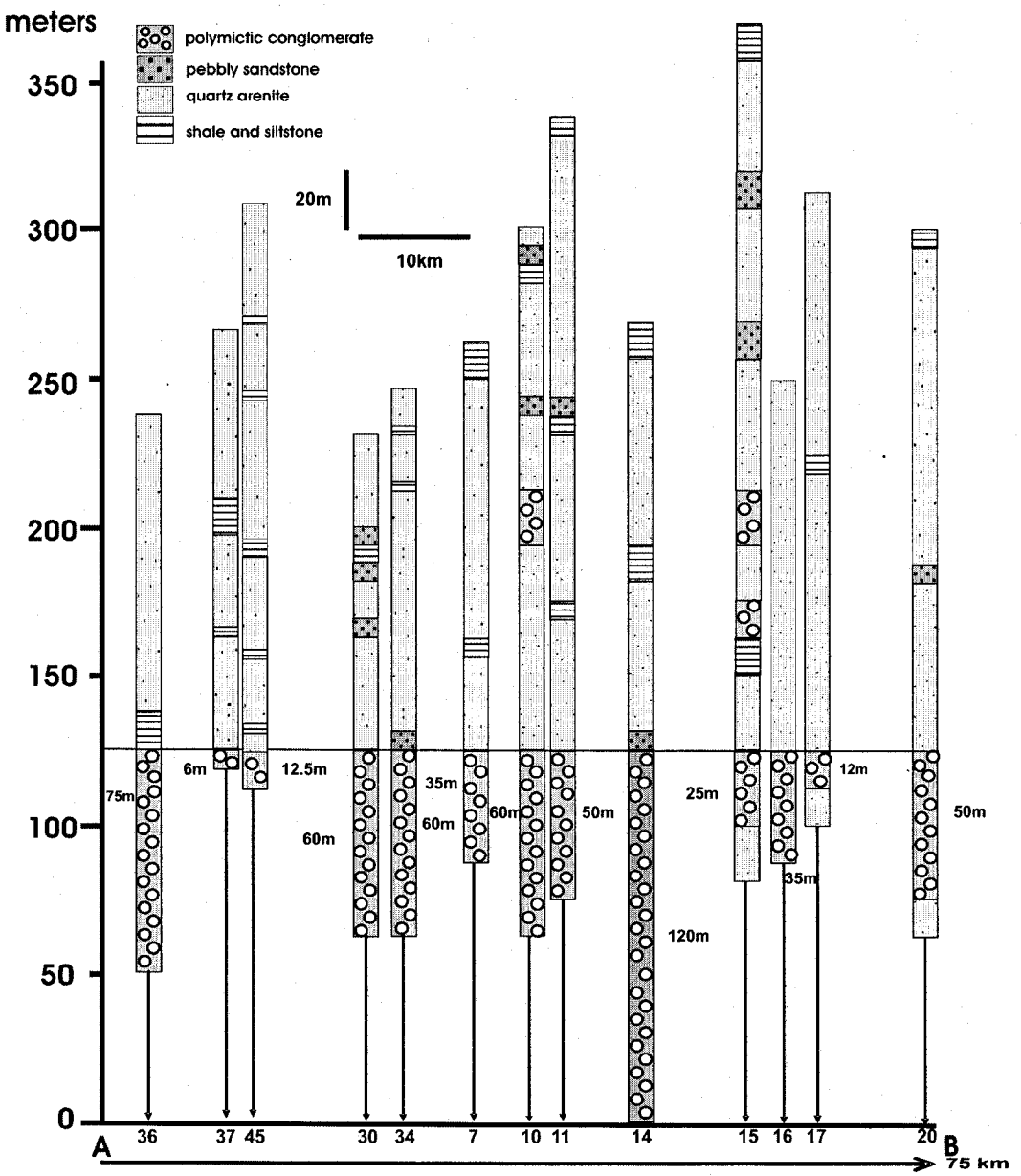

Figure 21: Correlation of sections along line A-B. Notice variation in conglomerate thickness along strike. Shale and siltstone intervals are rare.

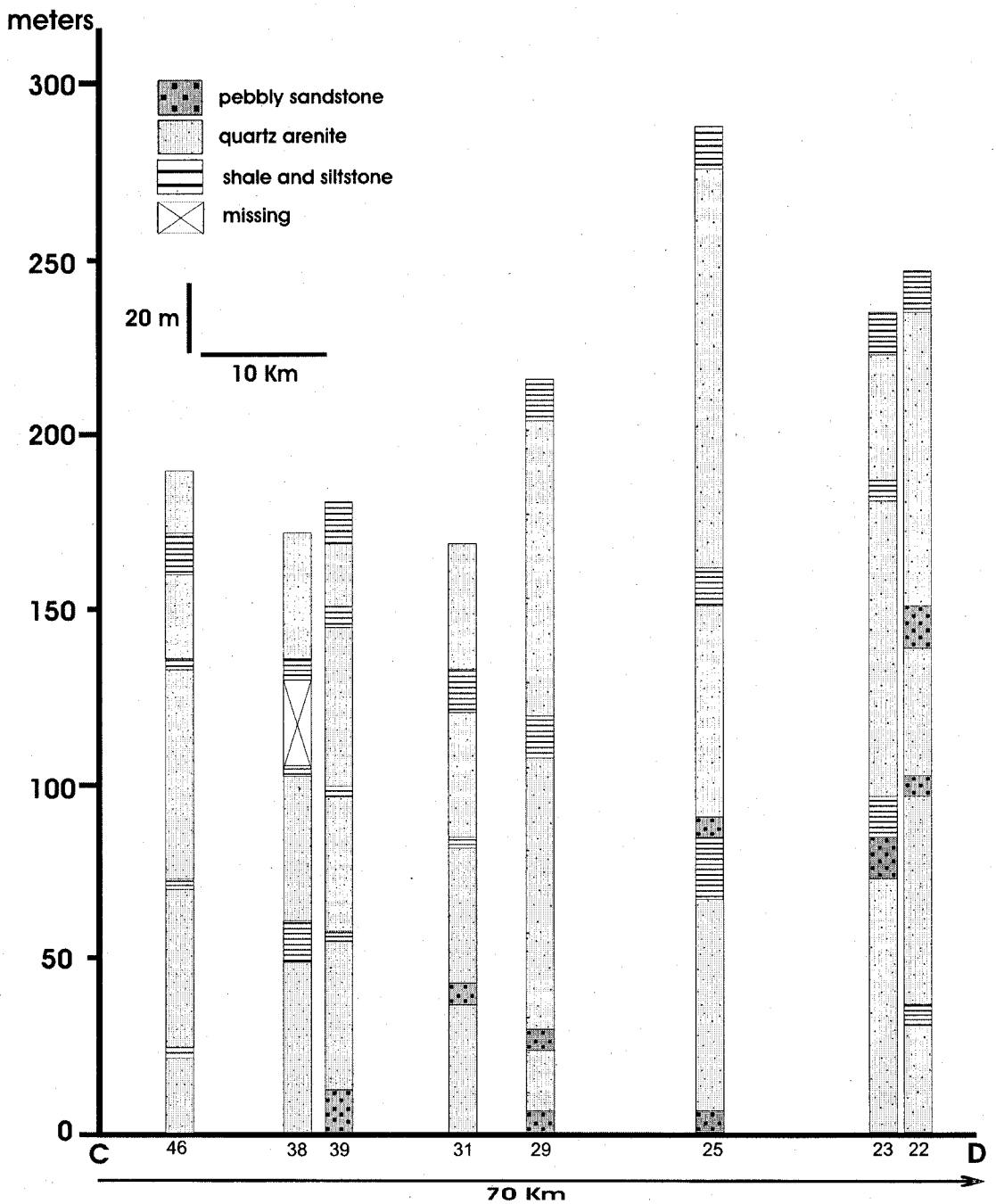

Figure 22: Sections of Hubert (1973) using his numbers projected onto line C-D (Fig. 20). Notice increase in shale and siltstone intervals compared to line A-B (Fig. 21).

trending northwest-southeast, in this model appear as canyon or channel meanders. Sections in the meanders may show alternating conglomerate and quartz arenite horizons (Hubert's sections 10, 15 and 28) and reflect canyon or channel shifting. The circle in Figure 23 depicts a complex meander bend that has shifted several times. Figure 24 illustrates a correlation between sections 9, 10 and 28 present in the complex meander. Channel shifting is associated with the presence of isolated conglomerate lenses. This lenticularity was noticed by Hubert (1973) but he envisaged alluvial fans as depositional environment.

The documented canyon (channel) only reflects the deepest parts of the conduit that supplied the deep-sea sand and conglomerate of the Kamouraska Formation. Two hatched lines were drawn to expand this channel, in order to encompass the wider distribution of the quartz arenites higher up in the sections that possibly reflects shifting meander bends. The geometry suggests that the Kamouraska Formation was deposited in a canyon, most likely on the slope. The canyon restricted the transport of the basal conglomerates to the southeast. A width of 15 km is estimated for the shifting meandering canyon belt in the northern parts of the study area (Fig. 24) that narrows to less than 7 km in the south. This width is probably underestimated due to folding. The estimated width is in line with widths of modern canyons (e.g., Zaire Canyon: maximum width of 15 km, Babonneau et al., 2002). The thickness of the canyon fill is in the order of 250-300 m similar to some modern submarine canyons (e.g. Cap-Timris Canyon offshore northwestern Africa; Krastel et al., 2004). Hubert (1973) reported a thickness of up to 370 m for the Kamouraska Formation.

In some locations northeast of the study area the Kamouraska Formation is not as thick and is characterized by a higher frequency of shale interbeds (for example on Ile Verte and at Matane). One might envisage another separate, NE-SW oriented canyon in the Matane area which is far away from the study area. However, on Ile Verte, the Kamouraska Formation most likely belongs to the same meandering canyon due to proximity and alignment with the envisaged

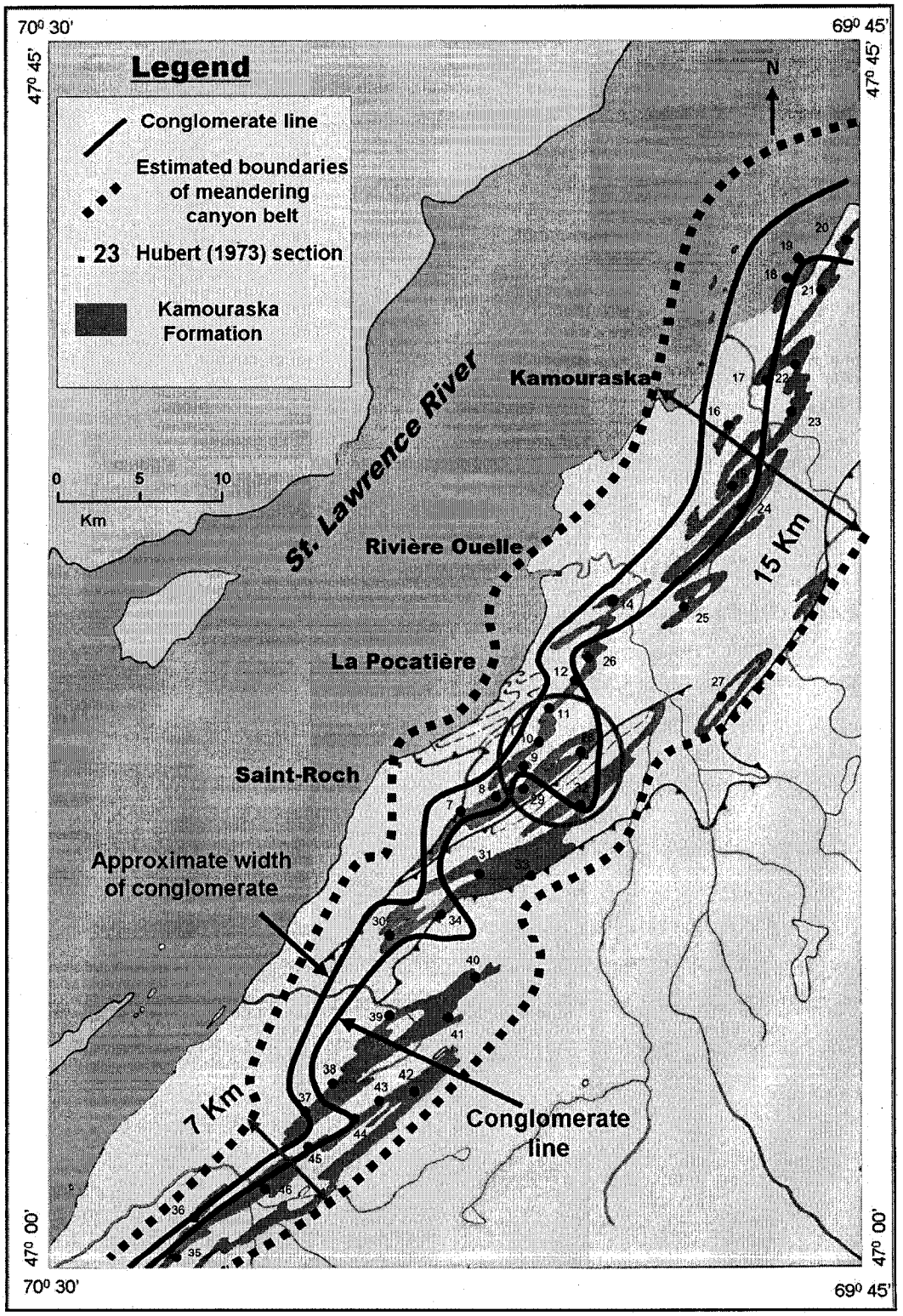

Figure 23: Approximate width of the conglomerate (solid lines) which reflects the basal parts of the meandering canyon. Complex meander bend circled in red. For correlation between sections 9, 10 and 28 see Figure 24. Hatched lines: Estimated width of shifting meandering canyon.

canyon of the study area. The lower thickness and the higher frequency of shale interbeds in the Ile Verte and Matane areas could be attributed to a position at the margin of the canyon where lower thickness and higher frequency of shale interbeds would be expected.

Unfortunately, apart from the few local measurements reported here and in Hubert (1973), regional paleocurrent maps are not available for the Kamouraska Formation in order to defend the hypothesis beyond doubt. Furthermore the regional distribution of the sandstones to conglomerates in the underlying Saint-Damase Formation that could serve as an analog at a lower stratigraphic level is not well enough constrained to support or contradict the proposed hypothesis. It is very difficult to delineate the exact depositional setting of the Kamouraska Formation. However, the coarseness of some of the channelized deposits in outcrops from the same region and similar age (e.g., Grosses Roches, Hendry; 1978) point towards a slope setting rather than a deep-sea channel system on the rise. The somewhat older canyon at L'Islet-sur-Mer (Walker, 1978) suggests that the same setting prevailed already in Cambrian time. The envisaged meandering canyon environment remains speculative, however, as it is not known whether the Kamouraska Formation is restricted to the present outcrop belt or had a much wider original distribution in rocks hidden in the subsurface or lost due to erosion.

11. CONCENTRATED DENSITY FLOWS OF EOLIAN SAND

Sarnthein and Diester-Haass (1977) documented the presence of thick beds of eolian sand on an abyssal plain of the eastern Atlantic, off West-Africa. These beds consist of clean quartz arenitic sand and are characterized by massive bedding and commonly coarse tail grading. These authors interpreted the deposits as turbidites and called them "eolian-sand turbidites" because they consist of eolian sand.

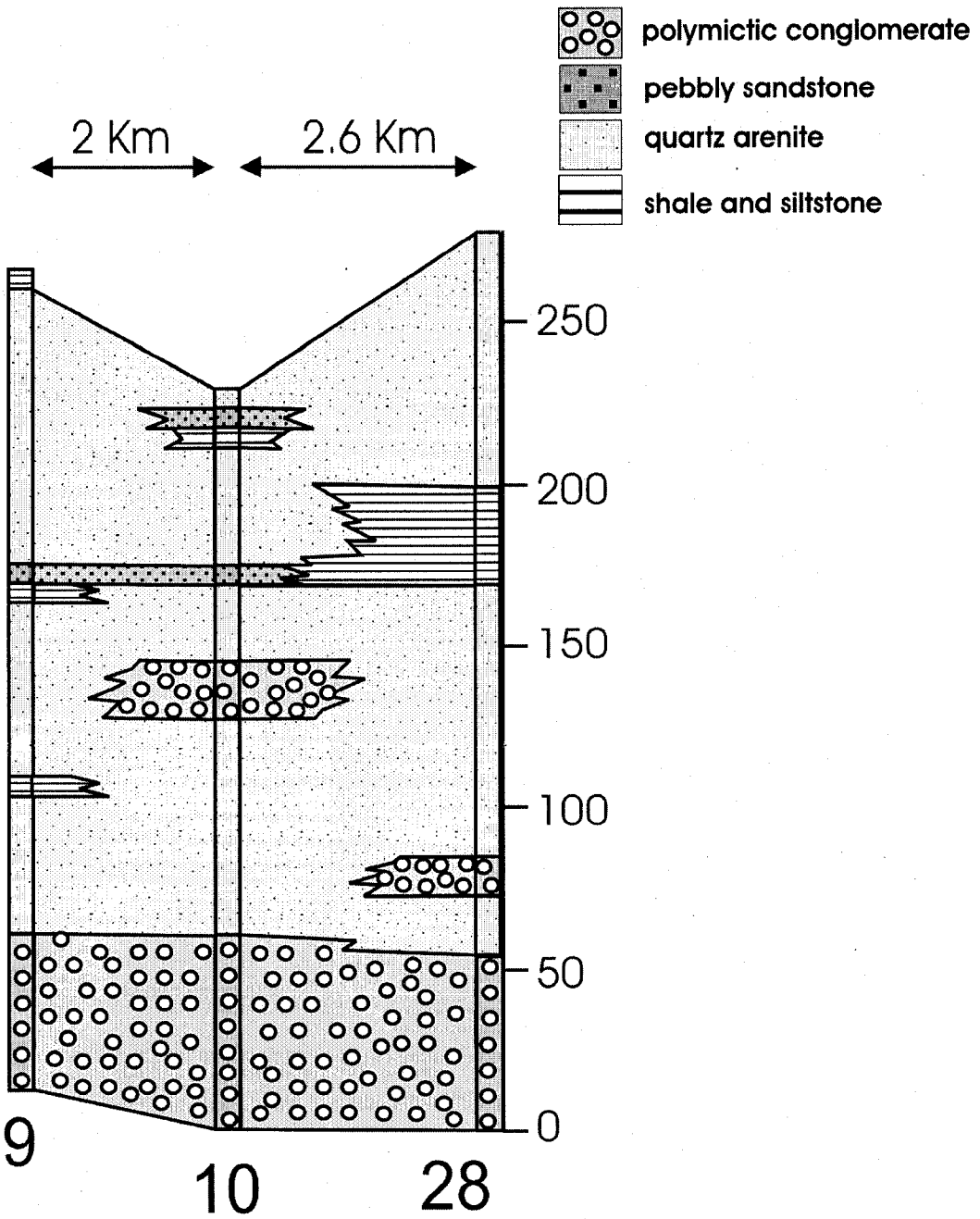

Figure 24: Correlation between sections 9, 10 and 28 within the complex meander bend (indicated by red circle in Fig. 24). Episode 2 of conglomerate deposition was localized in section 28. Channel shift is expressed in episode 3 of conglomerate deposition in section 10 as the channel shifts away from section 28. Section 28 is later topped by a thick shale and siltstone interval which suggest a halt in deposition as this part of the channel was abandoned. As other parts of the channel were filled sedimentation later resumed in 28. Notice lenticularity of the conglomerates.

Sarnthein and Diester-Haass (1977) related the occurrence of the eolian sand turbidites off West Africa to Pleistocene glacial sea level low-stands. The drop in sea level permitted eolian sand dunes of the Western Sahara to cross the exposed continental shelf to the shelf edge, where the eolian sand would be blown into the near-shore zone, entrained by long-shore currents and ultimately trapped in the heads of submarine canyons. Turbidity currents triggered in the canyons subsequently moved the sand into the deep sea as turbidites where the sand still retained its eolian characteristics.

Detailed investigation has shown that the quartz arenites of the Kamouraska Formation resemble and retain characteristics of eolian (desert) sand. This finding is supported by the following facts:

1) The bulk of the grain sizes present range from 0.125 to 0.5 mm in diameter (Figs. 15 and 16). Grain sizes measured by Sarnthein and Diester-Haass (1977) range from 0.15 to 0.45 mm. This range of grain sizes is characteristic of wind-blown sand. Wind-blown sand from deserts around the world has grain sizes that range from 0.06 to 2 mm (Pye and Tsoar, 1990); however the bulk diameter is between 0.125 and 0.25 mm (Ahlbrandt, 1979).
2) The near vertical cumulative grain size curves frequently indicate moderately well sorted (this study) to well sorted sand (Hubert, 1973). Desert dune-sands are usually moderately well sorted (Ahlbrandt, 1979; Edgell, 2006). In this respect the moderately well to well sorted quartz arenites of the Kamouraska Formation resemble eolian sand, in line with the observations of Sarnthein and Diester-Haass (1977).
3) The dominance of well rounded grains with pitted and frosted surfaces support an eolian phase of transport, also in accordance with Sarnthein and Diester-Haass' (1977) observations.
4) The SEM study of grain surface textures revealed surface textures characteristic of wind-blown sand. Smoothed over upturned plates,

bulbous edges, and irregular depressions (pits) all favor an eolian stage in the history of these sands.

5) The predominance of quartz (averaging more than 96% and frequently more than 99%) in itself is not a necessary attribute of eolian sand (e.g. Folk, 1968); however many eolian sands have a high quartz content.

For these reasons, the quartz arenites of the Kamouraska Formation are interpreted to have inherited eolian characteristics, either from residence in an inland desert or, less likely, in eolian beach dunes. Many of the characteristics discussed are in line with the observations of Sarnthein and Diester-Haass (1977).

The position of the northern margin of Laurentia during the Late Cambrian and Early Ordovician was between $10^0 - 30^0$ south. This position would have placed Laurentia in the desert belt thus locating the study area in the proper latitudes for desert formation. The absence of land plants during Late Cambrian and Early Ordovician times would have promoted the formation of deserts on a barren earth.

If the quartz arenites of the Kamouraska Formation are of eolian origin, then how did they reach the deep sea?

A sea level lowstand has been documented for the end of the Cambrian (Sloss, 1963; James et al. 1989; Salad Hersi et al., 2002a, b; Lavoie et al., 2003) and correlates with the onset of deposition of the Kamouraska Formation (age range from latest Cambrian to earliest Ordovician (middle Tremadocian); see Section 5). Following the model proposed by Sarnthein and Diester-Haass (1977), the sea level lowstand would have paved the way for the eolian sand to cross the continental shelf and end up in the deep sea (Fig. 25).

As has been discussed in the petrography section there is evidence from thin sections for some mixing (Fig. 14, sub-lithologies 2, 3 and 4) in the form of feldspar grains that are coarser than the average grain size (Fig. 13D). Thin

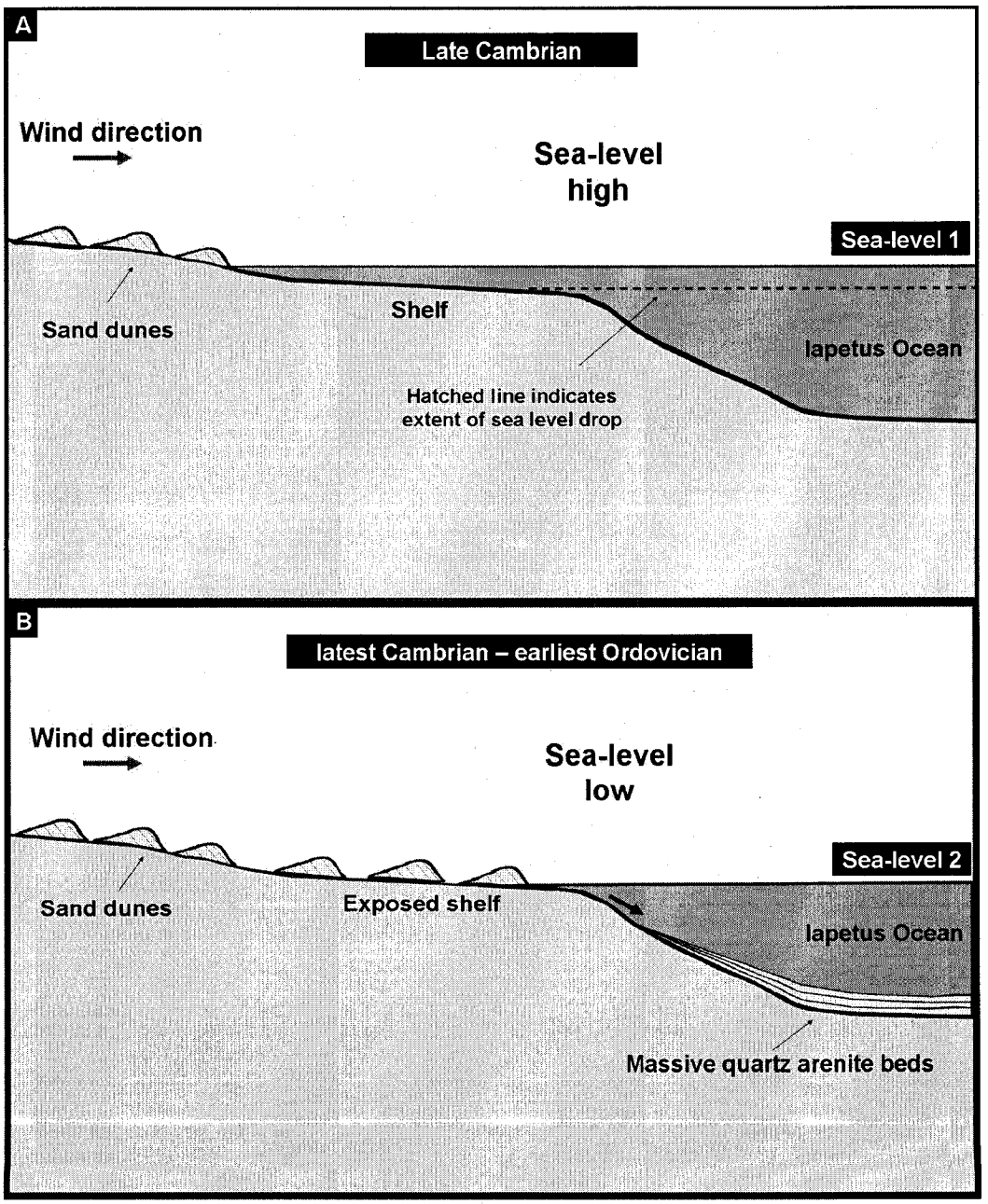

Figure 25: Eolian-sand turbidite model. A) Seaward eolian dune migration ends at the coast and sand is subsequently redistributed on the shelf. B) After a sea-level drop, eolian dunes cross the exposed shelf and reach the shelf edge, from where the sand is transferred into the deep sea by sediment gravity flows. See text for details (modified after Sarnthein and Diester-Haass, 1977).

sections containing oversized feldspar also have poorer sorting and a higher than average feldspar content. Quartz arenite samples that contain no or very little feldspar and are well sorted (Fig.14, sub-lithologies 1 and 5), apparently represent the quartz rich source of eolian dune sand. In case of sublithologies 2, 3 and 4, material from this source likely has been mixed with a feldspar-rich source. This feldspar-rich source may have been the same source that supplied the sand for the underlying feldspathic arenites of the Saint Damase Formation.

The conglomeratic horizons in the basal parts of the Kamouraska Formation have a source different from the quartz arenites. Their provenance and that of other Paleozoic conglomerates in the Appalachian Humber Zone has been thoroughly documented in the literature. Lavoie et al. (2003) suggested significant tectonic activity near the Saguenay Aulacogen to explain the Lower to Upper Cambrian limestone clasts in the Trois Pistoles Group. An equally wide age range is not known in the time correlative conglomerates in Newfoundland. The widely accepted interpretation is that the conglomerates are of platform margin origin and have been supplied to the slope by instabilities on the shelf (Davies and Walker, 1974; Lajoie et al., 1974; St. Julien and Hubert, 1975; Hein, 1982; Hein and Walker, 1982; Vallières, 1984; James et al., 1989; Bernstein et al., 1992; Landing et al., 1992; Lavoie, 1997; Maletz, 1997; Salad Hersi et al. 2002a, Lavoie et al., 2003), an interpretation that is adopted for the basal Kamouraska Formation.

12. PROVENANCE OF EOLIAN SAND

Figure 26 shows age correlations between platform formations in southern Quebec and the slope formations of the featured Rivière Boyer Nappe. These correlations are based on data from various studies summarized in Lavoie et al. (2003).

The Potsdam Group sandstones represent the earliest terrestrial and shallow-marine siliciclastic sediments on the (autochthonous) platform of

southern Quebec. The Potsdam Group lies unconformably on Precambrian basement and is divided into the basal Covey Hill Formation and the overlying Cairnside Formation. The Covey Hill Formation consists of arkosic sandstones and conglomerates deposited by braided rivers and on alluvial fans. The Cairnside Formation consists of clean quartz arenite of medium to coarse, well sorted and well rounded sand and is shallow marine (Clark, 1966, 1972, Lewis, 1972). Like the Covey Hill, the Cairnside is unfossiliferous; however some ichnofossils occur. The Covey Hill and the Cairnside formations are separated by an erosional unconformity. This unconformity has been described as sub-aerial and related to eolian activity (Clark, 1972). Another intraformational unconformity was described from within the Cairnside Formation (Clark, 1966). The Potsdam Group extends into Ontario where both the Covey Hill and the Cairnside formations are present. The latter is referred to as the Nepean Formation in Ontario where it is Tremadocian in age (Brand and Rust, 1977). Wolf and Dalrymple (1984, 1985) differentiated 5 sandstone facies in the Nepean Formation in Southeastern Ontario. Most regionally widespread is a facies consisting of alternating cross-bedded and bioturbated quartz arenite which represents a prograding tide-dominated shallow marine environment (facies 3, Wolf and Dalyrmple, 1985). The second most extensive facies is characterized by large scale cross-bedding and was interpreted as an inland eolian dune system which is uniquely preserved in many outcrops all over eastern Ontario (facies 2, Wolf and Dalrymple, 1985). The remaining three facies are much less widespread and are: wave-dominated near shore environment, storm-dominated marine environment and braided fluvial to estuarine environments.

The Cambrian formations of the Phillipsburg Group represent the extension of the Potsdam Group into a carbonate shelf (Lavoie et al., 2003), (Fig. 26) The Ordovician formations of the Beekmantown and the Phillipsburg groups reflect a major transgression in the Early Ordovician (Late Tremadocian) which flooded the platform and culminated in the formation of a carbonate shelf (Lavoie et al., 2003).

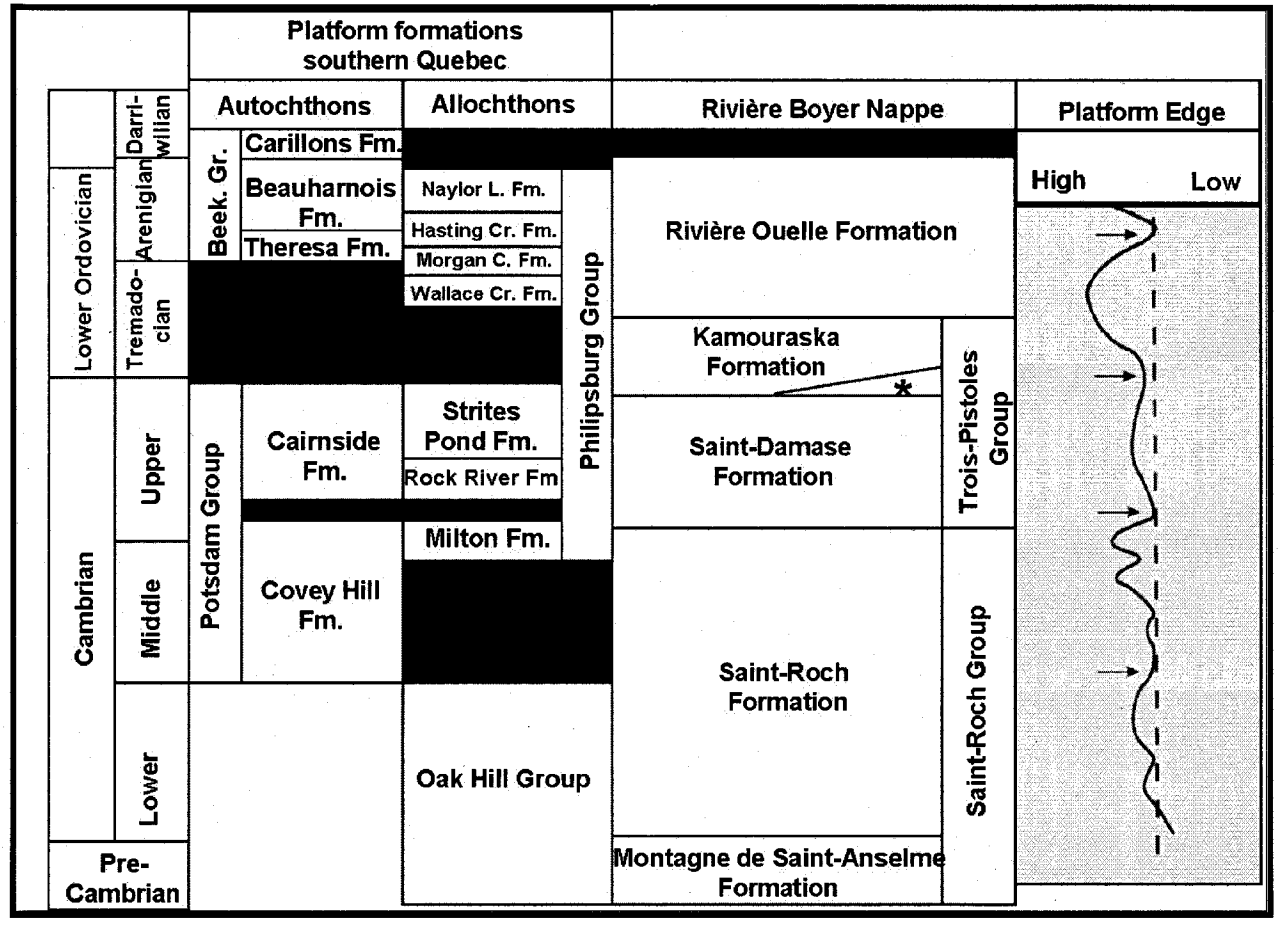

Figure 26: Correlation between platform formations in southern Quebec and the Rivière Boyer Nappe (modified after Lavoie et al., 2003; Sea level curve after James et al., 1989). Dark areas are periods of non-deposition and erosion. Notice correlation of hiatus (on the platform) at the end of the Cambrian with the Kamouraska Formation. Arrows indicate sea level low. (*) = Rivière-du-Loup Formation. Beek Gr. = Beekmantown Group; Fm. = Formation; L. = Ledge; Cr. = Creek; C. = Corner. See text for detail.

For the problem of the provenance of the eolian quartz sands of the Kamouraska Formation it is important that Salad Hersi et al. (2002a) documented the presence of an erosional unconformity at the top of the Cairnside Formation in southwestern Quebec and southeastern Ontario, by which it is separated from the overlying basal parts of the Theresa Formation of the Beekmantown Group (Fig. 26). The Theresa Formation is characterized by dolomitic sandstone, sandy dolomite, and dolomite beds which accumulated in a deeper marine shelf environment (Salad Hersi et al., 2002a). Conodonts recovered from the basal parts of the Theresa Formation indicate an Early Ordovician age (Late Tremadocian to Early Arenigian). No fossils were ever recovered from the Cairnside Formation and thus the age of the unconformity and the span of the hiatus are not constrained. Salad Hersi and Lavoie (2001) documented a similar erosional unconformity in the Philipsburg slice of southern Quebec which is the westernmost Taconian Nappe in the Humber Zone of the Quebec Appalachians. This unconformity is located at the top of the Strites Pond Formation of the Philipsburg Group and separates the latter (consisting of coarse crystalline dolostone and limestone) from the overlying Wallace Creek Formation (characterized by intraclastic and bioclastic wackestone and packstone). Conodonts recovered from the bottom of the Wallace Creek Formation indicate an Early Ordovician (Late Tremadocian) age and suggest a hiatus similar to that observed between the Cairnside and the Theresa Formation (Salad Hersi et al., 2002a, b; Lavoie et al., 2003) (Fig. 26). The erosional unconformity documented in both areas was correlated; hence the tops of both the Cairnside Formation and the Strites Pond Formation are considered time equivalent (Salad Hersi et al., 2002a; Salad Hersi et al., 2002b). Conodonts recovered close to the top of the Strites Pond Formation indicate a Late Cambrian age. This suggests that the erosional unconformity and associated hiatus spanned an interval from latest Cambrian into Early Tremadocian (Fig. 26). The erosional unconformity was described as sub-aerial and its extension onto the carbonate platform (Strites Pond Formation) is characterized by cavities filled with medium to coarse sand resembling that of the Cairnside Formation.

This Late Cambrian – Early Ordovician unconformity has been documented in various parts of the Laurentian margin (Salad Hersi et al., 2002a). It has been correlated from Ottawa to Montreal to Sainte-Croix (Salad Hersi et al., 2002a). In northeastern Quebec an unconformity is documented between the Arenigian Romaine Formation (Lower Paleozoic succession on Mingan and Anticosti islands) and the underlying Precambrian rocks (Nowlan, 1981; Desrochers, 1988) and could be indirectly correlated. It is documented in New York State, on the southern flank of the Adirondack Mountains, including the Mohawk Valley, Saratoga Springs and southern Champlain Valley (Mazzullo et al., 1978; Westrop et al., 1993; Landing et al., 1996). This unconformity has been interpreted as a result of a eustatic sea level fall at the end of the Cambrian (Salad Hersi et al., 2002a; Lavoie et al., 2003) which persisted on the platform of southern Quebec into the Early Tremadocian.

This erosional unconformity and the associated hiatus suggest that a long period of erosion and non-deposition prevailed on the platform and eroded the exposed platform formations during latest Cambrian-early Tremadocian. Denudation has been reported for the Cairnside Formation (Wilson, 1937; Salad Hersi et al. 2002a – their stratigraphic sections 6 & 7) where entire sections are missing. The equivalent of the unconformity on the slope is characterized by the shedding of conglomerates and quartz arenites (Salad Hersi et al. 2002a; Lavoie et al., 2003) preserved in the Humber Zone of the Quebec Appalachians, in Western Newfoundland (James and Stevens, 1986; James et al., 1989), and in the Taconian belt of eastern New York (Landing, 1993).

The model presented here of eolian sand crossing the shelf and being deposited in the deep sea fits into the regional shelf – slope correlations. The age range assigned for the Kamouraska Formation, from latest Cambrian to early Tremadocian appears to correlate with the hiatus on the platform. The model would explain the presence of extensive quartz sand on the slope. If a desert had existed on the platform and migrated seaward, then an erosional unconformity and

hiatus are to be expected. The presence of shallow marine facies of the Cairnside Formation reflects the Late Cambrian paleogeography when eolian dunes were restricted to inland areas (Napean Formation). Only during the latest Cambrian sea level drop were the dunes able to cross the shelf. Eolian sand dunes are the fastest moving sand bodies with average migration rates of 10-30 m/year or 1000-3000 km/100,000yrs (Cooke et al., 1993). The apparent absence of preserved eolian dunes in the Cairnside Formation (except for remnants in the Nepean Formation) is attributed to the poor preservation potential of eolian dunes in the geological record. It needs to be remembered that the total thickness of inland deserts may be very limited. The present Sahara has an average sand thickness of 26 m. Wolf and Dalrymple (1985) advocated an eolian dune system on the platform during the time of deposition of the Nepean Formation. They believed that eolian conditions continued in coastal zones of the advancing sea until marine waters drowned the dune complex. The other facies of Nepean Formation documented by Wolf and Dalrymple (1985) have been attributed to sand reworking in various marine environments upon subsequent sea level rise. The absence of an inland dune facies in the Cairnside Formation of southern Quebec is similarly attributed to the rise in sea level which probably reworked the dunes and dispersed the sand on the shelf.

It is suggested here that the bulk of the quartz sand of the Kamouraska Formation was supplied by eolian environments equivalent to those of the eolian part of the Nepean Formation (Cairnside Formation). This is supported by the arguments presented above: the tentative correlation of the Kamouraska Formation with the unconformity and hiatus at the top of the Cairnside; the evidence of erosion and denudation in the Cairnside Formation; the presence of Cairnside sand in karstic cavities on the shelf; the preservation of a cross-bedded inland dune system in the Nepean Formation in Ontario. Furthermore, the lithological similarity between the quartz arenites of Kamouraska and the Cairnside formations supports this argument. The Cairnside Formation is characterized by clean quartz sand (predominantly monocrystalline quartz)

containing no feldspar or clay matrix. Grain sizes are dominantly of medium to coarse sand. The sand is well sorted and the grains are well rounded.

The slightly finer grain size observed in the Kamouraska Formation (medium to fine sand) is attributed to the longer transport distance in active migrating dunes. Examples from modern dune fields in Arabia show a change in granulometry from inactive inland dunes to coastal dunes (Edgell, 2006). Migrating dunes are dominantly associated with finer grain sizes. Stabilized or inactive dune fields are associated with coarser grain sizes. Studies have shown that there is a direct relationship between granulometry and relative ages of barchans. The youngest dunes have the finest sizes (fine sand) averaging (63-125 μm). In the active (migrating) dunes, the mode shifts to coarser sizes of medium to fine sand averaging 125-250 μm. Inactive dunes have the coarsest fractions (medium sand) averaging 260-500 μm (Belser, 2002). This relationship is clearly observed in the Great Nafud sand sea of Arabia which consists of 95% stable dunes. Whitney et al. (1983) attributed the better sorting of active dunes in the Great Nafud to winnowing of pre-existing stable dunes. This relationship was also noticed in Ad Dahna sand sea of Arabia (Edgell, 2006), in Al Qashiniyah and Al Wafra sand sheets of Kuwait (Khalaf et al., 1985, Khalaf et al., 1989a, Khalaf et al., 1989b), in Ash Shamiya desert in southern Irak (Skoček and Saadalah, 1972), and in Ramlat Al Wahibah in eastern Oman (Goudi et al., 1987).

The presence of oversized feldspar grains and slight deterioration in the degree of sorting of some of the quartz arenites of the Kamouraska Formation (sub-lithologies 2, 3 and 4) is attributed to mixing as previously discussed. The presence of some, albeit low matrix content in the Kamouraska Formation (~ 2%) is attributed to admixture of eroded clayey sediment (including the churning up of mudclasts) by the concentrated gravity flows and turbidity currents.

For the above reasons we suggest that the Cairnside Formation or an equivalent quartz arenite formation provided most of the sand to the deep sea

Kamouraska Formation. The Cap-aux-Oies Formation (Belt et al., 1979) in the La Malbaie Area on the north shore of the Gulf of St. Lawrence is the northernmost known occurrence of quartz arenites on the platform at about the same latitude as the outcrops of the Kamouraska Formation. The source of the Kamouraska Formation must have still been located farther to the north. The Cap-Aux-Oies Formation is shallow marine but could have had eolian equivalents farther inland as the Cairnside Formation has which could have been the source of eolian quartz sand in the deep sea. The Cap-Aux-Oies Formation is overlain by the pre-Middle Ordovician Cap-a-L'Aigle Formation, but otherwise its age is not constrained.

Under normal circumstances linking a deep sea deposit with a platform formation might not be possible. This is because the transport of sand in the various environments leads to mixing of different sources and the resultant sand does not have a single provenance. The unique mode of deposition of the quartz arenites of the Kamouraska Formation as redeposited eolian-sands in the deep sea renders such a correlation possible.

13. RELATIONSHIP TO DICKINSON AND SUCZEK'S (1979) TECTONIC SANDSTONE PROVENANCE MODEL

The last point in this discussion pertains to sandstone provenance schemes pioneered by Krynine in the 1940s and revolutionized by Dickinson and Suczek (1979).

Dickinson and Suczek (1979) noticed that provenance, mode of transport and the receiving basin are all inter-related and directly related to tectonic setting of the source areas. According to these authors the plate tectonic position of the source area is the main controlling factor for sandstone composition. Dickinson and Suczek (1979) established a systematic relationship between sandstone composition and tectonic setting and classified sandstones into three provenance groups: Those of continental block provenance, those of magmatic arc

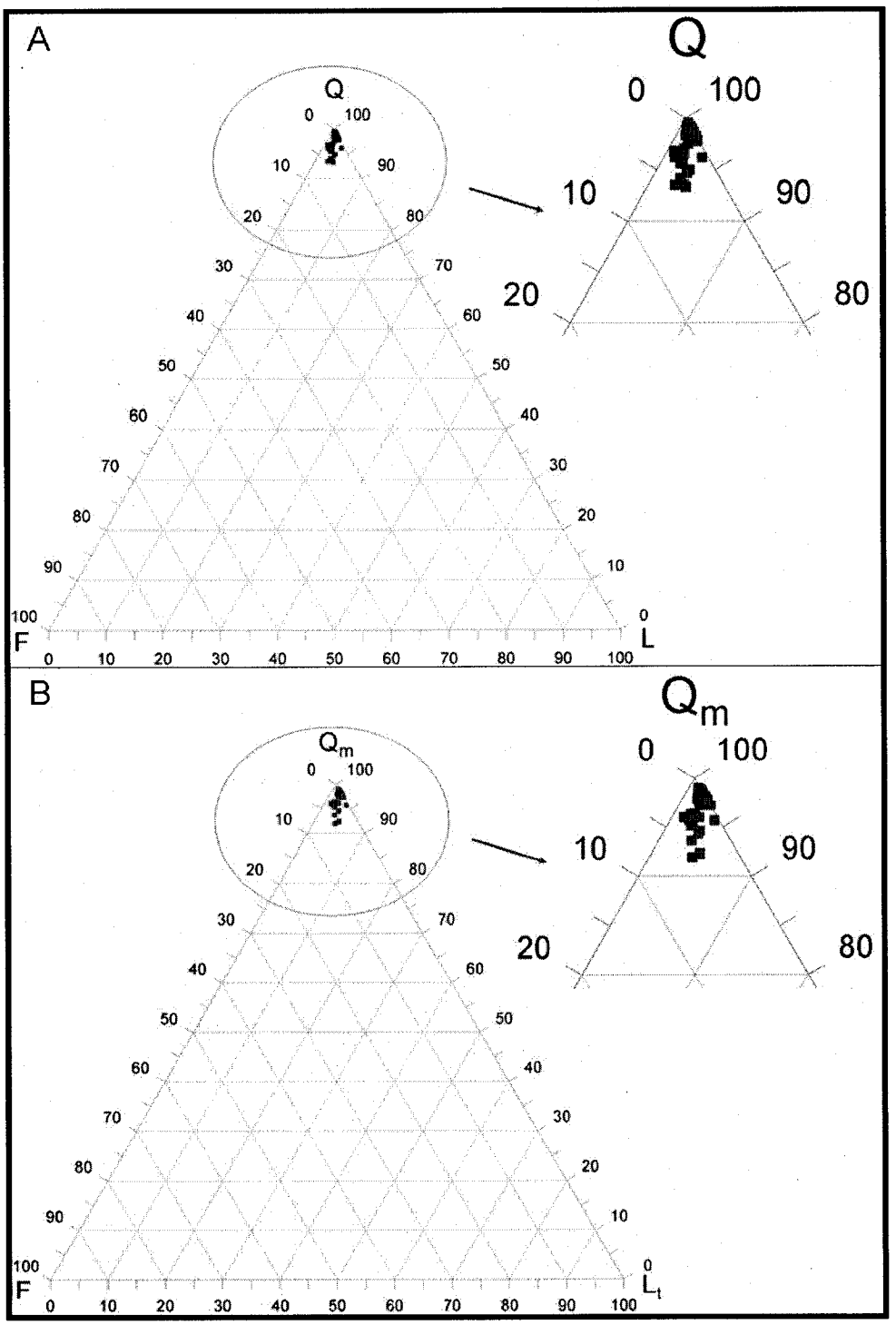

Figure 27: QFL and Q_mFL_t plots for the quartz arenites of the Kamouraska Formation. Q - total quartz, both monocrystalline and polycrystalline, including chert; Q_m - monocrystalline quartz; F - total feldspar; L – lithic fragments without quartz lithic fragments (Q_p); L_t - total lithic fragments. Notice the clustering of data points near the Q and Q_m poles in both the QFL and Q_mFL_t diagrams.

provenance and those of recycled orogen provenance; all of which plot in different areas of ternary QFL and QmFLt diagrams.

The presence of thick massive beds of clean quartz sand of the Kamouraska Formation in the deep sea provokes interesting questions in the light that they differ from the feldspathic arenites and wackes of the underlying deep sea formations (the Saint Damase and Saint Roch, respectively). The quartz arenites of the Kamouraska Formation plot in the field of continental block provenance on both the QFL and QmFLt triangles (Figure 27). According to Dickinson and Suczek (1979) these sandstones would have a cratonic provenance and are associated with long distances of transport and deposition in shallow continental basins. Indeed, the Kamouraska Formation must have had a cratonic provenance and its sands did travel long distances; however, deposition in the deep sea reflects a variant to its expected depositional site in a shallow basin. The mode of transport and deposition of these eolian sands by concentrated flows and turbidity currents suggests unique conditions for the occurrence of quartz arenites in the deep sea.

14. CONCLUSIONS

A) The Kamouraska Formation represents quartz arenites and conglomerates that have been shed onto the continental slope by means of subaqueous gravity flows. These flows change from north to south from hyperconcentrated density flows (disorganized or reversely graded grain-supported conglomerates) to concentrated flows (massive sand beds with coarse tail grading) to turbidity currents (thin beds with turbidite structure divisions).

B) Field evidence from numerous sections visited by Hubert (1973) suggests that the likely depositional environment of the Kamouraska Formation is a meandering northeast-southwest trending submarine canyon on the slope.

The estimated width of the shifting canyon belt decreases from 15 km in the north to less than 7 km in the south over a distance of 75 km. The width of the canyon is underestimated because no palinspastic section was constructed from the fold structures in which the Kamouraska Formation occurs.

C) The quartz arenites of the Kamouraska Formation have an eolian provenance. The conglomerates have a different provenance and are associated with sediment shedding from the shelf edge.

D) The likely source for the quartz arenites of the Kamouraska Formation is an equivalent of Cairnside Formation (uppermost formation of the Potsdam Group) or a similar correlative formation (e.g. eolian equivalent of the Cap-aux-Oies Formation). This is based on lithological similarities; the assumed time equivalence of the hiatus and erosional unconformity at the top of the Cairnside Formation and its northern equivalents with the time of deposition of the Kamouraska Formation; the large areas where the Cairnside Formation and its equivalents are absent and most likely denudated; the presence of Cairnside Formation sand filling karstic pockets in at the top of the Strites Pond Formation caused by sea level fall; the presence of prominent large scale cross-bedded eolian dunes in inland equivalents of the Cairnside Formation (the Nepean Formation of Ontario).

E) The following points summarize the reasons for advocating an eolian-sand turbidite model:

1- The dominance of quartz sand in the deep sea.

2- The presence of well sorted sand in the deep sea.

3- The grain sizes characteristic of eolian sand.

4- The well rounded nature of the quartz grains.

5- The presence of pitted and frosted surfaces.

6- The presence of eolian signatures confirmed by SEM.

7- The orientation of Laurentia during the Late Cambrian and Early Ordovician, between 10^0 and 30^0 South, which positions it in the desert belt.

8- The absence of land plants during Late Cambrian and Early Ordovician promoting wind activity.

9- The presence of a sea level lowstand at the end of the Cambrian and early Ordovician which allowed eolian sand migration across the shelf.

10- The presence of an erosional unconformity on the platform at the Cambrian-Ordovician boundary and a hiatus during the latest Cambrian - early Tremadocian that correlate with the time of deposition of the Kamouraska Formation on the slope.

11- The presence of a platform equivalent, the Cairnside Formation, with preserved remnants of an eolian dune system (Nepean Formation in southeastern Ontario).

12- The presence of Cairnside-like sand preserved on the shelf in karstic voids of the Strites Pond Formation which indicates seaward sand migration on the shelf.

13- The presence of modern equivalents of eolian sand reaching the deep sea by means of turbidity currents (e.g., off-shore West Africa) and showing that such a mechanism is feasible.

None of the 13 points listed above taken alone has the power to exclusively suggest an eolian heritage for deep-sea sands. It is the combination of all these arguments which led to the proposed eolian-sand turbidite model. The sea level lowstand at the end of the Cambrian is a crucial part of the suggested model. Sarnthein and Diester-Haass (1977) showed that when dealing with rapidly migrating landforms such as desert dunes, this model could operate over a few millions years. Dune migration at average rates of 1000-3000km/100,000yrs would provide large

quantities of sand to the shelf in a short period of time. A short period of exposed shelf (i.e. short period of sea level fall) is sufficient for sand to reach canyon heads and subsequently being deposited in the deep sea.

F) The presence of quartz arenites in the deep sea has implications on the tectonic sandstone provenance scheme of Dickinson and Suczek (1979). It is an exception to their continental block provenance for quartz arenites.

ACKNOWLEDGMENTS

I would like to take the opportunity to acknowledge my research supervisor Dr. Reinhard Hesse for his dedicated support of this study. His interest, experience, and guidance have provided invaluable help for this work and insight into the problems studied. I would also like to thank Dr. Aicha Achab and Esther Asselin from the Institute National de Recherche Scientific, Eau, Terre et Environment (INRS-ETE) for their help in organic matter extraction and search for siliceous microfossils. Special thanks go to Dr. John Riva for his help in identifying controversial ramified dendroids in the quartz arenites. I would also like to acknowledge Mr. Jake Ross who assisted me in parts of the field work, Ms. Yuliana Proenza who provided timely help in sample preparation, Mrs. Anne-Marie Abi-Nader who conducted the French translation of the abstract and Dr. Jeanne Paquette who revised and enhanced the translation. I also extend my thanks to the Department of Earth and Planetary Sciences at McGill University for providing the use of its facilities. NSERC funding of this research through a discovery grant to R. Hesse is gratefully acknowledged.

BIBLIOGRAPHY

Ahlbrandt, T.S. (1979). Textural parameters of eolian deposits. *In* E. D. McKee (ed.) A Study of Global Sand Seas, Profesional Papers, U.S. Geological Survey, no.1052, pp. 21–51.

Asselin, E., Achab, A. and Soufiane, A. (2004). Biostratigraphic significance of lower Paleozoic microfaunas from eastern Canada. Canadian Journal of Earth Sciences, 41: 489-505.

Babonneau, N., Savoye, B., Cremer, M., Klein, B. (2002). Morphology and architecture of the present canyon and channel system of the Zaire deep-sea fan. Marine and Petroleum Geology 19: 445–467.

Bagnold, R.A. (1954). Experiments on a gravity-free dispersion of large solid spheres in a Newtonian fluid under shear. Proceedings of the Royal Society of London, A225: 49-63.

Barnes, N.E. and Normark W.R. (1985). Diagnostic parameters for comparing modern submarine fans and ancient turbidite systems. In A.H. Bouma, W.R. Normark, N.E. Barnes (Eds.), Submarine Fans and Related Turbidite Systems, Springer-Verlag, New York, pp.13-14.

Besler, H. (2002). Complex barchans in the Libyan Desert: dune traps or overtaking solitons? Zeitschrift fur Geomorphologie N.F., 126: 59-74.

Belt, E.S., Riva, J., and Bussières, L. (1979). Revision and correlation of Late Middle Ordovician stratigraphy northeast of Québec City. Canadian Journal of Earth Sciences, 16: 1467 -1483.

Bernstein, L., James, N.P., and Lavoie, D. (1992). Cambro-Ordovician stratigraphy in the Québec Reentrant, Grosses-Roches – Les Méchins area, Gaspésie, Québec. *In* Current research, part E. Geological Survey of Canada, Paper 92-1E, pp. 381–392.

Bouma, A.H. (1962). Sedimentology of some flysch deposits: A graphic approach to facies interpretation. Elsevier, Amsterdam, 168pp.

Brand, U. and Rust, B.R. (1977). The age and upper boundary of the Nepean Formation in its type section near Ottawa, Ontario. Canadian Journal of Earth Sciences, 14: 2002-2006.

Burden, E. (2000). Palynomorph biostratigraphy of 13 outcrop samples from various localities in eastern Canada. Omnichron Associates, final report to the Geological Survey of Canada.

Burden, E. (2001). Palynomorph biostratigraphy of 30 outcrop samples from various localities in eastern Québec, Canada. Omnichron Associates, final report to the Geological Survey of Canada.

Carlson, P.R., and Karl, H.A. (1988). Development of large submarine canyons in the Bering Sea, indicated by morphologic, seismic and sedimentologic characteristics. Geological Society of America Bulletin, 100: 1594- 1615.

Castonguay, S., Tremblay, A., Ruffet, G., Féraud, G., Pinet, N., and Sosson, M., (1997). Ordovician and Silurian metamorphic cooling ages along the Laurentian margin of the Quebec Appalachians: Bridging the gap between New England and Newfoundland: Geology, 25: 583-586.

Castonguay, S., Dietrich, J.R., Morin, C., and Laliberté, J.-Y. (2001). Structural architecture of the St. Lawrence platform and Québec Appalachians: insights from reprocessed (MRNQ) seismic reflection data. Geological Survey of Canada, Open File 4028.

Cawood, P.A., Van Gool, J.A.M., and Dunning, G.R., (1995). Collisional tectonics along the Laurentian margin of the Newfoundland Appalachians. *In* J.P. Hibbard, et al. (Eds.), Current perspectives in the Appalachian-Caledonian Orogen: Geological Association of Canada Special Paper 41: 283–301.

Cawood, P.A., van Gool, J.A.M., and Dunning, G.R. (1996). Geological development of eastern Humber and western Dunnage zones: Corner Brook – Glover Island region, Newfoundland. Canadian Journal of Earth Sciences, 33: 182–198.

Cawood, P.A., McCausland, P.J.A., and Dunning, G.R. (2001). Opening Iapetus: Constraints from Laurentian margin in Newfoundland. Geological Society of America Bulletin, 113: 443-453.

Cheel, R.J. and Middleton, G.V. (1986). Horizontal laminae formed under upper flow regime plane bed conditions. Journal of Geology, 94: 489-504.

Clark, J. D., Kenyon, N. H., and Pickering, K. T. (1992). Quantitative analysis of the geometry of submarine channels: implications for the classification of submarine fans. Geology, 20: 633–636.

Clark, T.H. (1966). Chateauguay area. Ministère de l'Énergie et des Ressources du Québec, Geological Report RG-122.

Clark, T.H. (1972). Montréal area. Ministère de l'Énergie et des Ressources du Québec, Geological Report RG-152.

Cooke, R. U., Warren, A., and Goudie, A. S. (1993). Desert Geomorphology, London, UCL Press, 526 p.

Damuth, J. E., V. Kolla, R. D. Flood, R. O. Kowsmann, M. C. Monteiro, M. A. Gorini, J. J. C. Palma, and Belderson, R. H. (1983). Distributary channel meandering and bifurcation patterns on the Amazon deep-sea fan as revealed by long-range side-scan sonar (GLORIA). Geology, 11: 94–98.

Davies, I.C. and Walker, R.J. (1974). Transport and deposition of resedimented conglomerates: the Cap Enrage Formation, Cambro-Ordovician, Gaspé, Quebec. Journal of Sedimentary Petrology, 44: 1200-1216.

Desrochers, A. (1988). Stratigraphie de l'Ordovicien de la région de l'Archipel Mingan. Ministère de l'Énergie et des Ressources du Québec, MM87-01.

Dewey, J. F., and Bird, J. M. (1970). Mountain belts and the new global tectonics. Journal of Geophysical Research, 75: 2615-2647.

Dickinson, W.R. and Suczek, C.A. (1979). Plate tectonics and sandstone compositions. The American Association of Petroleum Geologists Bulletin, 63: no.12, 2164-2182.

Doolan, B.L., Gale, M.H., Gale, P.N., and Hoar, R.S. (1982). Geology of the Quebec re-entrant: possible constraints from early rifts and the Vermont–Quebec serpentine belt. *In* Major structural zones and faults of the northern Appalachians. *Edited by* P. St-Julien and J. Béland. Geological Association of Canada, Special Paper, 24: 87–115.

Dresser, J.A. (1912). Reconnaissance along the National Transcontinental Railway in Southern Quebec. Geological Survey of Canada, Memoir 35, 40p.

Dzulynski, S. and Sanders, J.E. (1962). Current marks on firm mud bottoms. Connecticut Academy of Arts and Science, Transactions, 42: 57-96.

Edgell, S. (2006). Arabian deserts: nature, origin and evolution. Springer, Netherlands, 592p.

Fisher, R.V. (1983). Flow transformations in sediment gravity flows. Geology, 11: 273-274.

Folk, R.L. (1968). Bimodal supermature sandstones: product of the desert floor. Reports of the 23rd International Geological Congress, 8: 9-32.

Gani, R. (2004). From turbid to lucid: a straightforward approach to sediment gravity flows and their deposits. The Sedimentary Record, SEPM 2: 4-8.

Goudi, A. S., Warren, A., Jones, D. K. C., & Cooke (1987). The character and possible origins of the aeolian sediments of the Wahiba sand sea, Oman. Geographical Journal, 153: 231-256.

Hagen, R. A., Bergersen, D. D., Moberly, R., and Coulbourn, W. T. (1994). Morphology of a large meandering submarine canyon system on the Peru - Chile forearc. Marine Geology, 119: 7-38.

Hampton, M.A. (1975).Competence of fine grained debris flows. Journal of Sedimentary Petrology, 45: 834-844.

Hand, B.M. (1997). Inverse grading resulting from coarse-sediment transport lag. Journal of Sedimentary Research, 67: 124-129.

Hein, F.J. (1982). Depositional mechanism of deep-sea coarse clastic sediments, Cap Enragé Formation, Quebec. Canadian Journal of Earth Sciences, 19: 267-287.

Hein, F.J., and Walker, R.G. (1982). The Cambro-Ordovician Cap Enragé Formation, Québec, Canada: conglomeratic deposits of a braided submarine channel with terraces. Sedimentology, 29: 309-329.

Hendry, H.E. (1978). Cap des Rosiers Formation at Grosses Roches, Quebec – deposits of the mid-fan region on an Ordovician submarine fan. Canadian Journal of Earth Sciences, 15: 1472 – 1488.

Hesse, R., and Chough, S. K. (1980). The Northwest Atlantic Mid-Ocean Channel of the Labrador Sea: II. Deposition of parallel laminated levee muds from the viscous sublayer of low-density turbidity currents. Sedimentology, 27: 697-711.

Hiscott, R.N. (1994a). Loss of capacity, not competence, as the fundamental process governing deposition from turbidity currents: Journal of Sedimentary Research, A64: 209-214.

Hiscott, R.N. (1994b). Traction-carpet stratification in turbidites; fact or fiction?: Journal of Sedimentary Research, A64: 204-208.

Hiscott, R.N. and Middleton, G.V. (1979). Depositional mechanics of thick-bedded sandstones at the base of a submarine slope, Tourelle Formation (Lower Ordovician), Quebec, Canada. *In* L.J. Doyle and O.H. Pilkey (eds.), Geology of continental slopes. Society of Economic Paleontologists and Mineralogists, Special Publication, 27: 307-326.

Hiscott, R.N. and Middleton, G.V. (1980). Fabric of coarse deep-water sandstones, Tourelle Formation, Quebec, Canada. Journal of Sedimentary Petrology, 50: 703-722.

Hubert, C. (1965). Stratigraphy of the Quebec Complex in the L'Islet-Kamouraska area, Quebec. McGill University, Ph.D. Thesis, 192p.

Hubert, C. (1973). Kamouraska, La Pocatière, and Saint-Jean-Port-Joli area. Mistère des Richesses Naturelles, Québec, Geological Exploration Service, Geological Report 151, 205p.

James, N.P., and Stevens, R.K. (1986). Stratigraphy of the Cambro-Ordovician Cow Head Group, western Newfoundland. Geological Survey of Canada, Bulletin 366, 143p.

James, N.P., Stevens, R.K., Barnes, C.R., and Knight, I. (1989). Evolution of a Lower Paleozoic continental-margin carbonate platform, northern Canadian Appalachians. *In* P.D. Crevello, J.L. Wilson, R. Sarg, and J.F. Read (eds.) Controls on carbonate platform and basin development. Society of Economic Paleontologists and Mineralogists, Special Publication, 44: 123–146.

Kamo, S.L., Gower, C.F., and Krogh, T.E. (1989). Birthdate for the Iapetus Ocean? A precise U–Pb and baddeleyite age for the Long Range dykes, southeast Labrador. Geology, 17: 602–605.

Kamo, S.L., Krogh, T.E., and Kumarapeli, P.S. (1995). Age of the Grenville dyke swarm, Ontario-Quebec: implications for the timing of Iapetan rifting. Canadian Journal of Earth Sciences, 32: 273-280.

Kean, B.F., and Strong, D.F., (1975). Geochemical evolution of an Ordovician island arc of the central Newfoundland Appalachians; American Journal of science, 275: 97-118.

Khalaf, F. I. (1989a). Textural characteristics and genesis of the aeolian sediments in the Kuwaiti desert. Sedimentology, 36: 252-271.

Khalaf, F. I. (1989b). Desertification and Aeolian processes in the Kuwait desert. Journal of Arid Environments, 16: 125-145.

Khalaf, F. I., & Gharib, I. M. (1985). Roundness parameters of quartz grains of Recent Aeolian sand deposits in Kuwait, Sedimentary Geology, 45: 147-158.

Kneller, B.C., and Branney, M.J. (1995). Sustained high-density turbidity currents and the deposition of thick massive beds. Sedimentology, 42: 607-616.

Kolla, V., Bourges, Ph., Urruty, J.-M., and Safa, P. (2001). Evolution of deep-water Tertiary sinuous channels offshore Angola (west Africa) and implications for reservoir architecture. American Association of Petroleum Geologists Bulletin, 85: 1373-1405.

Krastel, S., Hanebuth, T.J.J., Antobreh, A.A., Henrich, R., Holz, C., Kölling, M., Schulz, H.D., Wien, K., and Wynn, R.B. (2004). Cap Timiris Canyon: a newly discovered channel system offshore of Mauritania. EOS 85: 417–432.

Krinsley, D.H., and Doornkamp, J. (1973). Atlas of Quartz Sand Surface Textures. Cambridge University Press, Cambridge, England.

Krinsley, D.H. and Wellendorf, W. (1980). Wind velocities determined from the surface textures of sand grains. Nature, 283, no. 5745, pp. 372-373.

Krinsley, D.H., Friend, P. and Klimentidis, R. (1976). Eolian transport textures on the surfaces of sand grains of early Triassic age. Geological Society of America Bulletin, 87: 130-132.

Kuenen, Ph. H. (1960). Experimental abrasion 4: eolian action. Journal of Geology, 68: 427-449.

Lajoie, J. (1979). Origin of the megarhythms in flysch sequences of the Quebec Appalachians. Canadian Journal of Earth Sciences, 16: 91-104.

Lajoie, J. Heroux, Y., and Mathey, B., (1974). The Precambrian shield and the lower Paleozoic shelf: the unstable provenance of the lower Paleozoic flysch sandstone and conglomerates of the Appalachians between Beaumont and Bic, Quebec: Canadian Journal of Earth Sciences, 11: 951-963.

Landing, E. (1993). Cambrian-Ordovician boundary in the Taconic allochthon, eastern New York, and its interregional correlation. Journal of Paleontology, 57: 1-19.

Landing, E., and Benus, A.P. (1985). The Lévis Formation: Passive margin slope process and dynamic stratigraphy in the "western area". *In* Riva, J. (ed.): Canadian paleontology and biostratigraphy seminar, field excursion guidebook.. Ste-Foy, Quebec.

Landing, E., Benus, A.P., and Whitney, P.R. (1992). Early and early Middle Ordovician continental slope deposition: shale cycle and sandstones in the New York Promontory and Quebec Reentrant region. New York State Museum, Bulletin 474: 1-40.

Landing, E., Westrop, S.R., and Knox, L.A. (1996). Conodonts, stratigraphy, and relative sea-level changes of the Tribes Hill Formation (Lower Ordovician, east-central New York). Journal of Paleontology, 70: 656-680.

Lavoie, D. (1997). Cambrian-Ordovician slope conglomerates in the Humber Zone, Québec. *In* Current research 1997-D. Geological Survey of Canada, pp. 9-20.

Lavoie, D., Burden, E., and Lebel, D. (2003). Stratigraphic framework for the Cambrian–Ordovician rift and passive margin successions from southern Quebec to western Newfoundland. Canadian Journal of Earth Sciences, 40: 177-205.

Lebel, D., and Hubert, C. (1995a). Géologie de la région de Saint-Raphaël (Chaudière-Appalaches). Ministère des Ressources Naturelles du Québec, ET 93-02, 81p.

Lebel, D., and Hubert, C. (1995b). Géologie de la région de Saint- Malachie (Chaudière-Appalaches). Ministère des Ressources Naturelles du Québec, ET 93-03, 63p.

Lebel, D., and Kirkwood, D. (1998). Nappes and mélanges in the Québec – Bellechasse area: their regional tectonic and stratigraphic significance in the Humber Zone. Geological Association of Canada – Mineralogical

Association of Canada, Joint Annual Meeting, Québec, Que., 1998, Field Trip Guidebook A5, pp.15- 17.
Legros, F. (2002). Can dispersive pressure cause inverse grading in grain flows? Journal of Sedimentary Research, 72: 166-170.
Le Roux, J.P. (2003). Can dispersive pressure cause inverse grading in grain flows?— discussion. Journal of Sedimentary Research, 73: 333-334.
Lewis, D.W. (1971). Qualitative petrographic interpretation of the Potsdam Sandstone (Cambrian), southwestern Quebec. Canadian Journal of Earth Sciences, 8: 858-882.
Logan, W.E. (1863). Geology of Canada. Geological Survey of Canada, Report of progress from its commencement to 1863, 983 p.
Lowe, D.R. (1975). Water escape structures in coarse-grained sediments: Sedimentology, 22: 157-204.
Lowe, D.R. (1982). Sediment gravity flows, II: Depositional models with special reference to the deposits of high-density turbidity currents. Journal of Sedimentary Petrology, 52: 279-297.
Lowe, D.R., and LoPiccolo, R.D. (1974). The characteristics and origins of dish and pillar structures. Journal of Sedimentary Petrology, 44: 484-501.
Mahaney, W.C. (2002). Atlas of Sand Grain Surface Textures and Applications. Oxford University Press, Oxford, 237 pp.
Mahaney, W.C., and Andres, W. (1996). Scanning electron microscopy of quartz sand from the north-central Saharan desert of Algeria. Zeitschrift für Geomorphologie N.F., Suppl-BD., 103: 179-192.
Maletz, J. (1992). Yapeenain (Early Ordovician) grapolites in the Quebec Appalachians. Canadian Journal of Earth Sciences, 29: 1330-1334.
Maletz, J. (1997). Arenig biostratigraphy of the Pointe-de-Lévy slice, Quebec Appalachians, Canada. Canadian Journal of Earth Sciences, 34: 733–752.
Maletz, J. (2001). A condensed Lower to Middle Ordovician grapolite succession at Matane, Quebec, Canada. Canadian Journal of Earth Sciences, 38: 1531-1539.
Margolis S.V. and Krinsley, D.H. (1971). Submicroscopic frosting on eolian and subaqueous quartz sand grains. Bulletin Geological Society of America, 82: 3395-3406.
Mattern, F. (2002). Amalgamation surfaces, bed thicknesses, and dish structures in sand-rich submarine fans: numeric differences in channelized and unchannelized deposits and their diagnostic value. Sedimentary Geology, 150: 203-228.
Mazzullo, S.J., Agostino, P., Seitz, J.N., and Fisher, D.W. (1978). Stratigraphy and depositional environment of the Upper Cambrian – Lower Ordovician sequence, Saratoga Springs, New York. Journal of Sedimentary Petrology, 48: 99-116.
Middleton, G.V. (1967). Experiments on density and turbidity current. III. Deposition of sediment. Canadian Journal of Earth Sciences, 4: 475-505.
Middleton, G. V. (1970). Experimental studies related to problems of flysch sedimentation. In J. Lajoie, Flysch sedimentology in North America, Geological Association of Canada Special Paper, 7: 253-272.

Middleton, G.V. and Hampton, M.A. (1973). Part I. Sediment gravity flows: mechanics of flow and deposition. *In* Middleton, G.V. and Bouma, A.H. (eds.):Turbidity Currents and Deep Water Sedimentation, , SEPM, Pacific Section, Short Course Lecture Notes, pp. 1-38.

Mulder, T. and Alexander, J. (2001). The physical character of subaqueous sedimentary density flows and their deposits: Sedimentology, 48: 269-299.

Mutti, E. (1992). Turbidite Sandstones. Agip, Instituto di Geologia, Università di Parma, San Donato Milanese, 275p.

Mutti, E. and Nilsen, T.H. (1981). Significance of intraformational rip-up clasts in deep-sea fan deposits. *In* R. Valloni, A. Colella, M. Sonino, E. Mutti, and G.G. Ori (eds.), International Association of Sedimentologists, 2nd European Regional Meeting, Bologna, Italy, pp. 117-119.

Mutti, E., and Normak, W.R. (1987). Comparing examples of modern and ancient turbidite systems: problems and concepts. *In* J.K. Leggett, and G.G. Zuffa (eds.), Marine Clastic Sedimentology. Concepts and Case Studies. Graham & Trotman, London, pp.1-38.

Nelson, C.H., Twichell, D.C., Schwab, W.C., Lee, H.J. and Kenyon, N.H. (1992). Upper Pleistocene turbidite sand beds and chaotic silt beds in channelized, distal, outer-fan lobes of the Mississippi fan. Geology, 20: 693-696.

Normark,W.R., AND Carlson, P.R. (2003). Giant submarine canyons; is size any clue to their importance in the rock record?; in Chan, M.A., and Archer, A.W., eds., Extreme Depositional Environments; Mega End Members in Geological Time. Geological Society of America, Special Paper 370: 175–190.

Nowlan, G. (1981). Stratigraphy and conodont faunas of the Lower and Middle Ordovician Romaine and Mingan formations, Mingan Islands, Québec. Maritime Sediments and Atlantic Geology, 17: 67.

O'Connell, S., Ryan, W.B.F., and Normark, W.R. (1987). Modes of development of slope canyons and their relation to channel and levee features on the Ebro sediment apron, off-shore northeastern Spain. Marine and Petroleum Geology, 4: 308-319.

Osberg, P.H. (1978). Synthesis of the geology of the north-eastern Appalachians, U.S.A. Geological Survey of Canada, Paper 78-13, pp. 137-147.

Pantin, H.M. (1979). Interaction between velocity and effective density in turbidity flow: phase-plane analysis, with criteria for autosuspension. Marine Geology, 31: 59-99.

Parker, G., Fukushima, Y., Pantin, H.M. (1986). Self-accelerating turbidity currents. Journal of Fluid Mechanics, 171: 145-181.

Paull, C.K., Mitts, P., Ussler,W., Keaten, R., AND Greene, H.G. (2005). Trail of sand in upper Monterey Canyon: Offshore California. Geological Society of America Bulletin, 117:1134–1145.

Pickering, K.T., Hiscott, R.N., and Hein, F.J., (1989). Deep Marine Environments; Clastic Sedimentation and Tectonics. London, Unwin Hyman, 416 p.

Pinet, N., and Tremblay, A. (1995). Tectonic evolution of the Québec-Maine Appalachians: from oceanic spreading to obduction and collision in the northern Appalachians. American Journal of Science, 295: 173-200.

Piper, D.J.W., Shor, A.N. and Hughes-Clarke, J.E. (1988). The 1929 "Grand Banks" earthquake, slump and turbidity current. Gological Society of America, Special Paper, 229: 77-92.

Postma, G., Nemec, W. and Kleinspehn, K.L. (1988). Large floating clasts in turbidites: a mechanism for their emplacement. Sedimentary Geology, 58: 47-61.

Pye, K. and Tsoar, H. (1990). Aeolian Sand and Sand Dunes. Unwin Hyman, London, 396 pp.

Rasetti, F. (1946). Cambrian and Early Ordovician stratigraphy of the Lower St. Lawrence Valley. Geological Society of America Bulletin, 57: 687-706.

Releves Geophysiques Inc. (1978). Interprétation des données aéromagnétiques dans la région de Beauce – Charlevoix. Ministère de l'Énergie et des Ressources Québec; DPV-557, 78p.

Riva, J. (1972). Geology of the environs of Québec City. 24th International Geological Congress, Montréal, Quebec, Field Trip Guidebook B-19, 53p.

Salad Hersi, O., and Lavoie, D. (2001). Contributions to the sedimentology of the Strites Pond Formation, Cambro-Ordovician Philipsburg Group, southwestern Quebec. *In* Current research, part D. Geological Survey of Canada, Paper 2001-D11.

Salad Hersi, O., Lavoie, D., Hilowle Mohamad, A., and Nowlan, G.S. (2002*a*). Subaerial unconformity at the Potsdam–Beekmantown contact in the Quebec Reentrant (SW Quebec and Eastern Ontario, Canada): regional significance for the Laurentian continental margin history. Bulletin of Canadian Petroleum Geology, 50: 419-440.

Salad Hersi, O., Lavoie, D., and Nowlan, G.S. (2002*b*). Stratigraphy and sedimentology of the Upper Cambrian Strites Pond Formation, Philipsburg Group, southern Quebec, and implications for the Cambrian platform in eastern Canada. Bulletin of Canadian Petroleum Geology, 50: 542-565.

Sandford, B.V. (1993). St. Lawrence Platform—Geology. *In* Sedimentary cover of the Craton in Canada. *Edited by* D.F. Scott and J.D. Aitken. Geological Survey of Canada, Geology of Canada, no.5, Chap. 11, pp. 723–786.

Sarnthein, M., and Diester-Haass, L. (1977). Eolian-sand turbidites. Journal of Sedimentary Petrology, 47: 868-891.

Savage, S.B., and Sayed, M. (1984). Stresses developed by dry cohesionless granular materials sheared in an annular shear cell. Journal of Fluid Mechanics, 142: 391-430.

Shanmugam, G. (1996). High-density turbidity currents: are they sandy debris flows? Journal of Sedimentary Research, 66: 2-10.

Shanmugam, G. (2006). Deep water processes and facies models: implications for sandstone petroleum reservoirs. - (Handbook of petroleum exploration and production; v.5), Elsevier, 476p.

Shanmugam, G., and Moiola, R.J. (1995). Reinterpretation of depositional processes in a classic flysch sequence (Pennsylvanian Jackfork Group), Ouachita Mountains, Arkansas and Oklahoma. American Association of Petroleum Geologists Bulletin 79: 672–695.

Skoček, V. and Saadallah, A.A. (1972). Grain size distribution, carbonate content and heavy minerals in eolain sands, southern desert, Iraq. Sedimentary Geology, 8: 29-46.

Slivitzky, A., St-Julien, P., and Lachambre, G. (1991). Synthèse géologique du Cambro-Ordovician du nord de la Gaspésie. Ministère de l'Energie et des Ressources, Québec, ET 88-14, 61p.

Sloss, L.L. (1963). Sequences in the cratonic interior of North America. Geological Society of America Bulletin, 74: 93–114.

Sohn, T.K. (1995). Traction-carpet stratification in turbidites; fact or fiction? (Discussion). Journal of Sedimentary Research, A65: 703-704.

Sohn, T.K. (1997). On traction-carpet sedimentation. Journal of Sedimentary Research, 67: 502-509.

Stanley, R.S., and Ratcliffe, N.M. (1985). Tectonic synthesis of the Taconian orogeny in western New England. Geological Society of America Bulletin, 96: 1227-1250.

St. Julien, P. (1979). Structure and stratigraphy of platform and Appalachian sequences near Québec City. Geological Association of Canada, Annual Meeting, Québec, Que., Field Trip Guidebook A-9, 31 pp.

St. Julien, P., and Hubert, C. (1975). Evolution of the Taconian Orogen in the Québec Appalachians. American Journal of Science, 275A: 337-362.

St. Julien, P., Slivitzky, A., and Feininger, T. (1983). A deep structural profile across the Appalachians of southern Québec. *In* R.D. Hatcher, H. Williams, and I. Zeitz (eds.): Contributions to the tectonics and geophysics of mountain chains. Geological Society of America Memoir 158: 103-111.

Strong P.G., and Walker, R.G. (1981). Deposition of the Cambrian continental rise: the St. Roch Formation near St. Jean-Port-Joli, Quebec. Canadian Journal of Earth Sciences, 18: 1320-1335.

Vallières, A. (1984). Stratigraphie et structure de l'orogénie taconique de la région de Rivière-du-Loup. Unpublished Ph.D. thesis, Université Laval, Québec, Que.

Vallières, A., Hubert, C., and Brooks, C. (1978). A slice of basement in western margin of the Appalachian orogen, Saint-Malachie, Quebec. Canadian Journal of Earth Sciences, 15: 1242-1249.

Walker, R.G. (1978). Deep-water sandstone facies and ancient submarine fans: models for exploration for stratigraphic traps: American Association of Petroleum Geologists Bulletin, 62: 932-966.

Westrop, S.R., Knox, L.A., and Landing, E. (1993). Lower Ordovician (Ibexian) trilobites from the Tribes Hill Formation, central Mohawk Valley, New York State. Canadian Journal of Earth Sciences, 30: 1618–1633.

Whitney, J. W., Faulkender, D. J., & Rubin, M. (1983). The environmental history and present condition of Saudi Arabia's northern sand seas. U. S. Geological Survey Open-File Report 83-749, 39 p., Jiddah.

Williams, H. (1978). Tectonic-Lithofacies Map of the Appalachian Orogen. Memorial University of Newfoundland, Map No.1.

Williams, H. (1979). Appalachian Orogen in Canada. Canadian Journal of Earth Sciences, 16: 792–807.

Williams, H. (1995). Temporal and spatial subdivisions of the rocks of the Canadian Appalachian region. *In* Geology of the Appalachian-Caledonian Orogen in Canada and Greenland. *Edited by* H. Williams. Geological Survey of Canada. Geology of Canada, no.6, pp. 21-44.

Williams, H., and Stevens, R.K. (1974). The ancient continental margin of eastern North America. *In* C.A. Burk and C.L. Drake (eds.): The geology of continental margins. Springer-Verlag, New York, pp. 781-796.

Williams, H. and St. Julien, P. (1978). The Baie Verte-Brompton Line in Newfoundland and regional correlations in the Canadian Appalachians. Commission géologique du Canada, étude préliminaire 78-1A: 225-229.

Williams, H. and St-Julien, P. (1982). The Baie Verte-Bromton Line: Early Paleozoic continent-ocean interface in the Canadian Appalachians. *In* St-Julien, P. and Béland, J. (eds.): Major Structural Zones and Faults of the Northern Appalachians, , Geological Association of Canada, Special Paper 24:177-207.

Wilson, A.E. (1937). Erosional intervals indicated by contacts in the vicinity of Ottawa, Ontario. Transactions of Royal Society of Canada. Section IV: 45-60.

Wolf, R.R. and Dalrymple, R.W. (1984). Sedimentology of the Cambro-Ordovician sandstones of eastern Ontario. *In* Geoscience Research Grant Program, Summary of Research 1983–1984, Ontario Geological Survey, Miscellaneous Paper 121: 240–252.

Wolf, R.R. and Dalrymple, R.W. (1985). Sedimentology of the Cambro-Ordovician sandstones of eastern Ontario. *In* Geoscience Research Grant Program, Summary of Research, 1984–1985. Ontario Geological Survey, Miscellaneous Paper 127: 112–118.

APPENDIX A: GRAIN SIZE ANALYSIS DATA

Sample number: GSA 3

Dry weight at start(g) = 17.7

Sieve opening (mm)	Sieve opening (Φ)	Weight retained (g)	Cumulative % retained
2	-1	0	0.000%
1	0	0	0.000%
0.5	1	0.27	1.525%
0.25	2	9.02	52.486%
0.125	3	7.69	95.932%
0.0625	4	0.56	99.096%
0.032	5	0.05	99.379%
< 0.32	> 5	0.09	99.887%

Size analysis of fines (pipette method)

sodium hexametaphosphate (calgon) = 0.1862 (g/l)

Grain size (mm)	Grain size (Φ)	Weight (g/20cc)	Weight (g/l)	Calgon (g)	Net weight (g)	Cumulative % retained
0.0156	6	0.0047	0.235	0.1862	0.0488	99.654%
0.0078	7	0.004	0.2	0.1862	0.0138	99.732%
0.0039	8	0.0039	0.195	0.1862	0.0088	99.782%
0.00195	9	0.004	0.2	0.1862	0.0138	99.860%
0.00097	10	0.0038	0.19	0.1862	0.0038	99.881%

Summary

Grain size (Φ)	Grain size (mm)	Cumulative % retained	Weight % retained		mm	Φ
-1	2	0.000%	0.000%	Q5	0.462	1.114
0	1	0.000%	0.000%	Q16	0.388	1.366
1	0.5	1.525%	1.525%	Q25	0.349	1.5187011
2	0.25	52.486%	50.960%	Q50	0.26	1.9434165
3	0.125	95.932%	43.446%	Q75	0.181	2.4659384
4	0.0625	99.096%	3.164%	Q84	0.159	2.6529013
5	0.032	99.379%	0.282%	Q95	0.129	2.954557
6	0.0156	99.654%	0.276%	Ma =	0.26	1.943
7	0.0078	99.732%	0.078%	Gm =	0.252193	1.987
8	0.0039	99.782%	0.050%	σ =	NA	0.6006244
9	0.00195	99.860%	0.078%	S =	1.388588	NA
10	0.00097	99.881%	0.021%	log S =	0.142573	NA

Sample number: GSA 7

Dry weight at start(g) = 19.01

Sieve opening (mm)	Sieve opening (Φ)	Weight retained (g)	Cumulative % retained
2	-1	0	0.000%
1	0	0	0.000%
0.5	1	0.75	3.945%
0.25	2	8.05	46.291%
0.125	3	8.77	92.425%
0.0625	4	1.04	97.896%
0.032	5	0.2	98.948%
< 0.32	> 5	0.13	99.632%

Size analysis of fines (pipette method)
sodium hexametaphosphate (calgon) = 0.1871(g/l)

Grain size (mm)	Grain size (Φ)	Weight (g/ 20cc)	Weight (g/l)	Calgon (g)	Net weight (g)	Cumulative % retained
0.0156	6	0.005	0.25	0.1871	0.0629	99.279%
0.0078	7	0.0041	0.205	0.1871	0.0179	99.373%
0.0039	8	0.0038	0.19	0.1871	0.0029	99.388%
0.00195	9	0.0045	0.225	0.1871	0.0379	99.588%
0.00097	10	0.004	0.2	0.1871	0.0129	99.655%

Summary

Grain size (Φ)	Grain size (mm)	Cumulative % retained	Weight % retained		mm	Φ
-1	2	0.000%	0.000%	Q5	0.485	1.044
0	1	0.000%	0.000%	Q16	0.388	1.366
1	0.5	3.945%	3.945%	Q25	0.34	1.5563933
2	0.25	46.291%	42.346%	Q50	0.236	2.0831412
3	0.125	92.425%	46.134%	Q75	0.168	2.5734669
4	0.0625	97.896%	5.471%	Q84	0.148	2.7563309
5	0.032	98.948%	1.052%	Q95	0.113	3.1456053
6	0.0156	99.279%	0.331%	Ma =	0.236	2.083
7	0.0078	99.373%	0.094%	Gm =	0.2384159	2.068
8	0.0039	99.388%	0.015%	σ =	NA	0.6660485
9	0.00195	99.588%	0.199%	S =	1.4226066	NA
10	0.00097	99.655%	0.068%	log S =	0.1530848	NA

Sample number: GSA 10

Dry weight at start(g) = 34.9

Sieve opening (mm)	Sieve opening (Φ)	Weight retained (g)	Cumulative % retained
2	-1	0	0.000%
1	0	0	0.000%
0.5	1	1.76	5.043%
0.25	2	14.11	45.473%
0.125	3	13.51	84.183%
0.0625	4	3.73	94.871%
0.032	5	1.05	97.880%
< 0.32	> 5	0.61	99.628%

Size analysis of fines (pipette method)
sodium hexametaphosphate (calgon) = 0.191 (g/l)

Grain size (mm)	Grain size (Φ)	Weight (g/20cc)	Weight (g/l)	Calgon (g)	Net weight (g)	Cumulative % retained
0.0156	6	0.0099	0.495	0.191	0.304	98.751%
0.0078	7	0.0064	0.32	0.191	0.129	99.120%
0.0039	8	0.0052	0.26	0.191	0.069	99.318%
0.00195	9	0.0053	0.265	0.191	0.074	99.530%
0.00097	10	0.0046	0.23	0.191	0.039	99.642%

Summary

Grain size (Φ)	Grain size (mm)	Cumulative % retained	Weight % retained		mm	Φ
-1	2	0.000%	0.000%	Q5	0.5	1.000
0	1	0.000%	0.000%	Q16	0.394	1.344
1	0.5	5.043%	9.742%	Q25	0.343	1.5437195
2	0.25	45.473%	44.040%	Q50	0.23	2.1202942
3	0.125	84.183%	36.648%	Q75	0.153	2.7083964
4	0.0625	94.871%	9.713%	Q84	0.126	2.9885044
5	0.032	97.880%	3.181%	Q95	0.062	4.011588
6	0.0156	98.751%	0.726%	Ma =	0.23	2.120
7	0.0078	99.120%	0.353%	Gm =	0.2251809	2.151
8	0.0039	99.318%	0.124%	σ =	NA	0.8674942
9	0.00195	99.530%	0.181%	S =	1.4972742	NA
10	0.00097	99.642%	0.110%	log S =	0.1753013	NA

Sample number: GSA 11

Dry weight at start(g) = 36.65

Sieve opening (mm)	Sieve opening (Φ)	Weight retained (g)	Cumulative % retained
2	-1	0	0.000%
1	0	0	0.000%
0.5	1	3.4	9.277%
0.25	2	15.37	51.214%
0.125	3	12.79	86.112%
0.0625	4	3.39	95.362%
0.032	5	1.11	98.390%
< 0.32	> 5	0.54	99.864%

Size analysis of fines (pipette method)
sodium hexametaphosphate (calgon) = 0.1867 (g/l)

Grain size (mm)	Grain size (Φ)	Weight (g/ 20cc)	Weight (g/l)	Calgon (g)	Net weight (g)	Cumulative % retained
0.0156	6	0.0088	0.44	0.1867	0.2533	99.081%
0.0078	7	0.0062	0.31	0.1867	0.1233	99.418%
0.0039	8	0.0046	0.23	0.1867	0.0433	99.536%
0.00195	9	0.005	0.25	0.1867	0.0633	99.709%
0.00097	10	0.0045	0.225	0.1867	0.0383	99.813%

Summary

Grain size (Φ)	Grain size (mm)	Cumulative % retained	Weight % retained		mm	Φ
-1	2	0.000%	0.000%	Q5	0.58	0.786
0	1	0.000%	0.000%	Q16	0.43	1.218
1	0.5	9.277%	9.277%	Q25	0.37	1.4344028
2	0.25	51.214%	41.937%	Q50	0.256	1.9657843
3	0.125	86.112%	34.898%	Q75	0.163	2.6170561
4	0.0625	95.362%	9.250%	Q84	0.134	2.8996951
5	0.032	98.390%	3.029%	Q95	0.065	3.9434165
6	0.0156	99.081%	0.691%	Ma =	0.256	1.966
7	0.0078	99.418%	0.336%	Gm =	0.2452474	2.028
8	0.0039	99.536%	0.118%	σ =	NA	0.8989413
9	0.00195	99.709%	0.173%	S =	1.5066316	NA
10	0.00097	99.813%	0.105%	log S =	0.1780071	NA

Sample number: GSA 22

Dry weight at start(g) = 23.27

Sieve opening (mm)	Sieve opening (Φ)	Weight retained (g)	Cumulative % retained
2	-1	0	0.000%
1	0	0	0.000%
0.5	1	3.12	13.408%
0.25	2	12.67	67.856%
0.125	3	5.95	93.425%
0.0625	4	0.93	97.422%
0.032	5	0.26	98.539%
< 0.32	> 5	0.29	99.785%

Size analysis of fines (pipette method)

sodium hexametaphosphate (calgon) = 0.1862 (g/l)

Grain size (mm)	Grain size (Φ)	Weight (g/20cc)	Weight (g/l)	Calgon (g)	Net weight (g)	Cumulative % retained
0.0156	6	0.0066	0.33	0.187	0.143	99.153%
0.0078	7	0.0061	0.305	0.187	0.118	99.661%
0.0039	8	0.0041	0.205	0.187	0.018	99.738%
0.00195	9	0.0039	0.195	0.187	0.008	99.772%
0.00097	10	0.0038	0.19	0.187	0.003	99.785%

Summary

Grain size (Φ)	Grain size (mm)	Cumulative % retained	Weight % retained		mm	Φ
-1	2	0.000%	0.000%	Q5	0.641	0.642
0	1	0.000%	0.000%	Q16	0.475	1.074
1	0.5	13.408%	13.408%	Q25	0.416	1.2653446
2	0.25	67.856%	54.448%	Q50	0.317	1.6574453
3	0.125	93.425%	25.569%	Q75	0.218	2.1976
4	0.0625	97.422%	3.997%	Q84	0.176	2.5063527
5	0.032	98.539%	1.117%	Q95	0.112	3.1584294
6	0.0156	99.153%	0.615%	Ma =	0.317	1.657
7	0.0078	99.661%	0.507%	Gm =	0.2981411	1.746
8	0.0039	99.738%	0.077%	σ =	NA	0.7394252
9	0.00195	99.772%	0.034%	S =	1.3813967	NA
10	0.00097	99.785%	0.013%	log S =	0.1403184	NA

Formulas and symbols used:

Q5 = 5^{th} percentile (retained)

Q16= 16^{th} percentile (retained)

Q25= 25^{th} percentile (retained)

Q50= 50^{th} percentile (retained)

Q75= 75^{th} percentile (retained)

Q84= 84^{th} percentile (retained)

Q95= 95^{th} percentile (retained)

Ma = arithmetic mean = Q50

Gm = geometric mean = (Q16 + Q50 + Q84) / 3

σ = standard deviation = [(Q84 - Q16) / 4] + [(Q95 - Q5) / 6.6] -- (Using Φ scale)

S = sorting coefficient = $(Q25/Q75)^{1/2}$ -- (Using mm scale)

APPENDIX B: EXTRACTION OF ORGANIC MATTER FOR PALYNOLOGICAL STUDY

Organic matter extraction was conducted in search for siliceous microfossils (chitinozoans and achritarchs). The process of organic matter extraction comprises a set of steps. Essentially samples need to be treated with acid in order to separate the organic matter from the rock. Although different people use slightly different techniques, the following paragraphs present the detailed procedure conducted.

1. Organic matter extraction for chitinozoans

1) The first step begins with the crushing of the shale samples. A metallic mortar and pestle are used. The sample to be crushed should be 20 to 35 grams. Samples should be crushed down to dimensions less than 7-8 mm. the mortar and pestle should be disinfected after every crushing to avoid contamination. This is done with distilled water or alcohol.
2) The second step would be to place each of the crushed samples into a beaker. The beakers should be properly numbered.
3) First the calcareous samples have to be separated from the siliceous. The simple HCl test would suffice. After placing the beakers under the fume hood, add a few ml of 10% HCl to all the beakers. The beakers that effervesce with the HCl would then be separated and fully covered by HCl. These samples need to be treated until they are devoid of any carbonates. The procedure might take a whole day until no effervescence is present. Safety precautions are vital when dealing with acid. Always wear proper clothing. Goggles and gloves are a must. Always remember to keep acid bottles and beakers treated with acid under the fume hood.
4) In the mean time the remaining samples would be treated with hydrofluoric acid (HF) at 70% concentration. At this stage greater safety measures should be taken. This is why it is recommended that a special acid resistant apron be worn, and the regular goggles be replaced by larger

more protective ones. Hydrofluoric acid is deadly at such concentrations; furthermore the escaping fumes are highly corrosive. Make sure to keep the HF bottle under the fume hood at all times. It is recommended to lower the fume hood window half-way during the HF attack. At first, HF is added in small quantities to every beaker; this is in order to asses how aggressive the reaction will be in each. The beakers should be widely spaced in order to avoid any contamination. Some reactions are aggressive and the beakers might spill. HF is added again slowly to each beaker so that the whole sample is covered. The beakers that show vigorous aggressive reactions should be waited out before being filled up by HF. Once the attack is done, it is very important to close the bottle of HF and place its neck and lid under running water. This will dilute any spills. Do not forget to also wash the gloves you're wearing before taking them off. The beakers should be left for at least 12 hours or more before any neutralization is attempted.

5) The following day neutralization takes place for both HCl and HF treated beakers.
    a. The neutralization of HCl beakers is carried out by first emptying the HCl from the beakers and then adding distilled water. Care should be taken while emptying the beakers so as not to drop the sample. The samples are then waited out for at least three hours and then this procedure is repeated again for a second time. After the second decantation, the water is emptied and the sample becomes ready to be attacked by HF. The carbonate treated samples then follow the same steps as the carbonate free samples.
    b. The neutralization of the HF treated beakers is more extensive. The decantation process is carried out 6 to 7 times until complete neutralization is achieved and the pH of the beakers is close to 7. The decantation process begins by first emptying the HF from the beakers into containers (or large beakers) containing water and bicarbonate crystals. HF should not be emptied directly into the

sink. Before HF can be disposed, it should be neutralized. Once the beakers are emptied from HF, distilled water is added to each beaker in order to neutralize the sample. At least three hours should be allowed between each decantation. For the first three HF decantations the water in the beakers should always be emptied in containers containing water and bicarbonate crystals. From the fourth decantation onwards, the water in the beakers can be emptied into a sink with running water. HF decantation is repeated over and over until the pH of the beaker is between 6 and 7. As for the bicarbonate containers, bicarbonate should always be added moderately until no reaction is observed.

6) Once the samples in the beakers are completely neutralized, the extraction of chitinozoans begins. This is done by collecting a drop of the organic matter (residue in beaker) and observing it under a binocular microscope.

2. Organic matter extraction for achritarchs

1) The extraction of achritarchs proceeds after all beakers are neutralized (as described in the previous section). The first step involves filling up some organic matter (residue in the beakers) into test tubes that can fit in the centrifuge at hand.
2) Add water to each test tube so that all the test tubes are filled equally (up to 1 cm from the top of test tube is ideal).
3) In each batch the test tubes should all be balanced and placed properly in the centrifuge. Once this is done, the centrifuge is operated at 2000 rpm for 2 minutes.
4) When the centrifuge is stopped, the organic matter would have settled to the bottom of the test tubes. Empty the water from each test tube leaving only the organic matter.
5) The next step requires the use of a high density liquid. The use of zinc bromide $ZnBr_2$ liquid (density 2 g/cm^3) is ideal for this next operation.

Add 15 ml of zinc bromide into each test tube. Mix and stir each test tube. Make sure to wear gloves and protective glasses when handling zinc bromide.

6) Next get transparent flexible plastic tubes and shape each into a u-shape. The arms of the u-tube should be equal. Holding a u-tube tightly at its center, fill a test tube equally into the arms of u-tube and then place the u-tube in the centrifuge. Repeat the same procedure to the whole batch.
7) Next operate the centrifuge at 1000 rpm for 10 minutes. The finer particles of achritarch size will float on top of the high density liquid. Particles of higher density will sink to the bottom.
8) During the 10 minute wait, wash and dry the test-tubes. Make sure to wear gloves as the test-tubes contained zinc bromide. Once the tubes are cleaned, place a 5 ml of hydrochloric acid (10%) in each of the test tubes.
9) When the u-tubes are taken out of the centrifuge, fine organic matter would float on top of each u-tube. With a pincer squeeze the top of both arms of the u-tube, thus isolating the floating portion. Empty the isolated floating portion into its corresponding test tube that contains 5 ml of hydrochloric acid. Repeat the same procedure to the entire batch.
10) What remains in the u-tubes is unwanted material and is emptied in a waste disposal container and marked as zinc bromide. The u-tubes are then washed.
11) Distilled water is added to all the test tubes up to 1 cm from the top. The equally filled test tubes are placed again in the centrifuge. The test tubes are centrifuged at 2000 rpm for 5 minutes. The tubes are then taken out and the water is very slowly emptied. One should not attempt to empty all the test tube in order not to discard any fine particles. It is recommended leave a quarter of the test tube filled with water. Distilled water is added again and the procedure is repeated over and over until the ph paper indicates that all the tubes are fully neutralized.
12) After neutralization, the organic matter in the test tube is emptied into transparent glass vials.

13) The final step involves mounting of achritarchs. This is done by collecting a drop of the organic matter (from vials) with a pipette and placing it on a glass cover slip. The pipette is then properly washed and used to add a drop of polyvinyl to the drop of organic matter on the cover slip. Mix the two drops and spread them so that the organic matter is equally scattered on the cover slip. Next, place the cover glass on a heating plate and wait for it to dry. When dry the organic matter will stick onto the cover glass. Flip the cover glass onto a larger microscope glass slide. The organic matter will now be sandwiched in between. The slide can now be sent for final mounting. Repeat this procedure to all samples.

Table 3: No achritarchs or chitinozoans were detected in any of the samples. Organic matter was extracted from interbedded shale, and shale from underlying and overlying formations. Samples ending with INT, BOT, and TOP are from interbedded shale, underlying shale, and overlying shale respectively. Description is courtesy of Esther Asselin (INRS-ETE).

Analysis of extracted organic matter (described by Esther Asselin)			
Sample #	Visible Chitinozoanz	Visible Acritarchs	Organic matter (Esther Asselin) Flakes:might be secondary precipitation
PM210505-I-AA1-INT	None	None	poor/ fragments
PM230505-I-AA2-INT	None	None	middle/ brown flakes and black organic matter
PM230505-I-AA3-INT	None	None	poor
PM230505-I-AA4-INT	None	None	middle/ brown flakes and black organic matter
PM230505-I-AA5-TOP	None	None	very poor
PM230505-I-AA6-INT	None	None	rich/ black fragments
PM230505-I-AA7-INT	None	None	middle for brown flakes but very rare black organic matter
PM230505-I-AA8-INT	None	None	middle-poor for brown flakes but very rare black organic matter
PM230505-I-AA9-INT	None	None	middle/ small black fragments
PM230505-I-AA10-INT	None	None	middle/ small black fragments
PM230505-I-AA11-INT	None	None	middle rich/ more brown flakes than black fragments
PM240505-I-AA12-INT	None	None	very poor
PM240505-I-AA13-INT	None	None	poor
PM240505-I-AA14-INT	None	None	poor/ black fragments
PM240505-I-AA15-INT	None	None	poor/ black organic matter
PM250505-I-AA16-INT	None	None	poor/ black organic matter
PM250505-I-AA17-INT	None	None	poor/ black organic matter
PM250505-I-AA18-INT	None	None	poor/ black organic matter
PM270505-I-AA19-INT	None	None	middle rich/ black flakes and small black fragments
PM270505-I-AA20-TOP	None	None	grey-brown flakes (middle) but rare small black flakes
PM270505-I-AA21-TOP	None	None	rare/ small black fragments and flakes
PM300505-I-AA22-INT	None	None	rich/ fine flakes and dark fragments
PM030605-I-AA23-BOT	None	None	very poor and some recent contamination
PM030605-I-AA24-BOT	None	None	none
PM030605-I-AA25-INT	None	None	very rare; dark fragments
PM030605-I-AA26-TOP	None	None	middle for flakes but rare for dark fragments
PM030605-I-AA27-BOT	None	None	very poor; more likely recent contamination
PM 040605-I-AA28-TOP	None	None	only red-brown flakes (secondary precipitation?): middle
PM040605-I-AA29-BOT	None	None	rich dark flakes but rare dark fragments
PM040605-I-AA30-INT	None	None	poor; dark and brown organic matter
PM040605-I-AA31-INT	None	None	rich; dark fragments and flakes
PM040605-I-AA32-BOT	None	None	poor; fragments; some recent contamination
PM040605-I-AA33-BOT	None	None	rich brown flakes but poor black fragments
PM040605-I-AA34-BOT	None	None	very rare; dark fragments
PM040605-I-AA35-TOP	None	None	middle/ only red-brown flakes
PM050605-I-AA36-TOP	None	None	middle/ dark organic matter
INT = 22, TOP = 7, BOT = 7			